Evaluation of Neuroimaging Biomarkers in Amyotrophic Lateral Sclerosis

A dissertation submitted to Trinity College Dublin for the degree of Doctor of Philosophy (PhD) 2017

Christina Schuster

Supervisor Dr. Peter Bede

Declaration

I declare that this thesis has not been submitted as an exercise for a degree at this or any other university and it is entirely my own work.

I agree to deposit this thesis in the University's open access institutional repository or allow the library to do so on my behalf, subject to Irish Copyright Legislation and Trinity College Library conditions of use and acknowledgement.

Christina Schuster .....

Date, Signature

Abstract

Amyotrophic lateral sclerosis (ALS) is a progressive neurodegenerative condition characterised by relentless upper and lower motor neuron degeneration. The clinical spectrum, symptoms onset, genetic vulnerability and cognitive profile of ALS is hugely heterogeneous making early diagnosis, accurate prognosis and disease monitoring particularly challenging. There is no cure available and life expectancy is limited to 2-3 years. Objective, accurate and validated biomarkers are urgently needed for diagnostic applications, disease-monitoring and as prognostic indicators.

The aim of this PhD thesis is to evaluate the role of magnetic resonance imaging (MRI) as a potential biomarker of ALS.

First, a comprehensive systematic literature review was conducted to explore the methods, design and pitfalls of existing longitudinal imaging studies across the spectrum of neurodegenerative conditions including Alzheimer's disease, amyotrophic lateral sclerosis, fronto-temporal dementia, Huntington disease, multiple sclerosis, Parkinson's disease, ataxia, HIV, alcohol dependence and healthy ageing.

Subsequently, ALS-associated structural brain changes were evaluated cross-sectionally and longitudinally. The results were used in diagnostic and prognostic models to assess the biomarker potential of MRI metrics. The multimodal analyses relied on complementary grey and white matter measures based on T1-weighted and diffusion-weighted images. The methods included voxel-based morphometry, vertex-based cortical thickness analyses and track-

based analyses of fractional anisotropy, mean -, radial - and axial diffusivity indices.

The most prominent imaging features identified in this ALS study are the progressive degeneration of the corpus callosum, corticospinal tracts, corticobulbar fibres and the precentral gyri.

The comprehensive analyses of longitudinal MRI data highlight progressive grey matter alterations and suggest that grey matter metrics are better suited for monitoring purposes than white matter indices.

Based on these imaging patterns, an automated classification protocol to distinguish blinded MR data sets of ALS patients and healthy controls with good accuracy and sensitivity was developed.

Finally, the prognostic value of MRI was demonstrated predicting 18-month survival based on MR data sets alone and in combination with clinical data. The supplementary prognostic value of neuroimaging measures in addition to more-established clinical and demographic prognostic factors was shown.

In conclusion, it was demonstrated that MRI can be used as a diagnostic or prognostic biomarker and it was shown that monitoring markers should focus on grey matter degeneration.

"Dicebat Bernardus Carnotensis
nos esse quasi nanos gigantum umeris insidentes,
ut possimus plura eis et remotiora videre, non utique proprii visus
acumine, aut eminentia corporis, sed quia in altum subvehimur et
extollimur magnitudine gigantea."

Johannes von Salisbury: Metalogicon 3,4,46-50

Acknowledgements

First and foremost, I would like to thank my supervisor **Dr. Peter Bede** and **Professor Dr. Orla Hardiman** for giving me the opportunity and the means to conduct the research on MRI as a biomarker in ALS. I would like to thank them for their time and support despite their busy schedule.

I would also like to thank their team, especially **Marta**, **Bahman** and **Mark**, for their words of wisdom that encouraged me to accomplish this project.

Thanks to **CAMI**, in particular **Keith**, **Alison** and **Jo**, who somehow made it possible to acquire more than 300 scans in a relative short period of time.

I am grateful to my **family** and **friends**, wherever they are: thank you for your patience and encouragement whenever I needed it. Thanks to **Marwa**, **Niamh**, **Polona**, **Spyros**, **Steffie** and **Tahnée** for the coffees and **mochas**, for listening, and distracting and for putting things in perspective whenever I needed to hear it.

Last, but not the least, a million thanks to all the **patients**, their **families** and control **participants** who took the time to travel repeatedly to James's Hospital to help me accomplish this project. Thank you for sharing your stories with me.

Contents

List of Figures

List of Tables

List of Publications arising from this thesis

Schuster, C., Elamin, M., Hardiman, O., & Bede, P. (2015). Presymptomatic and longitudinal neuroimaging in neurodegeneration—from snapshots to motion picture: a systematic review. *Journal of Neurology, Neurosurgery & Psychiatry*, 86(10), 1089-1096.

Schuster, C., Elamin, M., Hardiman, O., & Bede, P. (2016). The segmental diffusivity profile of amyotrophic lateral sclerosis associated white matter degeneration. *European Journal of Neurology*, 23(8), 1361-1371.

Schuster, C., Hardiman, O., & Bede, P. (2016). Development of an Automated MRI-Based Diagnostic Protocol for Amyotrophic Lateral Sclerosis Using Disease-Specific Pathognomonic Features: A Quantitative Disease-State Classification Study. *PloS One*, 11(12), e0167331.

Schuster, C., Hardiman, O., & Bede, P. (2017). Survival prediction in Amyotrophic Lateral Sclerosis based on MRI measures and clinical characteristics. *BMC Neurology* 17(1), 73.

Glossary of terms

AD	Alzheimer's Disease
AD	Axial Diffusivity
ADNI	Alzheimer's Disease Neuroimaging Initiative
aIC	Anterior limb of the internal capsule
ALS	Amyotrophic Lateral Sclerosis
ALSFRS-R	Amyotrophic Lateral Sclerosis Functional Scale – revised
bCC	Body of the corpus callosum
CC	Corpus Callosum
CR	Corona Radiata
CSF	Corticospinal Fluid
CST	Corticospinal Tract
d	Days
DTI	Diffusion Tensor Imaging
FA	Fractional Anisotropy
FALS	Familial Amyotrophic Lateral Sclerosis
FDR	False Discovery Rate
FTD	Fronto-temporal dementia
FU	Follow-up
FWE	Family-wise error
gCC	Genu of the corpus callosum
HC	Healthy Control
HD	Huntington's Disease
IC	Internal capsule
l	Left

MCI	Mild Cognitive Impairment
MD	Mean Diffusivity
MDT	Multidisciplinary
ME	Mesencephalic cruri
M	Mean
MND	Motor Neuron Disease
mo	Months
MR	Magnetic Resonance
MRI	Magnetic Resonance Imaging
MRS	Magnetic Resonance Spectroscopy
MS	Multiple Sclerosis
NISALS	Neuroimaging Society in ALS
NIV	Non-Invasive Ventilation
PD	Parkinson's disease
PET	Positon Emission Tomography
pIC	Posterior limb of the internal capsule
PLS	Progressive Lateral Sclerosis
PMA	Progressive Muscular Atrophy
r	Right
RD	Radial Diffusivity
ROI	Region of Interest
sCC	Splenium of the corpus callosum
SD	Standard Deviation
SNIP	Sniff Nasal Inspiratory Pressure
SPECT	Single Photon Emission Computed Tomography
SUP-CR	Lateral fibres of the corona radiata
TBSS	Tract-based spatial statistics
TFCE	Threshold-free Cluster Enhancement
TMS	Transcranial Stimulation
VBM	Voxel-based morphometry
wks	Weeks
yrs	Years

Chapter 1

Amyotrophic Lateral Sclerosis

1.1 Introduction and Terminology

Amyotrophic lateral sclerosis (ALS) is characterised by degeneration of upper motor neurons in the cerebral cortex and lower motor neurons in the spinal cord (Kiernan et al., 2011; Al-Chalabi et al., 2016; Ludolph et al., 2015). The symptoms are progressive muscle atrophy and weakness, fatigue, bulbar symptoms and eventually respiratory failure. Several heterogeneous phenotypes can be distinguished: classical ALS presents as a mixture of upper and lower motor signs and is the most common form, its variants include upper motor neuron dominant forms, i.e. primary lateral sclerosis (PLS) and lower motor neuron dominant forms, i.e. progressive muscular atrophy (PMA), flail arm or leg syndrome.

In Europe, the incidence of ALS is 2-3 people per 100,000 of the general population. The overall lifetime risk of developing ALS is 1:400 (Alonso et al., 2009; Cronin et al., 2007; Johnston et al., 2006). Men are more commonly affected than women; the ratio is 1.2 - 1.5:1 (Logroscino et al., 2010).

1.2 Clinical manifestation

The clinical presentation varies regarding the site of symptoms onset: for the majority of cases (65%) limb symptoms are initially experienced, followed by symptoms of bulbar dysfunction (i.e. dysarthria or dysphagia; for 30% of all ALS cases). Five per cent of ALS patients report respiratory onset (Hardiman et al., 2011).
Cognitive or behavioural changes have been repeatedly reported. Fifty per cent of patients suffer from cognitive impairment and up to 10% present with frank frontotemporal dementia (FTD, Phukan et al., 2012).

1.3 Diagnosis

The average delay between first symptoms and formal diagnosis is 9-16 months (Chiò, 1999; Cellura et al., 2012). There is no definitive diagnostic test for ALS. The diagnosis relies on the integration of clinical signs, clinical progression and negative laboratory tests for alternative diagnoses. During the diagnostic phase, progressive neurodegeneration occurs, challenging biomarker studies and pharmaceutical trials (Wokke, 2009). The diagnostic delay may mask medication effects as too much deterioration has taken place to be able to measure the effectiveness of a new drug. The delay, furthermore, masks the subtle first degenerative changes which are the most likely candidates for a diagnostic biomarker. The role of standard magnetic resonance imaging (MRI) in the diagnosis of ALS is limited; it is used primarily to rule out alternative pathologies rather than to confirm the diagnosis. At present, research in various MRI techniques suggests its great potential as a novel *in vivo* biomarker for ALS.

1.4 Prognosis

The prognosis for ALS is poor. The median survival of patients with classical ALS is 2-3 years from symptom onset (Al-Chalabi and Hardiman, 2013). Several clinical and demographic factors have been identified to predict fast progression of classical ALS have been identified: older age at disease onset, bulbar site of onset, short diagnostic delay, presence of cognitive impairment or genotype (Chiò et al., 2009; Logroscino et al., 2010; Gordon et al., 2013; Elamin et al., 2011).
Other phenotypes i.e. pure upper or lower motor syndromes such as PLS or PMA carry a better prognosis.

1.5 Management

There is currently no cure for ALS; clinical management focuses on the treatment of symptoms and on the preservation of quality of life. The only evidence-based disease-modifying drug is riluzole, which is thought to block presynaptic glutamate release (Rothstein, 1996). It prolongs life by about three to six months (Miller et al., 2003).
Optimum care for patients with ALS is provided by a multidisciplinary (MDT) approach, where physiotherapist, occupational therapists, speech therapists, respiratory physicians, gastroenterologist, social workers and palliative care physicians collaborate (Van den Berg et al., 2005). The MDT approach has been linked to a better prognosis (Rooney et al., 2015).

The basic components of care are respiratory management, dietary management and palliative care: Respiratory care includes monitoring for potential respiratory muscle weakness. Eventually, non-invasive positive pressure ventilation (NIPPV) can assist spontaneous breathing. It has been shown that NIPPV increases quality of life and extends survival (Bourke et al., 2006). Dietary management aims to avoid excessive weight loss and malnutrition; both are associated with a poorer prognosis. The consistency of food and

fluids may need to be modified early, postural advice given or enteral feeding by gastrostomy initiated.

Early palliative care should focus on individual patient needs, dignity and autonomy (Bede et al., 2011). Advanced health care directives and early discussion of end of life decisions are paramount. Invasive mechanical ventilation should be discussed; even though most patients decide against it (Bourke et al., 2006).
The carefully assessment and management of caregiver burden is also essential. Counselling, support groups and a crisis management system represent some of the supportive strategies (Andersen and Al-Chalabi, 2011; Bede et al., 2011).

1.6 Genetics

Up to 10% of ALS cases have a strong family history suggesting familial ALS (fALS). The remaining 90% of cases appear sporadic, meaning they appear to occur randomly (Renton et al., 2014). The clinical presentation of familial ALS is very similar to sporadic ALS (Andersen and Al-Chalabi, 2011).

Genetics in ALS is a crucial research field. Recently, the gene *NEK1* was identified to be a risk variant in nearly 3% of ALS cases (Kenna et al., 2016). Some clinical trials specifically focusing on gene-carriers report promising results: Arimoclomol has been proven safe and well tolerable with clinically meaningful trends. [1]

There is a scarcity of studies correlating genotypes with clinical phenotypes: *C9orf72* mutation is associated with cognitive and behavioural changes and shorter survival (Byrne et al., 2012) and it is associated with a specific brain signature: Patients present with marked frontal lobe involvement (Bede et al.,

[1] http://orphazyme.com/index.php/news/news-releases/73-phase-ii-arimoclomol-als-sod1 accessed 15/12/2016

2013a).

1.7 Neuroimaging

As described above, MRI plays only a secondary role in the clinical diagnosis of ALS, but it is an important field of research (Turner et al., 2012; Chiò et al., 2014; Menke et al., 2017). MRI has improved our understanding of the pathological processes underlying ALS. It has been repeated suggested as biomarker (Turner et al., 2011). Multiple studies across various platforms have described the ALS-associated structural brain changes using group comparisons and healthy controls as a reference group.

T1-weighted images are used to analyse focal grey matter atrophy. Based on voxel-based morphometry or vertex-based cortical thickness analysis, ALS-associated grey matter changes include the degeneration of the precentral gyrus and supplementary motor cortex (Bede et al., 2012a; Schuster et al., 2013). Grey matter loss of the temporal and frontal lobes has been described (Verstraete et al., 2012; Agosta et al., 2012; Lillo et al., 2012) and, additionally, related to cognitive changes (Schuster et al., 2014a; Bede et al., 2013a).

White matter degeneration can be investigated using diffusion weighted imaging (DTI). It allows to calculate the diffusion of water molecules and thereby to characterise the integrity of the white matter tracts (Basser et al., 1994; Pierpaoli et al., 1996). Decreased factional anisotropy (FA) and increased mean diffusivity (MD) have been consistently described. Radial (RD) and axial diffusivity (AD) are examined less frequently, but are able to highlight ALS-associated structural white matter changes. Reliably reported brain changes based on group comparisons included degeneration of the cortico-spinal tract, particularly of the posterior limb of the internal capsule (Menke et al., 2012; Canu et al., 2011; Agosta et al., 2010b) and corpus callosum (Müller et al., 2012; Filippini et al., 2010; Kassubek et al., 2014). Extra-motor areas have been identified and linked to cognitive changes (Sarro et al.,

2011; Kasper et al., 2014).

Pathological grey and white matter changes have been reliably described based on group comparisons, but rarely replicated using single patient data. A successful biomarker needs to be meaningful for an individual patient.

1.8 Thesis Outline

This thesis investigates the potential of MRI as a biomarker for ALS. There are different types of biomarkers each focusing on a different aspect of the disease. Their aim is to either facilitate diagnosis, enable disease monitoring, which is crucial for clinical trials, or evaluating prognosis. In order to investigate MRI as one of these biomarkers, the first objective is to investigate which brain areas are most vulnerable to the disease and what type of MR images is able to reliably capture ALS-related brain changes. Eventually, these results then need to be evaluated for their potential as diagnostic, prognostic or monitoring biomarker for ALS.

The following chapter is systematic methodological literature review of longitudinal imaging studies in neurodegeneration which was used to design this PhD project (Chapter 2). Chapter 3 investigates patterns of ALS-associated white and grey matter degeneration in relation to clinical phenotypes and disability. Longitudinal brain changes are characterised in Chapter 4 evaluating the role of MRI as a potential monitoring biomarker. Chapter 5 outlines a computer-aided diagnostic tool based on key disease-associated brain regions exploring the role of MRI as a diagnostic biomarker. Finally, Chapter 6 explores the role of MRI in predicting survival. Chapter 7 summarizes the main findings of the thesis and reviews the overall clinical impact of MRI biomarkers in ALS.

1.9 Hypotheses

The primary hypothesis of this thesis is that MRI can be used as a biomarker for ALS. The individual hypotheses investigated within each chapter are stated below. For the background and justification please refer to the introduction section of each chapter.

Chapter 3 investigates the hypothesis that there is a segmental vulnerability of the cortico-spinal tract and the corpus callosum in ALS. This vulnerability can be linked to ALS-phenotype specific grey and white matter degeneration.

The hypothesis for Chapter 4 is that MRI is able to highlight longitudinally progressive neurodegenerative brain changes. This change can be found in the key disease-related brain regions: the precentral gyrus and the corticospinal tract. Furthermore, it can be described prior to symptom onset.

For Chapter 5, it is hypothesised that the diagnostic accuracy of a classification model is increased by incorporating multiple imaging indices of multiple disease-defining anatomical structures.

Finally, Chapter 6 investigated that MRI can predict the probability of 18-month survival based on an individual structural MR scan. It is, furthermore, hypothesised that structural MRI measures enhance prediction accuracy compared to more-established clinical and demographic factors.

Chapter 2

Methodological Review of Longitudinal Imaging Studies in Degenerative Disease

A concise version of this chapter has been published in the peer-reviewed Journal of Neurology, Neurosurgery & Psychiatry (Schuster et al., 2015).

In order to optimise the design of this longitudinal study in ALS, a systematic review of longitudinal imaging initiatives in neurodegeneration was performed. The focus lied on methodology, optimal statistical models, follow-up intervals, attrition rates, primary study outcomes and presymptomatic studies.

The findings of this review have been taken into account in the design of the longitudinal section of this PhD project and are discussed in detail in section 2.7 of this Chapter. Each of the subsequent chapters provides a detailed description of the sample used to investigate the hypotheses.

2.1 Introduction

In spite of their underlying pathological differences, neurodegenerative conditions share a number of strikingly common features, such as insidious symptom onset, diagnostic challenges, relentless disease progression, marked clinical and genetic heterogeneity, lack of sensitive biomarkers and prognostic indicators, a long preclinical phase, and lack of effective disease modifying agents. Moreover, many of these conditions have a relatively similar rate of decline, leading to considerable disability within a few years from diagnosis. These similarities provide the rationale to appraise research methodologies in imaging across a seemingly diverse set of conditions. While the core pathology is different in various neurodegenerative conditions, the commonly used imaging techniques, MRI pulse sequences and the methodological challenges are surprisingly similar. Furthermore, the initiatives of setting up multicentre studies, validating cross-platform protocols and establishing multicentre data repositories are also analogous, for example, the Alzheimer's disease neuroimaging initiative (ADNI, Jack et al., 2008), TRACK-HD (Tabrizi et al., 2009) or the Neuroimaging society in ALS (NISALS, Turner et al., 2011). While most researchers are experts of a specific neurodegenerative condition and attend disease-specific meetings, the imaging studies of other neurodegenerative conditions are a valuable source of learning and potential methodological templates for study design. Quantitative imaging measures have been repeatedly proposed as candidate biomarkers of neurodegenerative conditions. Non-invasive MRI-based approaches have successfully captured disease-specific pathology *in vivo* in Alzheimer's disease (AD), mild cognitive impairment (MCI), fronto-temporal dementia (FTD) and amyotrophic lateral sclerosis (ALS). Phenotype-specific imaging signatures have been described in variants of AD, FTD (Lam et al., 2014) and ALS (Bede et al., 2012a; Schuster et al., 2013).

The sensitivity of specific imaging techniques has been further demonstrated by correlations between imaging parameters and clinical measures across the spectrum of neurodegenerative conditions. For example, imaging measures

have been correlated with neuropsychological performance in AD (Grothe et al., 2013), FTD (Knopman et al., 2009) and with motor disability in ALS (Bede et al., 2013a; Schuster et al., 2013). Novel imaging techniques have been successfully utilised to describe genotype-specific changes, such as *MAPT*-related and *PGRN*-related changes in FTD (Whitwell et al., 2009), *APO-E*-associated changes in AD and MCI (Lu et al., 2011), *C9orf72*-specific changes in ALS (Bede et al., 2013a,b), repeat length-dependent changes in Huntington's disease (HD) (Ruocco et al., 2008), and *PRKN*-related changes in in Parkinson's disease (PD, Pavese et al., 2010). Imaging parameters are routinely used in pharmaceutical trials in MS, but imaging-based outcome measures have also been proposed in HD (Tabrizi et al., 2012) and ALS (Kalra et al., 2006). While MRI is routinely used to establish the diagnosis of MS and Ioflupane single-photon emission CT (SPECT; DaTSCAN) scan to confirm PD, recent classifier models also show promise of aiding the diagnosis of early ALS and AD (Orrù et al., 2012). Recently, quantitative imaging techniques have been successfully utilised to highlight changes in grey and white matter integrity in presymptomatic mutation carriers in HD (Aylward et al., 2004), AD (Fox and Warrington, 1996), PD (Tang et al., 2010) and ALS (Turner et al., 2005).

The majority of imaging studies in neurodegeneration are cross-sectional, even though longitudinal studies are crucial for the characterisation of natural disease trajectories, evaluation of the presymptomatic disease phase, description of genotype-specific progression rates, reporting patterns of pathological spread and appraisal of medication effects. Furthermore, longitudinal imaging has the potential to contribute to the validation of prognostic markers, establish imaging-based staging systems, define progression milestones and identify triggers for clinical interventions. Finally, multimodal longitudinal imaging studies can help to establish the relative sensitivity of the various imaging techniques.

2.2 Aims

The aim of this chapter is to systematically review longitudinal neuroimaging studies in neurodegeneration, focusing on imaging methodology, sample size considerations, enrolment bias, number of time points, statistical models, follow-up intervals, attrition rates and study deliverables. An additional objective of this work is to review presymptomatic and preclinical studies in neurodegeneration and outline the optimal methodological framework for large, multi-centre, longitudinal neuroimaging studies.

2.3 Methods

Longitudinal imaging studies published between 1990 and 2014 were identified using PubMed. The search terms "longitudinal", "imaging" and "MRI" were combined with one of the following keywords: "Alzheimer's disease", "Amyotrophic lateral sclerosis", "Motor neuron disease", "Frontotemporal dementia", "Huntington disease", "Multiple sclerosis", "Parkinson's disease", "Ataxia", "HIV", "Alcohol", "Healthy ageing". A supplementary search included the term "presymptomatic" in combination with the above listed conditions. The search was performed between April and June 2014. Clinical trials, animal-model studies and paradigm-based functional MRI studies were excluded. Studies of multiple system atrophy, progressive supranuclear palsy, Lewy body dementia, posterior cortical atrophy, and corticobasal degeneration were also excluded due to their lower incidence compared with the most common neurodegenerative conditions. While innovative longitudinal spinal cord studies have been published in ALS (Agosta et al., 2009; El Mendili et al., 2014) and MS (Freund et al., 2010), because of the lack of longitudinal spinal cord studies in other neurodegenerative conditions, only brain imaging papers were systematically reviewed. The identified studies were systematically reviewed for sample size, reference control groups, follow-up intervals, attrition rates, statistical models and their ability to capture longitudinal changes.

2.4 Results

Based on the above search criteria a total of 526 publications were identified; 423 longitudinal imaging papers and 103 genotype-based presymptomatic studies. One hundred and twenty-six longitudinal imaging papers were reviewed in AD, 18 in ALS, 18 in FTD, 21 in HD, 156 in MS, 26 in PD, 3 in ataxia, 5 in HIV cognitive impairment, 7 in alcohol abuse and 43 publications in healthy ageing. A list of the identified papers is provided at the end of the chapter (section 2.11).

2.4.1 Sample size and cohort considerations

Relatively few studies disclose their formal power calculations and sample size estimations (Teipel et al., 2011a). The average sample size of longitudinal studies of AD and MS is approximately three times larger than studies of ALS or FTD (Table 2.1). This is because of disease-specific factors, such as sialorrhoea and orthopnoea in ALS. Behavioural impairment has implications on recruiting phenotypes of FTD cohorts, motor disability makes recruitment to ALS and MS studies difficult, and extrapyramidal impairment may limit the scanning of symptomatic PD and HD patients. In addition to differences in prevalence, these factors all contribute to the significant sample size differences observed in longitudinal studies across the neurodegenerative spectrum (Table 2.1).

The reviewed articles included both prospective longitudinal projects and retrospective studies, interrogating data from large international data repositories. Digital data repositories have been established for AD, healthy ageing, ALS and HD; such as the ADNI, NISALS (Turner et al., 2011) or TRACK-HD (Tabrizi et al., 2012). More than half of longitudinal AD studies and more than a quarter of longitudinal FTD and MS studies utilise pre-existing data banks (Table 2.1). In prospective longitudinal studies, recruitment of prevalence cases as opposed to incidence cases introduces another bias towards those who are progressing slowly, a cohort which is more likely to participate in longitudinal imaging studies.

	AD	ALS	FTD	HD	MS	PD	Ataxia	HIV Dementia	Alcohol Abuse	Healthy Ageing
Reviewed studies (n)	126	18	18	21	156	26	3	5	7	43
Sample selected from database (% of studies)	55.6%	5.6%	27.8%	23.8%	38.5%	11.5%	33.3%	40%	14.3%	74.4%
Average Sample size*	112.9	29.9	34.5	64.8	108.3	40.3	20.3	80	45.4	188.3
Median Sample size*	55	28	22	35	44	27.5	10	80	24	122
Min/ Max sample size*	5/ 590	11/ 48	9/ 107	7/ 243	4/ 1465	6/ 199	6/ 45	74/ 86	15/ 111	24/ 1924
Average Attrition rate (Year 1) Ł	6.8%	56.2%	28%	4%	5.3%	19.3%	33% ł	0% ł	0% ł	8% ł
Average follow-up interval (months)	15.7	5.7	22.2	15.9	15.4	29.2	36	15	1.7	34.4
Min/ Max follow-up interval	2wks/ 5yrs	1mth/ 1yr	6mth/ 15yrs	6mth/ 2yrs	1wk/ 12yrs	1yr/ 5yrs	1yr/ 4.5yrs	6mth/ 2yrs	1wk/ 6mth	2mth/ 12.7yrs

	AD	ALS	FTD	HD	MS	PD	Ataxia	HIV Dementia	Alcohol Abuse	Healthy Ageing
Overall follow-up period (years)	10	2.5	20	6	14	8	10	3.5	1	13
Average number of assessments	2.1	1.6	2.9	1.4	4.7	1.6	1	1	1.6	2.7
Min/ Max number of assessments	1/ 10	1/ 4	1/ 13	1/ 4	1/ 51	1/ 3	1/ 1	1/ 1	1/ 3	1/ 10
Single imaging technique (% of studies)	82.5%	83.3%	83.3%	90.5%	57.1%	84.6%	33.3%	100%	85.7%	93.0%
Multiple techniques (% of studies)	17.5%	16.6%	16.7%	9.5%	42.9%	15.4%	66.6%	0%	14.3%	7.0%
MRI studies (% of studies)	82.5%	100%	88.9%	100%	100%	38.5%	100%	100%	100%	97.7%
PET studies (% of studies)	19%	0%	16.7%	0%	0.6%	50%	0%	0%	0%	7.0%
SPECT studies (% of studies)	10%	0%	5.56%	0%	0%	11.5%	0%	0%	0%	0%

	AD	ALS	FTD	HD	MS	PD	Ataxia	HIV Dementia	Alcohol Abuse	Healthy Ageing
Structural MRI (% of studies)	78%	38.9%	77.8%	95.2%	100%	42.3%	100%	80%	85.7%	95.35%
Diffusion MRI (% of studies)	4.8%	50%	0%	14.3%	9.0%	0%	0%	0%	14.3%	4.7%
MR Spectroscopy (% of studies)	0.8%	22.2%	0%	0%	5.8%	0%	33.3%	20%	14.3%	0%
Whole-brain analyses (% of studies)	34.9%	38.9%	27.8%	38.1%	55.1%	26.9%	66.6%	20%	71.4%	34.9%
ROI-only analyses (% of studies)	38.9%	22.2%	11.1%	42.9%	9.6%	46.2%	0%	40%	28.6%	32.6%
Combined whole-brain & ROI analysis (% of studies)	24.06%	33.3%	33.3%	19.0%	1.3%	23.1%	0%	20%	0%	28.0%

Table 2.1: Key characteristics of longitudinal imaging studies in neurodegeneration. *Values at time point 1. ł Based on a single study. Ł Attrition rate is calculated based on prospective studies only.

2.4.2 Reference groups

It is well-established that physiological changes take place during healthy ageing (Fjell et al., 2013b). Volume reductions and ventricular expansion has been detected as early as at a 12-month follow-up interval (Fjell et al., 2013a). However, the majority of longitudinal imaging studies do not include a healthy control group, and accordingly do not account for physiological changes over time. This seems an essential requirement in order to separate disease-specific effects from those associated with healthy ageing.

Additionally, very few longitudinal studies enrol neurological control cohorts. The inclusion of disease controls is particularly important in neurodegeneration, where initial symptoms may considerably overlap. Despite the advantage of characterising distinct phenotypic signatures, the longitudinal evaluation of multiple phenotypes of the same condition is seldom carried out (Lam et al., 2014).

2.4.3 Attrition rates

Attrition rate refers to the gradual reduction of sample size over a certain period of time. Foreseeable attrition rates should ideally be estimated prior to recruitment and sample size calculations. In a condition with high-attrition rates, a larger initial sample size and shorter follow-up intervals are required to draw meaningful conclusions on longitudinal changes. Few studies directly disclose their attrition rate, but most provide sufficient information for its calculation. Attrition rates are largely condition specific, for example, due to the rapid disease progression of ALS the average attrition rate after 1 year is 56.2%, while in MS studies it is only 5.3%, in AD 6.8%, in PD 19.3% and in FTD studies 28% (Table 2.1). Interestingly, attrition rates in studies of healthy ageing is higher than in MS studies indicating a possible study adherence bias of patients with chronic progressive conditions who are anxious to participate in structured monitoring programmes. Attrition rate is also a function of the recruitment strategy; carefully selected patients, who

participate in clinical trials are less likely to drop out. However, participants of population-based incidence studies may include relatively sicker patients resulting in higher attrition rates. Ideally, the factors influencing attrition rates in longitudinal studies should be thoroughly examined and their effect on overall study results comprehensively discussed.

2.4.4 Imaging modalities

Positron emission tomography (PET)-based, SPECT-based and MRI-based techniques dominate the methodology of longitudinal studies in neurodegeneration. Very few longitudinal studies have been carried out on PET/MRI or magnetoencephalography platforms to date. Similarly, there is currently a lack of high-field, such as 7-Tesla, longitudinal MRI studies in neurodegeneration, which is likely to change dramatically in the coming years.

The most commonly used grey matter MR techniques include voxel-based morphometry, cortical thickness measurements and MR spectroscopy (MRS). Frequently used white matter approaches included diffusion tensor imaging, tractography, connectomic mapping or white matter density measurements. Longitudinal imaging studies often report observations on a single white or grey matter parameter (Lam et al., 2014; Ruocco et al., 2008). Over 85% of longitudinal HD and ALS studies establish their conclusions based on a single imaging measure, most frequently an imaging proxy of atrophy. Most PD studies (84%) also use a single imaging technique, most frequently PET. The majority of longitudinal MS and ataxia studies, however, rely on multiple, complementary methods (Table 2.1).

As opposed to single-technique studies, a multimodal approach is clearly required to comprehensively characterise a condition and also establish the relative sensitivity of the various techniques in the different disease stages. Combining multiple methods led to the observation that white matter pathology can be detected relatively early in ALS, but shows limited progression

over time compared with grey matter changes, which demonstrate progressive anatomical spread in the later stages of the disease (Menke et al., 2014). Observations on the detection thresholds of various techniques should have a major impact on the design of new studies and development of viable diagnostic applications (Figure 2.1).

In all neurodegenerative conditions, structural MRI is by far the most frequently utilised measure, followed by diffusion-based white matter techniques, and only a small minority of longitudinal studies focus on metabolic imaging using MRS. However, with the advent of whole brain MRS sequences, spectroscopy is likely to gain further momentum. A significant proportion of AD, HD and PD studies report longitudinal changes solely from a specific region of interest (ROI) such as the motor cortex or corticospinal tracts in ALS, caudate nuclei in HD, temporal lobes in AD, etc. ROI-based analyses are often performed to highlight focal changes in disease-defining brain regions; however, narrowing the ROI to a specific area introduces an anatomical selection bias and ignores the multisystem nature of these conditions. Another pitfall of 'ROI-only' studies is that considerable changes may have already taken place at the initial time point making the detection of further changes difficult. This review suggests that less than one-third of longitudinal MRI studies report both ROI and whole-brain findings.

Currently, MRI-based techniques dominate the methodology of longitudinal imaging, despite the significant contribution of PET studies to presymptomatic and genotype-based research (Ciarmiello et al., 2012; Pavese et al., 2010, Table 2.1). With the development of novel ligands however, PET is likely to increasingly contribute to our understanding of pathophysiological changes. In spite of its cost implications, the requirement for a near-site cyclotron to produce short half-life isotopes, and limited availability, PET offers unrivalled sensitivity to identify disease-specific pathology. For example, amyloid-imaging and recently τ-imaging have the potential to provide sensitive diagnostic and biomarker applications in AD. PET radioligands that bind specifically to serotonin 5HT1A/5HT2A receptors, dopamine D2/D3 re-

ceptors, opioid mu receptors, GABA-A benzodiazepine receptors or ligands such as [11C]PMP which measures acetylcholinesterase activity enable the selective assessment of neurotransmitter-specific networks.

While PET provides valuable functional insights, group-level interpretation remains challenging, and the widespread availability of MRI scanners, their high spatial resolution and relatively simple spatial registration renders the interpretation of longitudinal MR data more straightforward. This is likely to change with the availability of combined PET/MRI scanners.

2.4.5 Statistical methods

Most of the identified studies include 2–3 follow-up measurements with the exception of MS studies where an average of 4.7 assessments have been carried out. However, many studies have relied on a single follow-up assessment making modelling on non-linear decline impossible.

The majority of the reviewed studies have used fixed time intervals which were largely diagnosis dependent. Conditions with slower progression rates use relatively longer follow-up periods compared with more rapid neurodegenerative conditions. The overall follow-up period from first to the last assessment also shows significant variations from a maximum of 2 years in ALS to up to 14 years in MS (Table 2.1).

A wealth of statistical approaches was identified, ranging from relatively simple methods to complex models. Many longitudinal studies directly compare the first and second assessment (Aylward et al., 2004), calculating the rate of change, percentage change or annualised percentage change from assuming a linear decline (Grothe et al., 2013). It is well established, however, that linear models are not applicable to most neurodegenerative conditions (McDonald et al., 2009), or to physiological ageing (Fjell et al., 2013b, Figure 2.1).

Other frequently utilised approaches include generalised estimating equations, or mixed effect linear models. The latter is particularly useful in longitudinal studies as participants with only a single assessment can be included (Leung et al., 2013; Nowrangi et al., 2013; Teipel et al., 2011a). This approach may also be favourable in high attrition rate studies and to model non-linear trajectories of decline. Furthermore, these models can be readily utilised to correlate longitudinal brain changes with clinical measures (Nowrangi et al., 2013). The superiority of the mixed effects model with a random effects term, accounting for variable observation time points, compared with fixed effects analyses, has been demonstrated by a longitudinal study of AD (Teipel et al., 2011a).

Other approaches, such as the cumulative model or sigmoid model, have been recently applied to model the rate of atrophy in AD (Sabuncu et al., 2011). This model assumes initial acceleration of volume loss up to an inflection point following which deceleration of atrophy occurs. This model has also been applied to MCI cohorts where higher acceleration rates were associated with conversion to AD (Leung et al., 2013). Acceleration–deceleration models may also explain why relatively little change is observed longitudinally in disease-defining pathological regions, such as the primary motor cortex (PMC) in ALS once significant changes have already taken place at the initial time point (Verstraete et al., 2014, Figure 2.1).

Primary regions of vulnerability, such as the PMC in ALS, the frontal lobes in behavioural variant FTD, the hippocampus in AD, or the substantia nigra in PD are affected early and progressively (acceleration) leading to substantial pathology after which only modest further changes take place (deceleration). The 'deceleration phase' may clinically manifest as a symptomatic 'plateau' and explain why several studies fail to detect significant longitudinal changes (Laakso et al., 2000; Menke et al., 2014).

The same principle has been applied to neuropsychology data. The 'change point model' is based on the time at which rate of decline begins to ac-

celerate to predict conversion to disease (Hall and Lipton, 2000). Acceleration–deceleration models rely on the interpretation multi-time point observations to predict disease outcomes, but such models require relatively uniform inter-assessment intervals. Finally, multivariate classification analyses, such as the support vector machine approach, enables individual participant classifications (Orrù et al., 2012).

Longitudinal statistical models should ideally have the ability to manage missing data, incorporate participants with single assessments, interpret variable follow-up periods and model non-linear decline.

Cluster analysis of progression rates has implication for genetics, prognosis, diagnosis and stratification for clinical trials (Gomeni et al., 2014; Simon et al., 2014). Most neurodegenerative conditions, particularly ALS and PD, have a relatively uniform rate of clinical decline and short transition times between disease stages (Balendra et al., 2015). A predictable disease trajectory enables the planning of support measures and the timing of assistive interventions. In patients who do not progress significantly over time or progress very slowly, the diagnosis is sometimes revisited or restrictive phenotypes are identified such as monomelic forms of ALS or primary lateral sclerosis. Conversely, studying fast 'progressors' may help to identify and characterise unique genetic or environmental factors (Byrne et al., 2012). Consequently, cluster analysis of patients based on progression rates should be undertaken in studies with sufficiently large sample sizes using a combination of imaging and clinical data (Gomeni et al., 2014, Figure 2.1).

2.4.6 Presymptomatic studies

It is widely accepted that pathological changes occur long before the diagnosis of most neurodegenerative conditions. Patients often observe and report subtle changes before the diagnosis of dementia syndromes and family members often recognise behavioural changes many years before the diag-

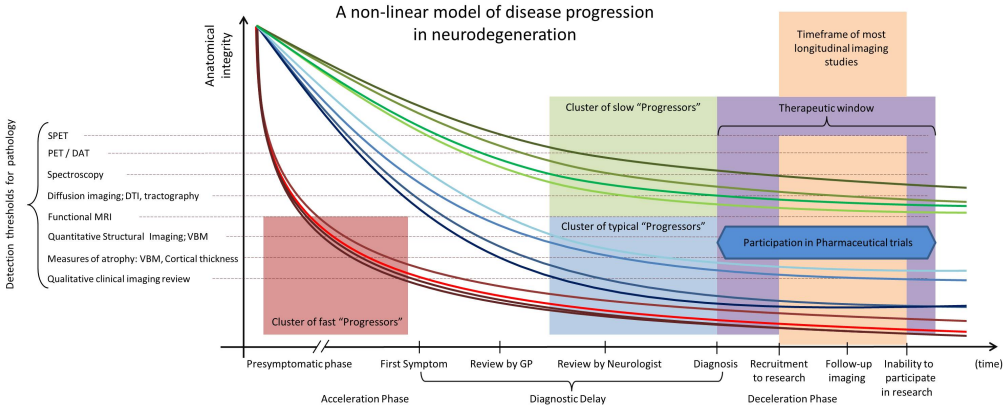

Figure 2.1: A schematic non-linear cumulative model of longitudinal change in neurodegeneration highlighting the effect of diagnostic delay on recruitment to pharmaceutical and longitudinal biomarker studies. The importance of multimodal, multiparametric imaging is illustrated by a hypothetical hierarchy of detection thresholds. Examples of colour coded progression rate clusters are shown. DAT, Ioflupane (123I) DaTSCAN; GP, general practitioner; PET, positron emission tomography; SPECT, single-photon emission CT; VBM, voxel-based morphometry; DTI, diffusion tensor imaging.

nosis of FTD is formally established. It is also increasingly recognised that ALS may have long preclinical phase (Eisen et al., 2014). Diagnostic delay in neurodegeneration is very significant compared with other neurological conditions and leads to considerable therapeutic delay as well as unnecessary interventions and investigations (Cellura et al., 2012). As illustrated in Figure 2.1, considerable neurodegenerative change may have taken place by the time patients are recruited into biomarker studies or pharmaceutical trials. Based on the acceleration–deceleration model, pathogenic mutation carriers in their preclinical stage are an optimal cohort to evaluate longitudinal changes. The preclinical, pre-manifest phase of neurodegenerative conditions also offers a valuable window for pharmacological and neuroprotective intervention. Presymptomatic longitudinal neuroimaging is one of the most novel trends of neurodegeneration research, an exciting interface of imaging, pathology and genetics (Table 2.8). The characterisation of key presymptomatic MRI signatures in neurodegeneration assists the development of more sensitive diagnostic protocols by identifying brain regions which

are affected early and the techniques which are most likely to detect these early changes. Presymptomatic studies may also have prognostic ramifications, by elucidating at what point a genotype is likely to translate into symptomatic brain pathology (Ciarmiello et al., 2012). In ALS, a few pioneering studies have examined the presymptomatic phase of the disease (Turner et al., 2005). Studies of repeat length dependent syndromes, such as the hexanucleotide repeats of *C9orf72*, or *CAG* repeats in HD have revealed repeat length-dependent structural changes (Ruocco et al., 2008).

2.4.7 Objectives, deliverables and outcomes of longitudinal imaging studies

The primary objective of the reviewed longitudinal studies ranges from the characterisation of disease phenotypes (van der Graaff et al., 2011), evaluation of disease genotypes (Rohrer et al., 2010), development of prognostic indicators (Grothe et al., 2013), establishment of study group-specific rates of decline (Frings et al., 2012), prediction of disease manifestation in presymptomatic cohorts (Ciarmiello et al., 2012), to the anatomical characterisation of pathological spread (Verstraete and Heuvel, 2010). Other study outcomes include the evaluation of the predictive value of baseline measures (Tabrizi et al., 2013), appraisal of the sensitivity of specific imaging techniques (Acosta-Cabronero et al., 2012), and correlation of longitudinal imaging changes to clinical variables (Menke et al., 2014). The most commonly stated study conclusion is that a specific imaging measure may serve as a biomarker in the future, which however, in most cases, remains aspirational (Tabrizi et al., 2012).

2.4.8 Optimal study designs

The systematic review of longitudinal imaging in neurodegeneration enabled the identification of a core list of desirable study considerations and statistical approaches, which are important for the design of future prospective studies (Table 2.2). Despite a trend of large multi-centre studies, single-site

studies have clear methodological benefits. Harmonising pulse-sequences and analysis pipelines across different field-strengths, manufacturer platforms and raw data formats requires complex quality control and validation procedures with phantom studies (Teipel et al., 2011b). Such studies are routinely undertaken in pharmacological studies of MS, but have to be carefully justified in a research setting. Even longitudinal single-centre, single-scanner studies are occasionally compromised by software updates, novel head coils, modification of pulse sequences which requires stringent post-processing corrections.

	Desirable study designs
-	Inclusion of both whole-brain and region of interest (ROI) analyses
-	Evaluation of multiple grey and white matter imaging parameters (structural, diffusion, metabolic) in the same study or multiplatform positron emission tomography/MRI designs
-	Incidence-based studies
-	Comprehensive clinical phenotyping and genotyping
-	Multiple (more than two) time-point designs
-	Inclusion of 'presymptomatic', 'premanifest' cohorts of pathological mutation carriers
-	Inclusion of a longitudinal healthy control group
-	Inclusion of neurological 'mimic' control groups also referred to as 'disease-controls'
-	Collection of longitudinal clinical data after imaging is no longer possible for validation of prognostic markers
-	Incorporation of standardised imaging protocols into pharmaceutical trials
-	Postmortem brain banking and correlation of *in vivo* imaging findings with post mortem evaluation

Optimised statistical frameworks
- Interpretation of variable follow-up periods
- Ability to model non-linear decline
- Meaningful correlations with clinical variables
- Cluster analysis of progression rates
- Multivariate classification analyses (support vector machine approach) to classify individual patients
- Comparative evaluation of the sensitivity of various imaging techniques
- Development, evaluation and validation of prognostic markers based on initial time-point or multiple-time point imaging data
- Definition of stage defining imaging measures

Disclosures and discussions
- Formal power and sample size calculations for established modalities
- Attrition rate estimations prior to recruitment
- Disclosure of recruitment strategies; incidence or prevalence cases
- Presentation of attrition rates, discussing factors contributing to attrition rates and discussion of the impact of attrition on overall findings
- Disclosure of negative results, such as lack of progression in specific ROIs

Table 2.2: Desirable design features of longitudinal studies in neurodegeneration.

2.5 Discussion

In this review, the academic, clinical and pharmaceutical potential of high-quality longitudinal studies in neurodegeneration were evaluated (Table 2.3). It is clear that longitudinal neuroimaging offers superior descriptive power to cross-sectional studies and is undoubtedly the optimal method to study progressive conditions. One of the biggest challenges of longitudinal analyses is the non-linear nature of disease progression, coupled with the relatively late recruitment of patients to biomarker studies (Figure 2.1). Presymptomatic studies, early recruitment to biomarker studies at the time of diagnosis, initiation of incidence-based prospective studies, multi-centre collaborations, comprehensive genotyping and implementation of robust statistical models are just some of the options that may enhance longitudinal imaging studies. The expected attrition rate associated with the target disease should be taken into account prior to study onset for accurate power calculations. This has cost implications for conditions with high attrition rates. Longitudinal scanning using MRI should seek to combine multiple complementary imaging modalities for sensitivity analyses. Cross-sectional studies often attempt to match patient groups for disease duration from symptom onset to the date of scan (Bede et al., 2015) assuming relatively uniform progression rates. Given the differences in rate of decline, however, this could be viewed as a sub-optimal approach. Longitudinal imaging can address this concern by generating models where single time point and longitudinal multipoint data can be integrated. Single time point imaging data can also be utilised to validate prognostic models by subsequent clinical assessments, when imaging may no longer be possible. Cluster analyses of longitudinal data using clinical, imaging and genetic data have the potential to identify protective factors in 'slow progressors' and potential risk factors in 'fast progressors'. The identification of 'atypical' patients based on objective imaging data makes targeted deep-phenotyping possible and may help to explore unique environmental and genetic factors in these cohorts.

One of the academic deliverables of well-designed longitudinal studies is the

	Pathophysiological insights
-	Characterisation of genotype-specific rate of decline, anatomical spread
-	Characterisation of phenotype-specific rate of decline, anatomical spread
-	Identification of distinct disease stages based on objective criteria
-	Development and validation of prognostic indicators
-	Characterisation of 'premanifest', 'presymptomatic' pathological changes
-	Identification of an optimal therapeutic window
	Clinical applications
-	Diagnostic applications: patient classification based on longitudinal changes
-	Prognostic indicators; introduction and withdrawal of interventions
-	Assessment for rehabilitation potential
	Pharmaceutical applications
-	Objective quantification of disease burden prior to therapy
-	Patient stratification based on predicted disease trajectories; fast versus slow 'progressors'
-	Evaluation of response to therapy
-	Discrimination of symptomatic versus disease modifying effect

Table 2.3: Potential deliverables of longitudinal studies in neurodegeneration.

confirmation or rejection of attractive, but empirical theories, such as 'focal spreading', 'spread along functional connections' (Verstraete and Heuvel, 2010), 'dying-back', 'dying-forward', 'selective vulnerability' (Schuster et al., 2016a), 'wires together-dies together' hypotheses (Bak and Chandran, 2012). The time interval from first symptom to definite diagnosis is often regarded as a prognostic indicator, suggesting that the longer it takes to establish the diagnosis the slower the progression rate may be (Chiò et al., 2009). Using well-constructed and adequately powered longitudinal imaging protocols, the current technology is now well placed to objectively examine these clinical observations.

Disease-state 'staging' is a fundamental medical concept widely used in neurology, oncology and other specialities. It enables patient stratification into clinical trials and examining the evidence for the introduction and withdrawal of treatment in progressive conditions. Clinical staging frameworks are extensively used in neurodegeneration, for example, Hoehn and Yahr in PD (Hoehn and Yahr, 1967), El Escorial in ALS (Ludolph et al., 2015; Brooks et al., 2000). Pathological staging systems, such as the Braak staging in AD (Braak and Braak, 1995), or the recently proposed TDP-43-based staging in ALS (Brettschneider et al., 2013), are used for post-mortem characterisation in neurodegeneration. Novel initiatives in biomarker research have the capability to integrate the two approaches by developing objective, imaging-based staging systems that rely on measurement of disease-specific pathological change *in vivo* (Kassubek et al., 2014). If 'staging' represents artificially defined phases of progressive conditions, functional 'rating scales' reflect on the continuum of clinical changes. Unified Parkinson Disease Rating Scale (UPDRS), Expanded Disability Status Scale (EDSS, Kurtzke, 1983), Revised ALS functional rating scale (ALSFRS-R, Cedarbaum et al., 1999), Alzheimer's Disease Assessment Scale-Cognitive (ADAS-Cog, Pea-Casanova, 1997), International Cooperative Ataxia Rating Scale (ICARS, Trouillas et al., 1997) are just some of the disease-specific clinical rating scales which are frequently utilised as end points of clinical trials. As has been demonstrated in MS, quantitative imaging protocols have the potential to complement these scales in neurodegeneration, and to assess response to therapy in randomised controlled trials by objectively measuring longitudinal changes in the various study groups (Radue et al., 2012).

2.6 Conclusion

Longitudinal studies in neurodegeneration are superior to cross-sectional studies in characterising specific disease phenotypes and genotypes. Well-designed longitudinal studies have both academic merits and important clinical benefits. They enable the characterisation of genotype-specific progres-

sion curves and presymptomatic changes, as well as the development of prognostic markers, staging of the disease and accurate measurement of response to therapy. While cross-sectional studies provide useful snapshots of group level pathology, longitudinal neuroimaging studies have the potential to dissect the dynamic and active biological processes underpinning neurodegeneration. The methodological challenges of longitudinal imaging are similar across the spectrum of neurodegenerative conditions, such as non-linear disease progression curves, high attrition rates, heterogeneous patient cohorts and relatively late recruitment to biomarker studies. Presymptomatic and prospective incidence-based studies utilising robust statistical models to interpret multimodal imaging data are likely to overcome these methodological challenges.

2.7 Implications of the existing imaging studies for the present project

This chapter comprehensively reviews the study parameters for an optimised longitudinal study in neurodegeneration. The findings of this review are highly relevant for the design of this imaging project to achieve its objectives in describing cross-sectional and longitudinal structural brain changes in ALS and assessing the value of MRI metrics as potential biomarkers.

An ideal ALS study should not only include prevalence but also an incidence cohort. An incidence cohort is essential for development of diagnostic aids (Chapter 5). Brain changes presented by a prevalence cohort may be too widespread and may mask the subtle changes associated with early-phase disease. In contrast, a pure prevalence cohort provides the opportunity to develop monitoring markers for the course ALS (Chapter 4).
The first scan should be performed shortly after diagnosis. This is essential to describe the initial brain changes. If possible studies should include presymptomatic cohorts, if ethics approval and formal genetic counselling is available. It is especially difficult to screen family members for gene muta-

tions, where penetrance, clinical ramifications and molecular biology is poorly understood.
Multiple assessments are required to capture a suspected non-linear radiological decline. Based on the available literature, the interval for follow-up assessments in an ALS study should be approximately 4 months in order to capture patients with faster rate of decline. Nonetheless, a drop-out rate of 20% per time point is to be expected (Table 2.4).

	Attrition rate after			
	3 months	**6 months**	**8-9 months**	**12 months**
mean	16.4%	12.5%	17.1%	36.7%
median	34.0%	38.0%	0%	55.0%
SD	48.1%	19.5%	26.0%	17.3%
available studies	2	5	3	5

Table 2.4: Attrition rate of longitudinal studies in ALS. SD = standard deviation.

At each MRI time-point, the clinical assessment should be carefully recorded. During the first assessment this includes site of onset (bulbar/ spinal/ respiratory), medication, a detailed family history and genotype. Subsequently, clinical progression and change in medications should be documented at each follow-up scan. Some medications may potentially influence MRI measurements - especially resting-state MRI - and should, therefore, be carefully documented. Neuropsychological assessments should be performed close to the MR acquisition. To investigate the prognostic value of MRI measures, clinical data should be continued to be gathered after the MRI scanning is no longer feasible due to respiratory failure or orthopnoea.

Ideally, multiple MR sequences should be included in the imaging protocol in order to comprehensively characterise white and grey matter alterations and to compare the sensitivity of the different approaches.
Healthy controls should undergo the same procedure as the patient cohort including multiple brain scans: at the first MRI time-point, a detailed med-

ical and family history should be recorded. At the subsequent time-points, change in medications needs to be enquired. It has been demonstrated that a healthy brain changes after only one year (Fjell et al., 2013a,b). Follow-up assessments of healthy controls enhance the evaluation of disease-related longitudinal changes, as the effect of healthy ageing can be regressed out of the analysis. Hence, the sample size requirement to detect longitudinal brain changes decreases. Inclusion of disease-controls or mimic neurodegenerative conditions may improve the accurate characterisation of disease-specific processes.

2.8 Methodology of the present project

2.8.1 Ethical approval

The imaging study was fully approved by Beaumont Hospital ethics committee. Informed consent was obtained from each participant.

2.8.2 Recruitment of participants

Patients were recruited through the Irish population-based ALS register (Donaghy et al., 2009; Rooney et al., 2013).
A group of neurologically healthy age- and gender-matched controls were recruited from spouses of ALS patients, unrelated family friends and though public advertising in accordance with the inclusion and exclusion criteria of the study.

2.8.3 Inclusion Criteria

Patients with a diagnosis of Motor Neuron Disease who are recorded in the Irish population-based ALS register were eligible.

2.8.4 Exclusion Criteria

Patients with a co-morbid diagnosis of any other neurodegenerative conditions (apart from frontotemporal dementia) or structural brain disease (e.g. stroke) were excluded. Controls with a family history of ALS or other neurodegenerative conditions were also excluded.

2.9 Data acquisition

2.9.1 Demographic and clinical data

For each participant the following demographic information were recorded: date of birth, gender, handedness, education, list of medications, family history of neurodegenerative disease (motor neuron disease, Parkinson's disease, Alzheimer's disease, frontotemporal dementia, Huntington's disease, multiple sclerosis). Additionally, for each patients the following clinical details were recorded: date and site of symptom onset, date of diagnosis, use of Riluzole, the presence of an enteral feeding tube, use of non-invasive ventilation (NIV), revised ALS functional rating scale (ALSFRS-R, Cedarbaum et al., 1999) at the date of the scan.

Statistical analysis of demographic and clinical data was conducted using t-test or analysis of variance (ANOVA). The assumption of normality and outliers were visually evaluated through histograms and boxplots of the corresponding data and statistically by using the Kolmogorov-Smirnov Test.

2.9.2 MRI acquisition

Each brain scan included a T1-weighted images, diffusion weighted images, resting-state MRI and a FLAIR imaging. Flair sequences were utilised to identify and exclude participants with severe white matter disease. MR data were acquired on a 3 Tesla Philips Achieva system with a gradient strength of 80 mT/m and slew rate of 200 T/m/s using an 8-channel receive-only head

coil.

T1-weighted images were obtained using a three-dimensional inversion recovery prepared spoiled gradient recalled echo (IR-SPGR) sequence with FOV: FH = 256 mm, AP = 256 mm, RL = 160 mm; Fast Imaging mode = TFE; TR = 8.5 ms; Rel. SNR = 0.864685357; Act. TR/TE = 8.5 ms / 3.9 ms; ACQ matrix M × P = 256 × 240; ACQ voxel MPS = 1.00 mm / 1.07 mm / 1.00 mm. The total scan duration was 07:32.1 min.

DTI images were acquired using a spin-echo planar imaging (SE-EPI) sequence with a 32-direction Stejskal-Tanner diffusion encoding scheme: FOV: RL = 245 mm, AP = 245 mm, FH = 150 mm; ACQ voxel size: RL = 2.5 mm, AP = 2.5 mm; slice thickness = 2.5 mm; reconstruction matrix = 112; P reduction (AP) = 2.5; TE = 59 ms; b-values = 0, 1100 s/mm^2; with SPIR fat suppression and dynamic stabilisation in an acquisition time of 5:27.8 min.

2.10 MRI database - Final Sample

For this PhD project, participants were recruited and scanned between the 29.04.2014 until the 07.06.2016 (Table 2.5). Imaging data of 38 ALS patients and 43 controls were also included in this study, which were acquired prior to the start of this research project.

Table 2.6 summaries the basic demographic and clinical data of this sample. Please note, each chapter described the sample available to the date of the analysis and additional exclusion criteria if applicable.

	ALS patients			
	Baseline	**FU 1**	**FU 2**	**FU 3**
Newly recruited	86	56	41	24
Existing data	38	14		
Total	124	70	41	24

	Healthy controls			
	Baseline	**FU 1**	**FU 2**	**FU 3**
Newly recruited	26	18	14	8
Existing data	43			
Total	69	18	14	8

Table 2.5: Newly acquired MRI scans acquired between 2014 and 2016. FU: Follow-up

	ALS patients	**Healthy controls**	**p-value**
N	124	69	
Age in years (mean/SD)	59.1 (11.1)	60.0 (9.9)	p = .57
Gender (male/female)	78/ 46	34/ 35	p = .09
Handedness (right/left)	107/ 17	64/ 5	p = .17
Site of onset (bulbar/ spinal/ respiratory/ cognition)	31/ 91/ 1/ 1		
Disease duration in months at first scan (mean/SD)	27.1 (20.6)		
ALSFRS-R at first scan (mean/ SD)	37.4 (7.6)		

Table 2.6: Demographic and clinical profile of the sample at the time of the first brain scan.

2.11 List of reviewed articles

The papers identified by the search criteria cited above (section 2.4) are listed here. These papers were systematically reviewed to draw conclusions about an optimal longitudinal study design in neurodegeneration.

Longitudinal studies in Alzheimer's Disease		
2012	Lehmann et al.	Alzheimers Dement
2012	Li et al.	Neurobiol Aging
2012	Lo et al.	Neurology
2012	McDonald et al.	Neurobiol Aging
2012	Okonkwo et al.	Neurology
2012	Ossenkoppele et al.	Eur J Nucl Med Mol Imaging
2012	Silbert et al.	Neurology
2012	Spulber et al.	Curr Alzheimer Res
2012	Stricker et al.	Brain Imaging and Behavior
2012	Vidoni et al	Neurobiol Aging
2012	Wang et al.	Alzheimer Dis Assoc Disord
2012	Yao et al.	PLoS One
2012	Zhang et al.	PloS One
2011	Bai et al.	J Alzheimers Dis
2011	Duara et al.	Am J Geriatr Psychiatry
2011	Farzan et al.	Diagn Pathol
2011	Honea et al.	Neurology
2011	Knight et al.	Neurobiol Aging
2011	Kume et al.	J Neurol
2011	Li et al.	Neuroradiology
2011	Lo et al.	Arch Neurol
2011	McEvoy et al.	Radiology
2011	Sabuncu et al.	Arch Neurol
2011	Skup et al.	Neuroimage
2011	Teipel et al.	World J Biol Psychiatry
2011	Villemagne et al.	Ann Neurol

2010	Carmichael et al.	Arch Neurol
2010	Fjell et al.	J Neurosci
2010	Goos et al.	Neurology
2010	Hanyu et al.	J Neurol Sci
2010	Ho et al.	Hum Brain Mapp
2010	Hua et al.	Neurobiol Aging
2010	Hua et al.	NeuroImage
2010	Marcus et al.	J Cogn Neurosci
2010	Risacher et al.	Neurobiol Aging
2010	Sluimer et al.	Neurobiol Aging
2010	Stoub et al.	Neurobiol Aging
2010	Teipel et al	J Alzheimers Dis
2010	Tosun et al.	Neurobiol Aging
2009	Apostolova et al.	Neurobiol Aging
2009	Davatzikos et al.	Brain
2009	Fouquet et al.	Brain
2009	Hua et al.	NeuroImage
2009	Jack et al.	Brain
2009	Leow et al.	NeuroImage
2009	McDonald et al.	Neurology
2009	Misra et al.	NeuroImage
2008	Barnes et al.	Neurobiol Aging
2008	Carlson et al	Neurology
2008	Chételat et al.	Neuropsychologia
2008	Hall et al.	Alzheimers Dement
2008	Hanya et al.	Eur J Nucl Med Mol Imaging
2008	Qiu et al.	NeuroImage
2008	Ridha et al.	J Neurol
2008	Schott et al.	Neuropsychologia
2008	Silbert et al.	Neurology
2008	Sluimer et al.	Radiology
2007	Carmichael et al.	Alzheimer Dis Assoc Disord
2007	Chen et al.	Am J Psychiatry

2007	de Leon et al.	J Neurol
2006	de Leon et al.	Neurobiol Aging
2006	Ridha et al.	Lancet Neurol
2005	Barnes et al.	Dement Geriatr Cogn Disord
2005	Chételat et al.	Neuroimage
2005	Fotenos et al	Neurology
2005	Godbolt et al.	Neurocase
2005	Kaye et al.	J Alzheimers Dis
2005	Mungas et al.	Neurology
2005	Schott et al.	Neurology
2005	Stoub et al.	Neurology
2004	Adak et al.	Neurology
2004	Ezekiel et al.	Alzheimer Dis Assoc Disord
2003	Cardenas et al.	Neurobiol Aging
2003	Chan et al.	Lancet
2003	Drzezga et al.	Eur J Nucl Med Mol Imaging
2003	Sakamoto et al.	J Neuroimaging
2003	Thompson et al.	J Neurosci
2003	Tonini et al.	Neurol Sci
2003	Wang et al.	NeuroImage
2002	Bradley et al.	Br J Radiol
2002	de Leon et al.	Neurosci Lett
2002	Matsuda et al.	J Nucl Med
2002	Mori et al.	Ann Neurol
2001	Whitwell et al.	AJNR Am J Neuroradiol
2000	Adalsteinsson et al.	Lancet
2000	Jack et al.	Neurology
2000	Kogure et al.	Ann Neurol
2000	Laakso et al.	Biol Psychiatry
1999	Wahlund et al.	Dement Geriatr Cogn Disord
1999	Wahlund et al.	Dement Geriatr Cogn Disord
1998	Fox et al.	Brain
1998	Lehtovirta et al.	J Nucl Med

1997	Sachdev et al.	J Neurol Neurosurg Psychiatry
1996	Brown et al.	Psychiatry Res
1996	Fox et al.	Ann N Y Acad Sci
1996	Fox et al.	Brain
1992	Smith et al.	Arch Neurol
1990	Haxby et al.	Arch Neurol

Longitudinal studies in Amyotrophic Lateral Sclerosis

2014	Menke et al.	Brain
2014	Verstraete et al.	Hum Brain Mapp
2013	Kwan et al.	NeuroImage: Clinical
2012	Keil et al.	BMC Neurosci
2012	Menke et al.	Arch Neurol
2012	Verstraete et al.	J Neurol Neurosurg Psychiatry
2011	van der Graaff et al.	Brain
2011	Zhang et al.	Amyotrophic Lateral Sclerosis
2009	Agosta et al.	Amyotrophic Lateral Sclerosis
2009	Agosta et al.	J Neurol Neurosurg Psychiatry
2009	Avants et al.	Archives of Neurology
2009	Nickerson et al.	Clin Neuroradiol
2007	Blain et al.	Amyotrophic Lateral Sclerosis
2007	Unrath et al.	J Neurol
2004	Rule et al.	Amyotroph Lateral Scler Other Motor Neuron Disord
2002	Suhy et al.	Neurology
2001	Hecht et al.	Journal of the Neurological Sciences
1998	Block et al.	Arch Neurol

Longitudinal studies in Frontotemporal Dementia

2013	Brodtmann	BMJ case reports
2013	Caso et al.	Behav Neurol
2013	Lu et al.	Dement Geriatr Cogn Disord
2012	Frings et al.	Human Brain Mapping

2012	Rohrer et al	J Alzheimers Dis
2010	Gordon et al.	NeuroImage
2010	Krueger et al.	Alzheimer Dis Assoc Disord
2010	Rohrer et al.	NeuroImage
2009	Knopman et al.	Neurology
2008	Czarnecki et al	Arch Neurol
2008	McKinnon et al.	Journal of Cognitive Neuroscience
2008	Rohrer et al.	Neurology
2008	Rohrer et al.	Nat Clin Pract Neurol
2008	Whitwell et al.	NeuroImage
2007	Brambati et al.	NeuroImage
2007	Diehl-Schmid et al.	Neurobiology of Aging
2004	Whitwell et al.	Dement Geriatr Cogn Disord
1999	Gregory et al.	Neuropsychiatry Neuropsychol Behav Neurol

Longitudinal studies in Huntington's Disease

2013	Tabrizi et al.	Lancet Neurol
2013	van den Bogaard et al.	AJNR Am J Neuroradiol
2012	Tabrizi et al.	Lancet Neurol
2011	Majid et al.	Mov Disord
2011	Tabizi et al.	Lancet Neurol
2011	Majid et al.	Mov Disord
2011	Wolf et al.	Experimental Neurology
2011	Rosas et al.	Mov Disord
2011	Awylard et al.	J Neurol Neurosurg Psychiatry
2010	Hobbs et al.	J Neurol Neurosurg Psychiartry
2010	Hobbs et al.	AJNR Am J Neuroradiol
2010	Sritharan et al.	J Neurol Neurosurg Psychiatry
2009	Weaver et al.	Experimental Neurology
2009	Vandenberghe et al.	J Neurol
2009	Squitieri et al.	CNS Neurosci Ther
2008	Ruocco et al.	J Neurol Neurosurg Psychiatry

2006	Henley et al.	Neurology
2004	Kipps et al.	J Neurol Neurosurg Psychiatry
2004	Aylward et al.	Neurology
2000	Aylward et al.	Movement Disorders
1997	Aylward et al.	Neurology

Longitudinal studies in Multiple Sclerosis

2014	Chen et al.	Radiology
2014	Gabilondo et al.	Ann Neurol
2014	Sumowski et al.	Neurology
2014	Walsh et al.	Radiology
2013	Bove et al.	BMC Neurology
2013	Calabrese et al.	Ann Neurol
2013	Calabrese et al.	Mult Scler
2013	Filippi et al.	Neurology
2013	Ikonomidou et al.	Mult Scler
2013	Perez-Miralles et al.	Mult Scler
2013	Popescu et al.	J Neurol Neurosurg Psychiatry
2013	Velez et al.	PLoS One
2012	Bendtfeldt et al.	Hum Brain Mapp
2012	Calabrese et al.	AJNR Am J Neuroradiol
2012	Calabrese et al.	J Neurol Neurosurg Psychiatry
2012	Hayton et al.	J Neurol
2012	Kalincik et al.	PLoS One
2012	Lebrun et al	Mult Scler
2012	Moodie et al.	J Neurol Sci
2012	Mowry et al.	Ann Neurol
2012	Orbach et al.	PLoS One
2012	Rigotti et al.	Neurology
2012	Sämann et al.	AJNR Am J Neuroradiol
2012	Teunissen et al.	Mult Scler
2012	Tian et al.	Neuroradiology
2012	Tourdias et al.	Radiology

2012	Vaneckova et al	Eur Neurol
2011	Calabrese et al.	Neurology
2011	Carabrese et al.	Radiology
2011	Deloire et al.	Neurology
2011	Fox et al.	AJNR Am J Neuroradiol
2011	Harrison et al.	Neurology
2011	Liguori et al.	J Neurol Neurosurg Psychiatry
2011	Liguori et al.	Genes Immun
2011	Loizou et al.	IEEE Trans Inf Technol Biomed
2011	Mesaros et al.	AJNR Am J Neuroradiol
2011	Sormani et al.	PLoS One
2010	Bendfeldt et al.	Hum Brain Mapp
2010	Calabrese et al.	Ann Neurol
2010	Coret et al.	Mult Scler
2010	Davis et al.	Neurology
2010	de Stefano et al.	Ann Neurol
2010	Di Filippo et al.	J Neurol Neurosurg Psychiatry
2010	Freund et al.	Mult Scler
2010	Furby et al	J Neurol
2010	Giorgio et al.	J Magn Reson Imaging
2010	Horakova et al.	Folia Biol
2010	Martola et al.	Neuroradiology
2010	Mesaros et al.	Mult Scler
2010	Raz et al.	Radiology
2010	van den Elskamp et al.	Neuroradiology
2010	Wattamwar et al.	J Neurol Sci
2010	Zhang et al.	J Neurol Sci
2009	Bellmann-Strobl et al.	Neurology
2009	Bellmann-Strobl et al.	Eur Radiol
2009	Bendfeldt et al.	NeuroImage
2009	Calabrese et al.	Neurology
2009	Calabrese et al.	Mult Scler
2009	Daumer et al.	Neurology

2009	Gauthier et al.	Arch Neurol
2009	Healy et al	Arch Neurol
2009	Healy et al	J Neurol Neurosurg Psychiatry
2009	Liguori et al.	Brain Res
2009	Martola et al.	Acta Radiol
2009	Neema et al.	J Neuroimaging
2009	Nielsen et al.	BMC Neurology
2009	Okuda et al.	Neurology
2009	Roosendaal et al.	Mult Scler
2009	Rudick et al.	J Neurol Sci
2009	Sampat et al.	AJNR Am J Neuroradiol
2009	Sormani et al.	Neurology
2009	Zhang et al.	NeuroImage
2008	Calabrese et al.	Neuroiamge
2008	Fisher et al.	Ann Neurol
2008	Fisniku et al.	Brain
2008	Jacobi et al.	Eur J Neurol
2008	Kezele et al.	Mult Scler
2008	Khaleeli et al.	Ann Neurol
2008	Perumal et al.	J Neurol
2008	Rashid et al.	J Neurol
2008	Rovaris et al.	J Neurol
2007	Agosta et al.	Brain
2007	Audoin et al.	Mult Scler
2007	Davies et al.	Mult Scler
2007	Garaci et al.	AJNR Am J Neuroradiol
2007	Juha et al.	J Neurol Neurosurg Psychiatry
2007	Khaleeli et al.	J Neurol Neurosurg Psychiatry
2007	Manfredonia et al.	Arch Neurol
2007	Rashid et al.	Mult Scler
2006	Audoin et al.	J Neurol
2006	Carbonell-Caballero et al	MAGMA
2006	Rashid et al.	J Neurol Neurosurg Psychiatry

2006	Richert et al	Neurology
2006	Rudick et al.	Ann Neurol
2005	Bielekova et al.	Neurology
2005	Ingle et al.	J Neurol Neurosurg Psychiatry
2005	Koziol et al.	J Clin Neuroscience
2005	Marrie et al.	J Neurol Sci
2005	Oreja-Guevara et al.	Arch Neurol
2005	Sastre-Garriga et al.	Brain
2005	Sastre-Garriga et al.	Neurology
2005	Tiberio et al.	Neurology
2005	Valsasina et al.	Neurology
2004	Cassol et al.	Mult Scler
2004	Chard et al.	Mult Scler
2004	Enzinger et al.	Ann Neurol
2004	Kallmann et al.	J Neurol
2004	Weißet al.	Mult Scler
2004	Wuerfel et al.	Brain
2004	Zwemmer et al.	Mult Scler
2003	Charil et al.	Neuroimage
2003	Cotton et al.	Neurology
2003	Ingle et al.	Brain
2003	van Veen et al.	J Neuroimmunol
2002	Brex et al.	N Engl J Med
2002	Caramia et al.	Magn Reson Imaging
2002	Kalkers et al.	Arch Neurol
2002	Tan et al.	AJNR Am J Neuroradiol
2001	Pelletier et al.	Arch Neurol
2001	Sperling et al.	Arch Neurol
2001	Zivadinov et al.	J Neurol Neurosurg Psychiatry
2000	Bagnato et al.	Mult Scler
2000	Brex et al.	Neurology
2000	Catalaa et al.	Radiology
2000	Filippi et al.	Neurology

2000	Ge et al.	Radiology
2000	Luks et al.	Mult Scler
2000	Mohr et al.	Neurology
2000	Pike et al.	Radiology
2000	Saindane et al.	Neurology
2000	Simon et al.	Neurology
1999	Blinkenberg et al.	Neurology
1999	Fulton et al.	AJNR Am J Neuroradiol
1999	Kappos et al.	Lancet
1999	Lee et al.	Brain
1999	Mainero et al.	J Neurol
1999	Mastronardo et al.	AJNR Am J Neuroradiol
1999	Miki et al.	Radiology
1999	Simon et al.	Neurology
1998	De Stefano et al.	Brain
1998	Dousset et al.	Neurology
1998	Fu et al.	Brain
1998	Molyneux et al.	Ann Neurol
1998	Narayana et al.	Ann Neurol
1998	Stevenson et al.	Neurology
1998	van Waesberghe et al.	AJNR Am J Neuroradiol
1997	De Stefano et al.	Neurology
1997	Filippi et al.	J Neuroimaging
1996	Filippi et al.	J Neurol Sci
1996	Kidd et al.	J Neurol Neurosurg Psychiatry
1994	Arnold et al.	Ann Neurol
1994	Frank et al.	Ann Neurol
1994	Khoury et al.	Neurology
1992	Feinstein et al.	J Neurol Neurosurg Psychiatry
1991	Harris et al.	Ann Neurol
1990	Baum et al.	Acta Neurol Scand

Longitudinal studies in Parkinson's Disease

2013	Compta et al	Parkinsonism Relat Disord
2013	Song et al	Parkinsonism Relat Disord
2013	Ulla et al	PLoS One
2012	Baba et al	Brain
2012	Ibarretxe-Bilbao et al	Mov Disord
2011	Camicioli et al	Mov Disord
2011	de la Fuente-Fernández	Ann Neurol
2011	Gallagher et al	Mov Disord
2011	Gallagher et al	Brain Imaging Behav
2011	Nandhagopal et al	Brain
2011	Pavese	NeuroImage
2010	Tang et al	J Neurosci
2009	Brück et al	Mov Disord
2009	Lewis et al	Eur J Neurol
2009	Marshall et al	Mov Disord
2009	Nandhagopal et al	Brain
2009	Osaki et al	Mov Disord
2007	Brenneis et al	J Neurol
2006	Burton et al	Am J Geriatr Psychiatry
2005	Hilker et al.	Arch Neurol
2005	Ramírez-Ruiz et al	J Neurol
2004	Schwarz et al	J Nucl Med
2003	Kaasinen et al.	J Neural Transm
2003	Pirker et al.	Mov Disord
2001	Hu et al	J Neural Transm
1994	Vingerhoets et al.	Ann Neurol

Longitudinal studies in Ataxia

2014	Mascalchi et al.	PLOS One
2012	D'Abreu et al.	J Neuroimaging
2011	Horimoto et al.	J Neurol

Longitudinal studies in HIV Dementia

2014	Pfefferbaum et al.	Neurobiol Aging
2011	Lentz et al.	J Neurovirol
2009	Cardenas et al.	J Neurovirol
1998	Stout et al.	Arch Neurol
1996	Dooneief et al.	J NeuroAIDS
1993	Post et al.	Radiology

Longitudinal studies in Alcohol abuse/dependence and Wernicke studies

2014	Durazzo et al.	Addict Biol
2014	Kühn et al.	JAMA Psychiatry
2014	Segobin et al.	Alcohol Clin Exp Res
2012	Alhassoon	Alcohol Clin Exp Res
2007	Bartsch et al.	Brain
1995	Pfefferbaum et al.	Alcohol Clin Exp Res
1994	Shear et al.	Alcohol Clin Exp Res

Longitudinal studies in Healthy Ageing

2013	Desikan et al	AJNR Am J Neuroradiol
2013	Erten-Lyons et al.	JAMA Neurol
2013	Fjell et al.	J Neurosci
2013	Fjell et al.	Neurobiol Aging
2013	Liu et al.	NeuroImage
2013	Maillard et al.	AJNR Am J Neuroradiol
2013	Pfefferbaum et al.	NeuroImage
2013	Taki et al.	Hum Brain Mapp
2012	Cherbuin et al.	Neurology
2012	Clark et al.	Neurobiol Aging
2012	Driscoll	Plos One
2012	Driscoll et al.	Hum Brain Mapp
2012	Durazzo et al.	Alzheimer's Dementia
2012	Holland et al.	Hum Brain Mapp

2012	Maillard et al.	Neurology
2012	Samieri et al.	Neurology
2012	Thambisetty et al	NeuroImage
2011	Driscoll et al.	Neurobiol Aging
2011	Glodzik et al.	Neurobiol Aging
2011	Lu et al.	J Alzheimers Dis
2011	Sojkova et al.	Arch Neurol
2011	Taki et al.	Neuroradiology
2011	Taki et al.	NeuroImage
2011	Taki et al.	Neurobiol Aging
2010	Barrick et al.	NeuroImage
2010	Chiang et al.	Neurology
2010	Crivello et al.	NeuroImage
2010	Donix et al.	NeuroImage
2010	Raz et al.	NeuroImage
2009	Driscoll et al.	Neurology
2009	Fjell et al.	J Neurosci
2009	Okada et al.	Spine
2009	Silbert et al.	Neurology
2007	Kramer et al	Neuropsychology
2005	Raz et al.	Cereb Cortex
2004	Tisserand et al.	Cereb Cortex
2003	Liu et al.	NeuroImage
2003	Resnick et al.	J Neurosci
2003	Rusinek et al.	Radiology
2003	Scahill et al.	Arch Neurol
2000	Moffat et al	Neurology
2000	Ylikoski et al.	Acta Neurol Scand
1998	Mueller et al.	Neurology

Table 2.7: List of reviewed longitudinal studies in neurodegeneration.

Presymptomatic studies in Alzheimer's Disease		
2014	Fagan et al.	Sci Transl Med
2014	McDade et al.	Neurology
2014	Roussotte et al.	Neurobiol Aging
2013	Cash et al.	Neurology
2013	Chhatwal et al.	Neurology
2013	Lee et al.	J Neurol Neurosurg Psychiatry
2013	Quiroz et al.	J Neurol Neurosurg Psychiatry
2013	Ryan et al.	Brain
2013	Sala-Llonch et al.	J Alzheimers Dis
2012	Fleisher et al.	Lancet Neurol
2012	Jagust et al.	J Neurosci
2012	Okonkwo et al.	Neurology
2012	Saint-Aubert et al.	J Alzheimers Dis
2011	Apostolova et al.	Dement Geriatr Cog Disord
2011	Johnson et al.	Alzheimers Dement
2011	Knight et al	Brain
2011	Knight et al	Neurobiolog Aging
2011	Lu et al.	J Alzheimers Dis
2010	Bendlin et al.	Alzheimers Dement
2010	Donix et al.	Am J Psychiatry
2010	Fortea et al.	J Alzheimers Dis
2010	Ringman et al.	J Neurol
2007	Klunk et al.	J Neurosci
2007	Ringman et al.	Brain
2006	Godbolt et al.	Neurocase
2006	Mosconi et al.	J Nucl Med
2006	Ridha et al.	Lancet Neurol
2005	Reiman et al.	Proc Natl Acad Sci USA
2003	Almkvist et al	Acta neurol Scand Suppl
2001	Johnson et al.	Neurology
1999	Wahlund et al.	Dement Geriatr Cogn Disord

Presymptomatic studies in Amyotrophic Lateral Sclerosis		
2011	Carew et al.	Neurology
2010	Vucic et al.	Clin Neurophysiol
2008	Ng et al.	J Magn Reson Imaging
2008	Vucic et al.	Brain
2005	Turner et al.	Brain
2002	Aggarwal et al.	J Neurol Neurosurg Psychiatry
2001	Aggarwal et al.	J Neurol Neurosurg Psychiatry

Presymptomatic studies in Frontotemporal Dementia		
2014	Dopper et al.	Neurology
2013	Jacova et al.	Neurology
2013	McDade et al.	J Neuroimaging
2013	Premi et al.	PloS One
2012	Lunau et al.	BMJ Open
2011	Pietroboni et al.	J Alzheimers Dis
2010	Miyoshi et al.	Parkinsonism Relat Disord
2009	Eskildsen et al.	Neuroimage
2009	Rohrer et al.	Dement Geriatr Cogn Disord
2008	Borroni et al.	Rejuvenation Res.
2008	Rohrer et al.	Nat Clin Pract Neurol
2008	Spina et al.	Brain
2007	Arvanitakis et al.	Parkinsonism Relat Disord
2004	Alberici et al.	J Neurol Neurosurg Psychiatry

Presymptomatic studies in Huntington's Disease		
2014	Phillips et al.	Cereb Cortex
2013	Dogan et al.	Neurodegener Dis
2013	Kincses et al.	Ideggyogy Sz
2013	Phillips et al.	PloS One
2013	Sanchez-Castaneda et al	Hum Brain Mapp

2013	Wolf et al.	Neurodegener Dis
2012	Ciarmiello et al.	Eur J Nucl Med Mol Imaging
2012	Di Paola et al.	Cereb Cortex
2011	Nopoulos et al.	Brain
2011	Panegyres et al.	J Neurol Sci
2011	Rizk-Jackson et al.	NeuroImage
2011	Wolf et al.	Exp Neurol
2011	Wolf et al.	J Cereb Blood Flow Metab
2010	Mandelli et al	AJNR Am J Neuroradiol
2009	Kloeppel et al.	Neurology
2009	Squitieri et al.	CNS Neurosci Ther
2007	Muehlau et al.	Mov Disord
2007	Tai et al.	Brain
2006	Ciarmiello et al.	J Nucl Med
2006	Rosas et al.	Mov Disord
2005	Reynolds et al.	Brain Res
2005	Rosas et al.	Neurology
2001	Feigin et al.	J Nucl Med
2000	Aylward et al.	Mov Disord
1999	Andrews et al.	Brain
1999	Harris et al.	Brain
1999	Sanchez-Pernaute et al.	Neurology
1998	Antonini et al.	Ann Neurol
1998	Campodonico et al	J Int Neuropsychol Soc
1996	Antonini et al.	Brain
1996	Aylward et al.	Arch Neurol
1994	Sedvall et al.	Eur Arch Psychiatry Clin Neurosci

Presymptomatic studies in Parkinson's Disease

2014	Thaler al al.	Mov Disord
2013	Sierra et al.	Neurology
2013	Szamosi et al	Neurodegenerative Dis
2012	Shi et al.	Neurobiol Aging

2011	Brockmann et al.	Mov Disord
2010	Eggers et al.	Neurology
2010	Pavese et al.	Exp Neurol
2010	Reetz et al.	Neurobio. Dis
2010	Sossi et al	Mov Disord
2009	Pavese et al.	Mov Disord
2008	Nandhagopal et al.	Neurology
2007	Hagenah et al.	J Neurol
2005	Adams et al.	Brain
2002	Hilker et al.	Neurosci Lett
2002	Khan et al.	Ann Neurol
2002	Khan et al.	Brain
2001	Hilker et al.	Ann Neurol
Presymptomatic studies in Ataxia		
2013	Jacobi et al.	Lancet Neurology
2013	Wang et al.	Mov Disord

Table 2.8: List of reviewed presymptomatic studies in neurodegeneration.

Chapter 3

The Segmental Diffusivity Profile of ALS-associated White Matter Degeneration

A concise version of this chapter has been published in the peer-reviewed European Journal of Neurology (Schuster et al., 2016a).

3.1 Introduction

Clinical trials in ALS mostly rely on survival and clinical rating scales as their primary end-points as no objective monitoring biomarkers have been validated to date. Despite considerable advances in ALS imaging (Bede and Hardiman, 2014; Schuster et al., 2015) the diagnosis of ALS remains primarily clinical. Diagnostic delay in ALS has crucial implications for belated recruitment to pharmaceutical trials (Zoccolella et al., 2006), unnecessary interventions (Cellura et al., 2012), and tardy introduction of neuroprotective therapy (Cellura et al., 2012). Longitudinal and presymptomatic studies suggest that considerable pathological change may have taken place by the time the diagnosis is established rendering neuroprotective therapy ineffective (Schuster et al., 2015; Eisen et al., 2014; Benatar and Wuu, 2012). While the urgency for biomarker development for diagnostic and monitoring purposes

in ALS is well recognised, sensitive biomarkers may also unveil patterns of anatomical spread and contribute to our understanding of cellular and molecular mechanisms.

Primary motor cortex (Bede et al., 2012a; Schuster et al., 2013) and corticospinal tract (CST, Bede et al., 2013a) pathology are the most extensively studied anatomical regions in ALS. Over 100 DTI studies have been published in ALS, most of which highlight CST and corpus callosum (CC) degeneration. Despite the significant number of imaging studies, striking inconsistencies can be identified in the literature (Bede and Hardiman 2014). While most ALS studies focus on CST degeneration in the posterior limb of the internal capsule (Menke et al., 2012), other key segments of the CST, such as the corona radiata (Ciccarelli et al., 2006) or cerebral peduncles (Hong et al., 2004) are surprisingly understudied. For the development of automated classifier-type analyses, it is pivotal to establish which segments of the CST best discriminate patients from controls and which diffusivity parameter is the most sensitive to capture early-stage neurodegeneration. While CST degeneration has been comprehensively characterised by numerous pathology studies (Smith, 1960), few neuroimaging studies investigated the segmental vulnerability of the CST *in vivo* (Toosy et al., 2003; Wong et al., 2007).

Corpus callosum degeneration has also been extensively evaluated in ALS by post-mortem studies (Smith, 1960) and genotype-based imaging studies (Bede et al., 2013a). Recent neuroimaging studies of ALS have focused on extra-motor involvement; characterising fronto-temporal (Schuster et al., 2014a), basal ganglia (Bede et al., 2013b), anterior cingulate (Woolley et al., 2011), cerebellar (Bede et al., 2015) pathology and have demonstrated network dysfunction of interconnected brain regions (Verstraete and Heuvel, 2010). With the emergence of automated classifier analyses (Chen et al., 2008; Wang and Summers, 2012), however, there is a renewed interest in the detailed characterisation of established, 'disease-defining' pathological sites, such as the CST.

CST degeneration in ALS is most commonly evaluated by diffusion weighted imaging (Bede et al., 2013a), but spectroscopy (Stagg et al., 2013), susceptibility - weighted imaging (Prell et al., 2015), white matter morphometry (Abrahams et al., 2005), connectivity analyses (Verstraete et al., 2014), fractal dimension analyses (Rajagopalan et al., 2013), functional approaches (Verstraete and Heuvel, 2010) and electrophysiological techniques, such as transcranial stimulation (TMS, Desiato et al., 2002) have also been utilised.

Despite the plethora of promising imaging and electrophysiological methods to assess CST integrity, diffusion weighted imaging remains one of the most reliable techniques with a number of analysis options to detect voxel-wise, tract-based, connectivity based or crossing fibre alterations. A number of diffusivity-derived, white matter integrity proxies are available, but no consensus exist as to which is the most sensitive to detect early CST degeneration in ALS. This is partly because the majority of studies continue to solely use fractional anisotropy (FA). The utility of other diffusivity measures, such as axial (AD) and radial diffusivity (RD), is increasingly recognised in ALS (Metwalli et al., 2010; Kasper et al., 2014). Importantly, these indices reflect on specific aspects of white matter microstructure. AD is generally regarded as an axonal marker (Sun et al., 2006; Budde et al., 2009), RD as a myelin related measure (Song et al., 2002, 2005). Fractional anisotropy and mean diffusivity (MD) are histologically less specific, yet sensitive composite markers of white matter integrity. While AD (λ_1) and RD ($(\lambda_2 + \lambda_3)/2$) are independent variables, MD is the mean of the three diffusion tensor eigenvalues λ_1, λ_2, λ_3. Additional DTI parameters such as volume ratio, relative anisotropy, linear component, planar component, spherical component are rarely utilised in ALS (Westin et al., 2002; Sundgren et al., 2004).

Corticobulbar and corticospinal tract degeneration are phenotype-defining features of ALS, yet these tracts are rarely examined separately and correlated with clinical disability. These tracts are relatively well separated in the internal capsule (IC) where corticobulbar tracts run in the genu of the IC

and corticospinal tracts run in the posterior limb of the IC in a somatotopic arrangement; representing the upper extremity, trunk, lower extremity in an anteromedial to posterolateral anatomical organisation (Lee et al., 2012).

Spastic speech, dysphagia, positive jaw-jerk, and pseudobulbar affect are some of the most frequently observed bulbar symptoms in ALS that can be directly linked to corticobulbar tract dysfunction.

The evaluation of the CST in the corona radiata offers another opportunity to examine somatotopically organised CST fibres and correlate white matter alterations to clinical disability. While previous neuroimaging studies of ALS linked motor disability to focal grey matter alterations in the precentral gyrus (Bede et al., 2012a; Mezzapesa et al., 2013; Schuster et al., 2013), this has not been replicated in white matter studies in the context of the functional architecture of the pyramidal tracts.

The main objective of this chapter is to evaluate the segmental vulnerability of CST and CC in order to assess which portions best discriminate patients and controls. A further aim of the study is to evaluate the sensitivity of various diffusivity measures in detecting ALS-associated white matter degeneration. Furthermore, the white matter signature of the main ALS phenotypes in the context of somatotopic anatomy was evaluated. Finally, clinical disability is correlated to white matter indices in anatomically-associated tracts.

3.2 Methods

3.2.1 Participants

Sixty-two ALS patients and 55 age-matched healthy controls were included in this study based on the following criteria: Participating ALS patients were diagnosed with either probable or definite ALS according to the revised El Escorial criteria (Brooks et al., 2000) and were negative for a compre-

hensive panel of established ALS-causing mutations, including *FUS*, *OPTN*, *SOD1*, *TARDBP*, *ANG*, *VAPB*, *VCP*, *SETX*, *ALS2* (Kenna et al., 2013). DNA samples were also screened by repeat-primed PCR for the presence of a GGGGCC hexanucleotide repeat expansion in *C9orf72*. Because of the significant imaging changes associated with this phenotype (Bede et al., 2013a), patients carrying the hexanucleotide expansion were excluded. Patients fulfilling the Rascovsky criteria for frontotemporal dementia (Rascovsky et al., 2011) were also excluded to avoid the confounding effect of imaging changes associated with comorbid frontotemporal dementia (Chang et al., 2005). Socio-demographic and clinical details of participating subjects are presented in Table 3.1.

3.2.2 Data pre-processing

Diffusion tensor imaging datasets underwent eddy current corrections, motion correction and brain-tissue extraction using FMRIB's software library (Smith et al., 2006, 2004). Subsequently, a diffusion tensor model was fitted, generating maps of fractional anisotropy (FA), mean diffusivity (MD), axial diffusivity (AD), and radial diffusivity (RD). Tract-based spatial statistics (TBSS, Smith et al., 2006) and permutation-based nonparametric inference was used for group comparisons in a study-specific white matter template applying the threshold-free cluster enhancement (TFCE) method (Salimi-Khorshidi et al., 2011).

Grey matter analyses were carried out using voxel based morphometry using the VBM tool in FSL (Douaud et al., 2007). Following brain extraction, and tissue-type segmentation, grey matter partial volume images were aligned to the Montreal Neurological Institute 152 standard space. The grey matter partial volume estimates were non-linearly co-registered to a study-specific template, modulated by a Jacobian field warp and smoothed with an isotropic Gaussian kernel with a sigma of 3 mm. A grey matter region of interest (ROI) was created based on the Harvard-Oxford probabilistic atlas

	ALS	**HC**	**p-value**	**Bulbar onset**	**Spinal onset**	**p-value**
N	62	55		26	36	
Gender (male/female)	36/26	29/26	$p = .56$	11/15	25/11	$p = .1$*
Age, years (mean/SD)	61.1 (9.7)	61.3 (8.5)	$p = .92$	62.3 (8.5)	60.3 (10.5)	$p = .7$*
Handedness (right/left)	55/7	52/3	$p = .26$	23/3	32/4	$p = .53$*
Disease duration, months (mean/SD)	30.3 (18.3)			25.4 (14.8)	33.8 (19.9)	$p = .07$
ALSFRS-R (mean, SD) (max 48)	35.5 (6.6)			36.3 (6.9)	34.9 (6.4)	$p = .41$
Bulbar subscore (mean, SD) (max 12)	8.7 (3.1)			6 (2.3)	10.7 (1.8)	$p < .01$
Spinal subscore (mean, SD) (max 24)	15.8 (6)			19.6 (4.7)	13.1 (5.4)	$p < .01$

Table 3.1: Demographic profile of participants. *comparison of HC vs bulbar onset/ spinal onset patients

for the motor cortex (Desikan et al., 2006). A voxel-wise generalised linear model was utilised for permutations-based non-parametric testing within this ROI 10,000 permutations (Winkler et al., 2014).

3.2.3 Statistical analyses

1. Whole-brain group comparisons were carried out between patients and healthy controls for the four diffusivity measures FA, MD, RD, and AD correcting for age and gender. The significance level was set at $p < .05$ corrected for multiple comparisons using family-wise error (FWE) and also visualised at $p < .01$ for FA and RD (Figure 3.1).

2. In order to explore the selective vulnerability of CST and CC, the CST was segmented into the superior corona radiata, inferior corona radiata, internal capsule, cerebral peduncle (mesencephalic crus) and the CC into the splenium, body and genu. These regions were defined using the Johns Hopkins University DTI-based white-matter atlas (JHU ICBM-DTI-81 white-matter labels atlas, Oishi et al., 2008). This atlas consists of 48 white matter tract labels created from the manual segmentation of DTI maps from 81 subjects. It does not include the lateral fibres of the corona radiata, therefore, this label was created manually. Figure 3.2 and Figure 3.3 shown the labels and the results.

   The white matter regions identified by the above whole-brain TBSS analyses, exhibiting significant alterations of FA and RD ($p < .01$ FWE) were anatomically segmented with the JHU labels and individual subject diffusivity data were extracted. The segmental diffusivity profile of study-groups was displayed in boxplots (Figure 3.2 and Figure 3.3).

3. The percentage change between patients and controls in the most relevant white matter segments was calculated. First, the average diffu-

sivity alterations was calculated in each white matter segment for all four DTI indices (Figure 3.4). Subsequently, diffusivity values were extracted from voxels in the relevant white matter segments which demonstrated intergroup differences in analysis 1 ($p < .05$, FWE; Figure 3.5).

4. Pyramidal tract involvement in bulbar and spinal onset patients was compared using ROI analyses restricted to the CST. Patients were stratified based on the site of symptom onset, and tract-based DTI analyses were conducted in comparison to healthy controls correcting for age and gender. Statistical significance was defined as $p < .05$ (FWE). To highlight the corresponding phenotype-specific grey matter degeneration, voxel-based morphometry analyses were also performed among the same study groups in the motor cortex adjusting for age and gender (Figure 3.6).

5. Additional correlative analyses were carried out between clinical variables and radial diffusivity values of individual patients in the corona radiata. Bulbar scores were defined as the sum of scores on questions 1-3 of the ALSFRS-R (max = 12) and spinal scores defined as the sum of scores on questions 4-9 (max = 24). The design matrix included age as a nuisance variable. The significance level was set to $p < .05$, FWE (Figure 3.7 and Figure 3.8).

3.3 Results

3.3.1 Whole-brain diffusivity analyses

Tract-based statistics over the entire brain revealed significant RD, MD and FA alterations in patients in comparison to controls at $p < .05$ (FWE). While FA and RD captured bilateral CST changes from the corona radiata to the brain stem, MD only revealed unilateral changes in the right hemisphere.

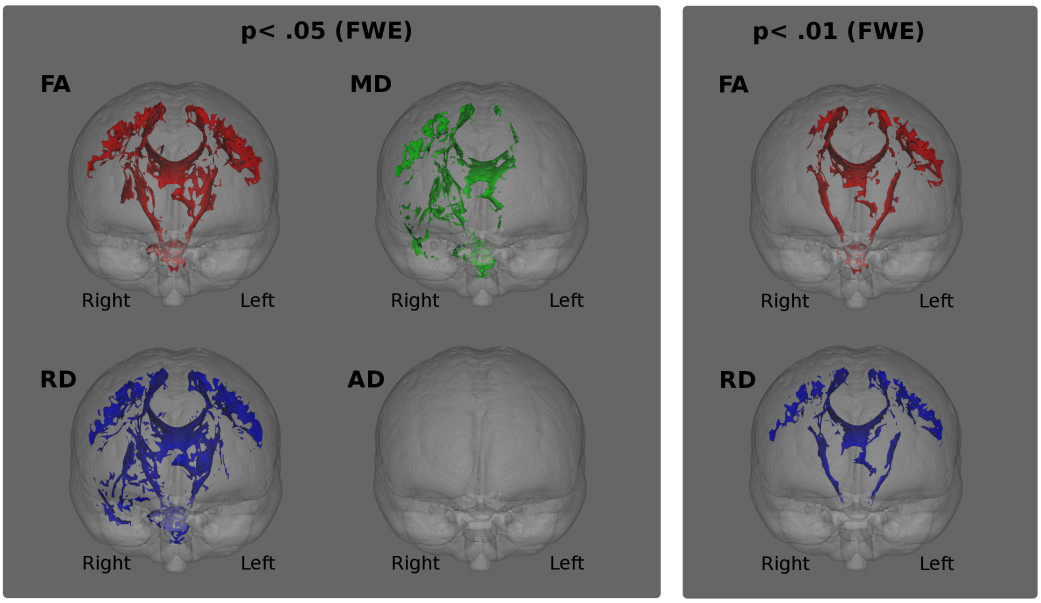

Figure 3.1: The sensitivity profile of diffusivity indices in capturing ALS-associated white matter degeneration. Fractional anisotropy (FA) alterations are displayed in red, radial diffusivity (RD) in blue, mean diffusivity (MD) in green.

Using a more stringent statistical threshold of $p < .01$ (FWE), the symmetrical CST alterations highlighted by RD remained significant; alterations highlighted by FA were more pronounced on the left side and no significant change was detected by MD (Figure 3.1). Degeneration of the fibres within the right temporal lobe was highlighted by MD and RD at $p < .05$ (FWE).

3.3.2 Individual patient data

The segmental evaluation of the CST and the CC using FA or RD demonstrated discriminating diffusivity profiles in patients and controls in the corona radiata, internal capsule, cerebral peduncle, and body of the corpus callosum (Figure 3.2 for FA and Figure 3.3 for RD).

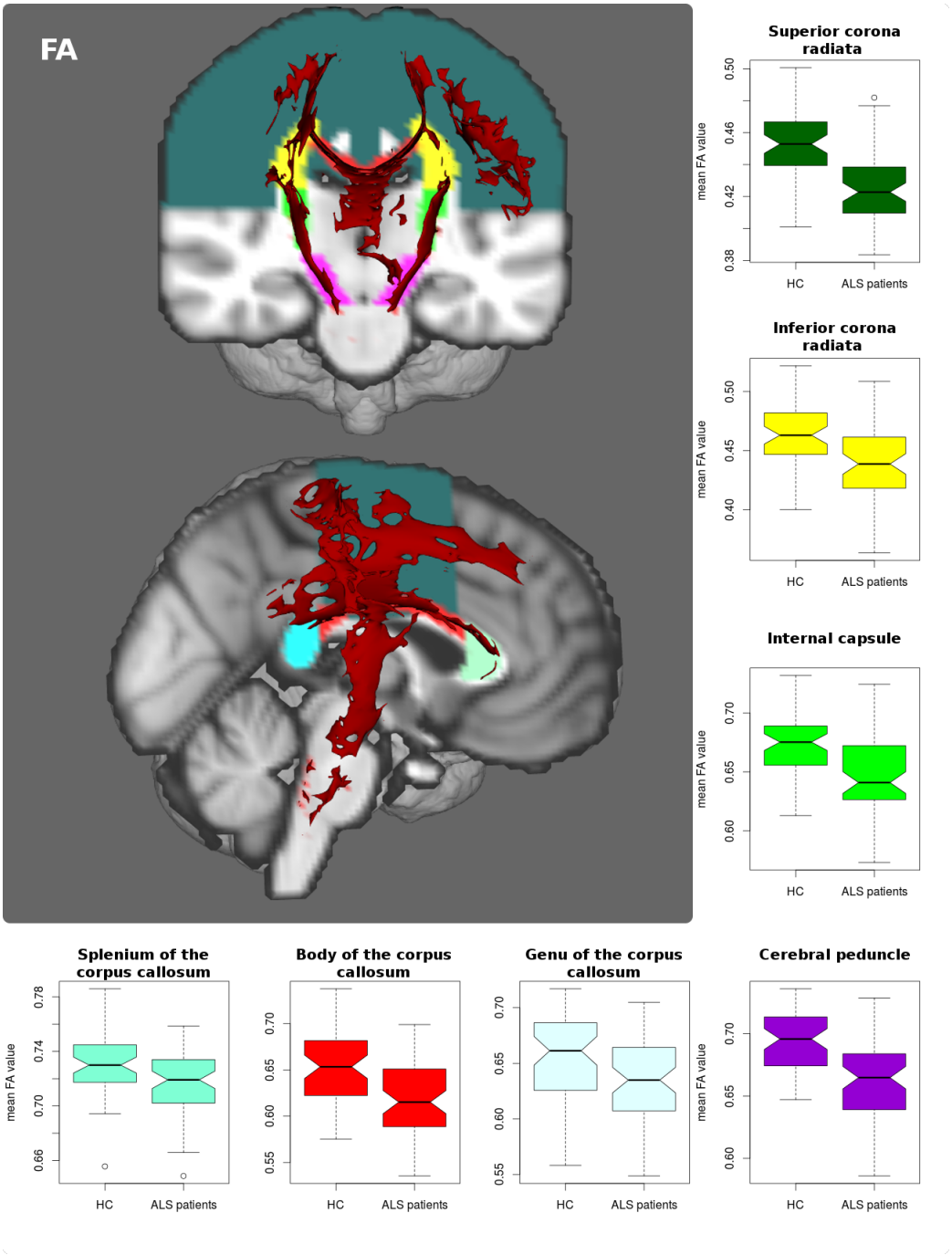

Figure 3.2: The segmental vulnerability of the corticospinal tracts and the corpus callosum. Average *fractional anisotropy* values of individual patients and controls are plotted in the voxels identified by the whole-brain ALS versus controls comparative analyses at $p < .01$ (FWE).

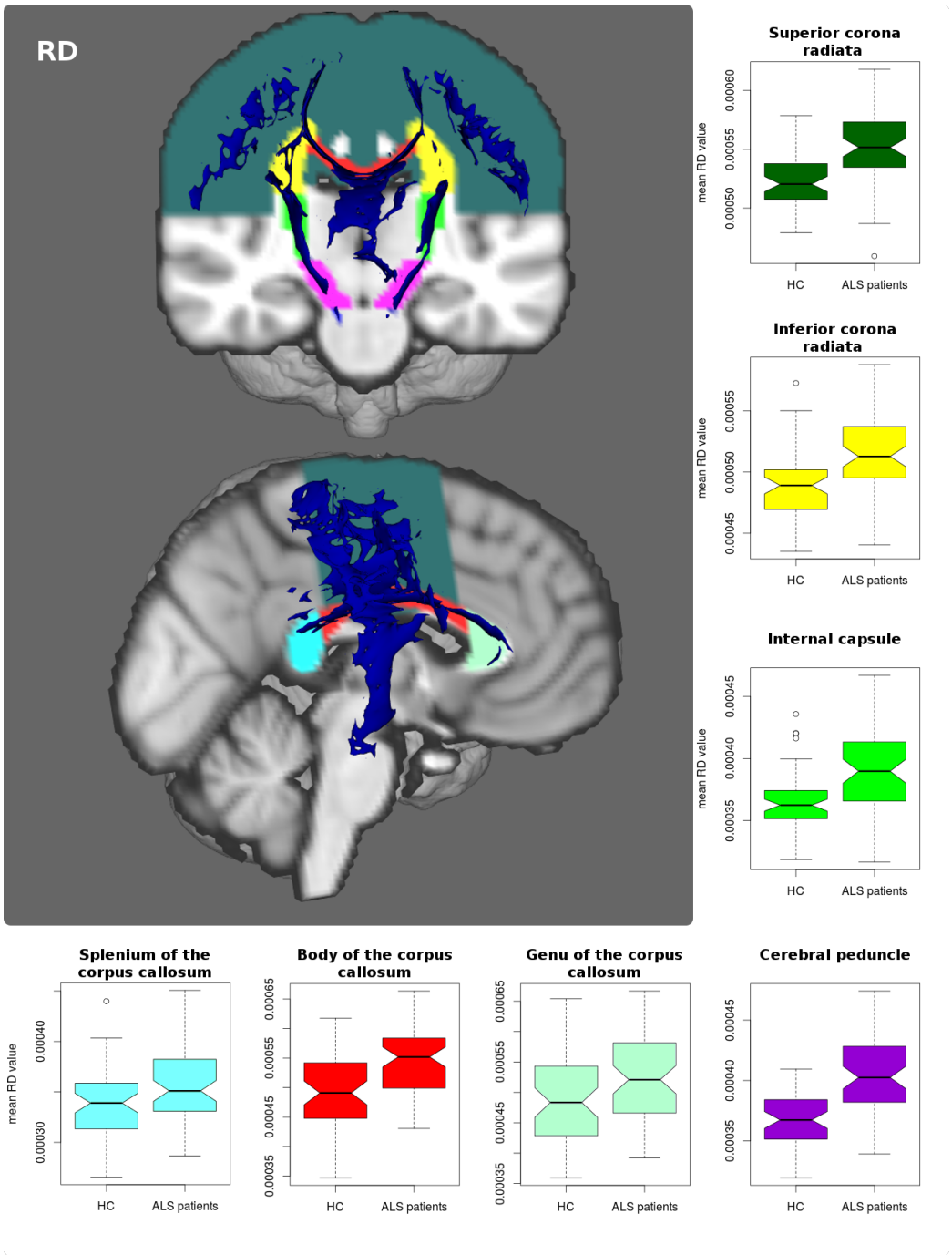

Figure 3.3: The segmental vulnerability of the corticospinal tracts and the corpus callosum. Average *radial diffusivity* values of individual patients and controls are plotted in the voxels identified by the whole-brain ALS versus controls comparative analyses at $p < .01$ (FWE).

3.3.3 Comparison of diffusivity measures

In this study, RD was identified as the most sensitive measure of white matter degeneration, followed by FA and MD. The body of the CC was the most affected white matter region followed by CST changes in the cerebral peduncle, splenium of the CC and internal capsule.

Figure 3.4 shows the percentage change based on the average diffusivity alterations in each white matter segments. Figure 3.5 displays the percentage change considering only voxels highlighting a significant change as described in analysis 1.

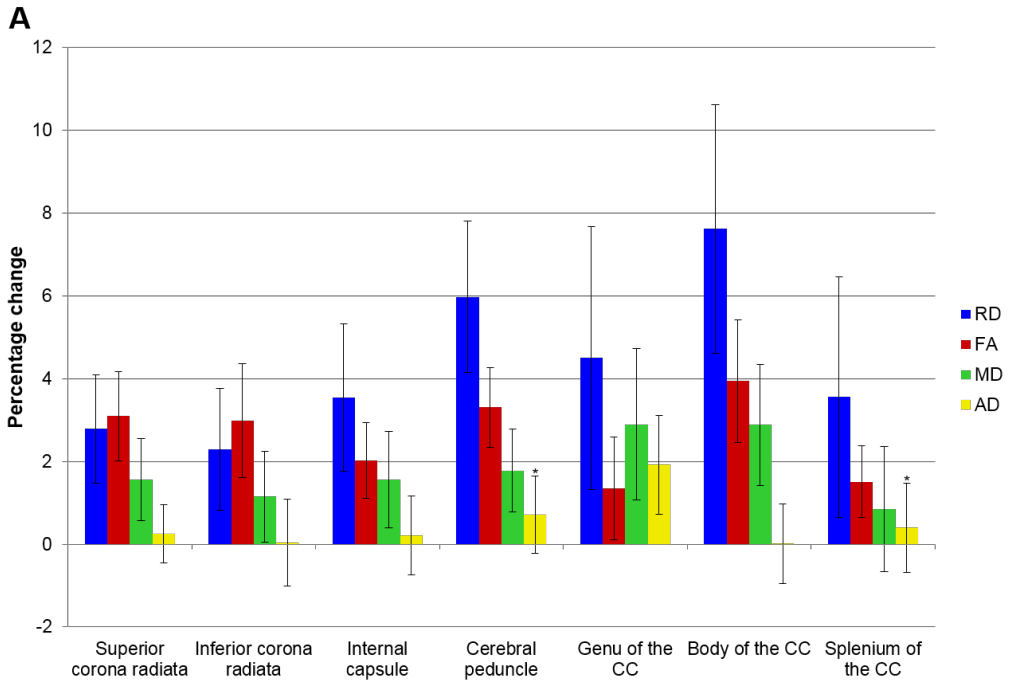

Figure 3.4: The segmental sensitivity profile of the diffusion metrics. Percentage change in patients compared to controls in specific CST and CC segments.

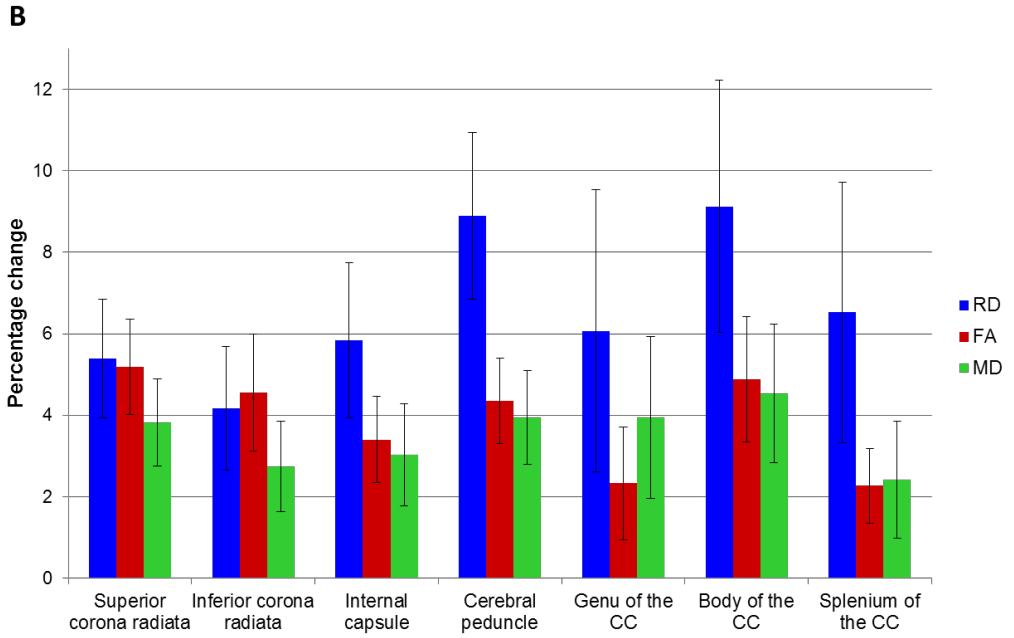

Figure 3.5: The segmental sensitivity profile of the diffusion metrics. Percentage change in patients compared to controls in voxels displaying statistically significant inter-group differences $p < .05$ (FWE).

3.3.4 Motor-phenotype specific degeneration

Based on RD, bulbar onset patients exhibit extensive white matter changes in the genu and posterior limb of the internal capsule and in the lateral fibres of the corona radiata subjacent to the bulbar representation of the motor homunculus ($p < .01$, FWE).

Spinal onset patients show predominantly posterior internal capsule involvement and medial corona radiata pathology based on RD ($p < .01$, FWE). The direct comparison of bulbar and spinal onset patients did not reveal statistically significant differences.

A concordant pattern of grey matter pathology was identified. Grey matter alterations of bulbar onset patients predominantly map to the inferior-lateral portions of the precentral gyrus ($p < .05$, FWE). In contrast, patients with

spinal onset show grey matter atrophy in the superior-medial region of the precentral gyrus ($p < .05$, FWE; Figure 3.5).

Patients with bulbar onset exhibit reduced grey matter density of the inferior precentral gyrus, which corresponds to the facial representation of the homunculus compared with spinal onset patients ($p < .05$, FWE).

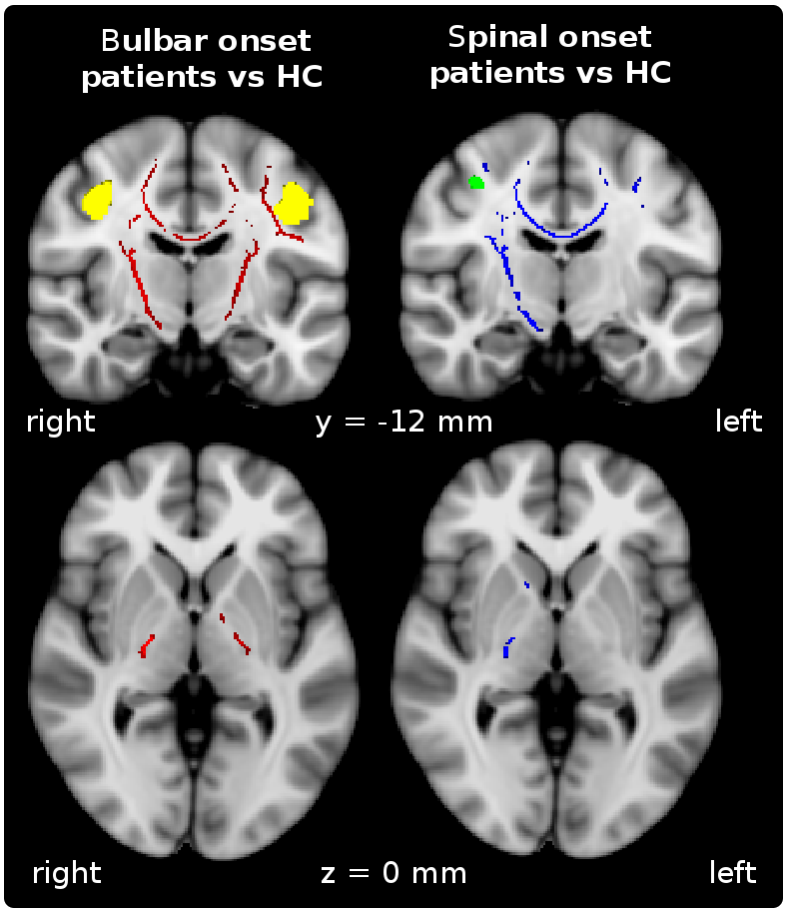

Figure 3.6: Motor phenotype-specific degeneration patterns.
Left: Bulbar onset patients versus controls; red colour indicates radial diffusivity changes at $p < .01$ (FWE), yellow colour indicates grey matter changes in the motor cortex at $p < .05$ (FWE).
Right: Spinal onset patients versus controls; blue colour indicates radial diffusivity changes at $p < .01$ (FWE), green colour indicates grey matter changes in the motor cortex at $p < .05$ (FWE).

3.3.5 Correlation with ALSFRS-R sub-scores

Bulbar sub-score shows a negative correlation with RD in the inferior-lateral fibres of the corona radiata ($p < .05$, FWE). Limb sub-scores shows a negative correlation with RD in the medial fibres of the corona radiata ($p < .05$, FWE; Figure 3.8). A similar pattern of positive correlation was identified for FA (Figure 3.7). For illustrative purposes, bulbar and spinal sub-scores were plotted against average RD values in the relevant white matter regions.

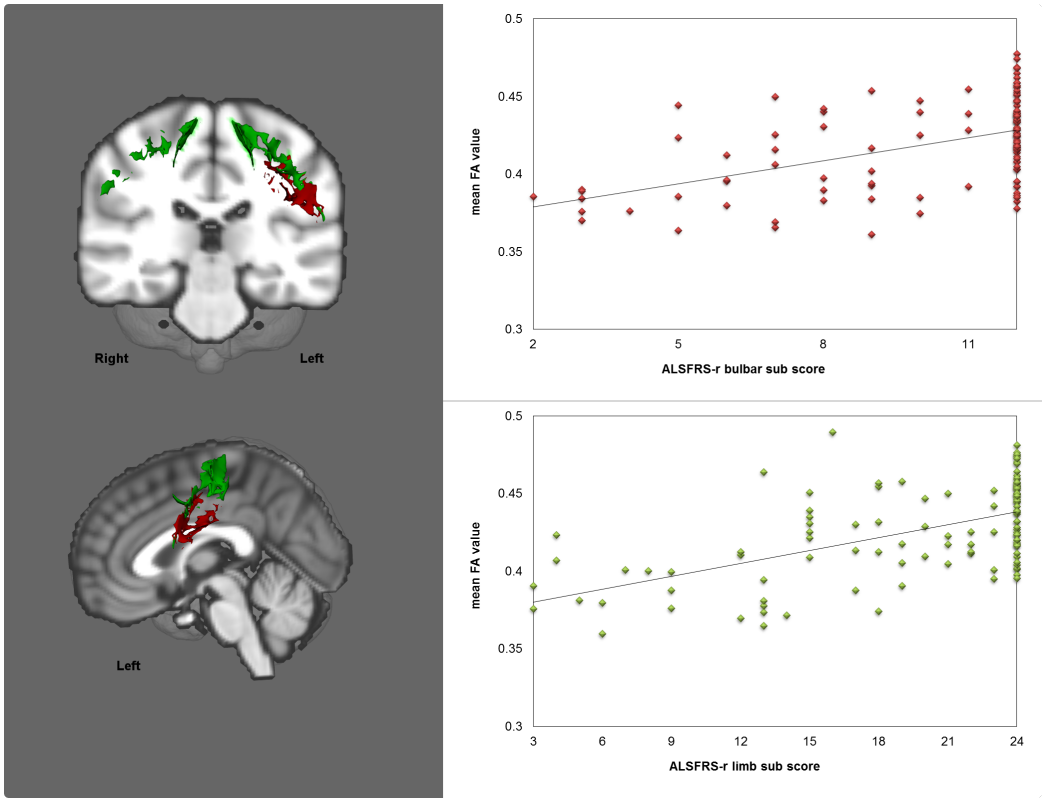

Figure 3.7: Fractional anisotropy correlates with clinical scores in the corona radiata. Regions of statistically significant positive correlation between FA and the bulbar sub-scores of the ALSFRS-R are displayed in red. Green colour indicates white matter regions in the corona radiata where spinal sub-scores show positive correlations with FA ($p < .05$, FWE).

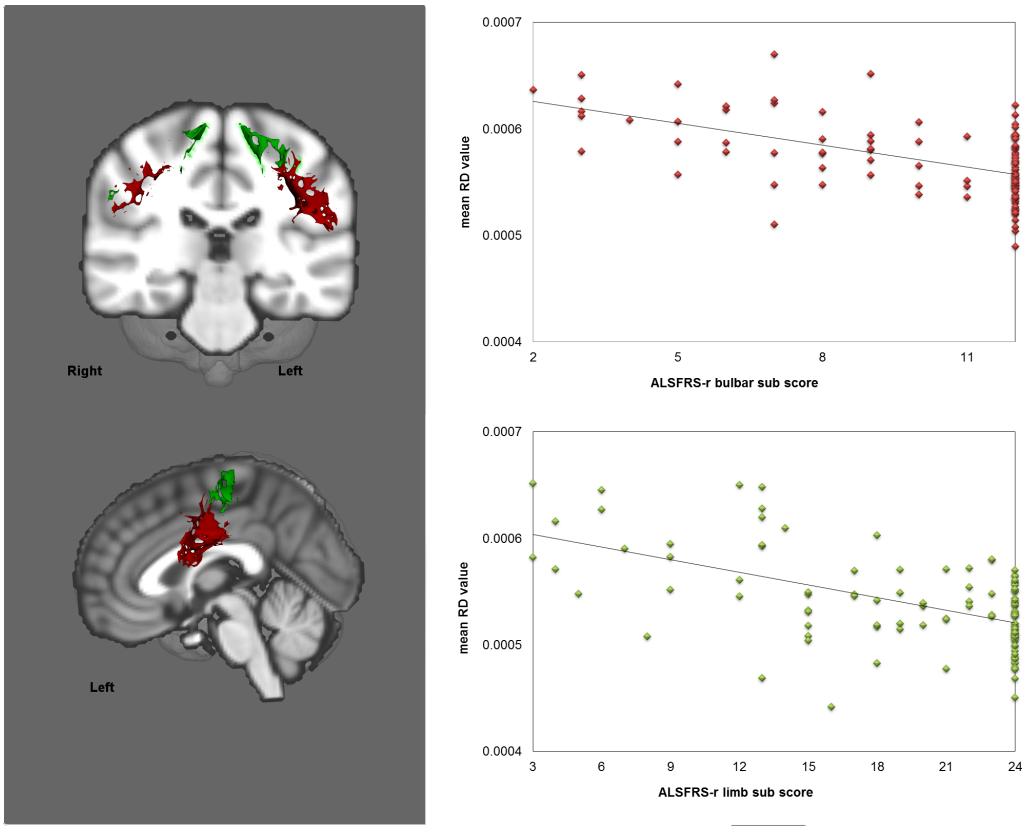

Figure 3.8: Radial diffusivity correlates with clinical scores in the corona radiata. Regions of statistically significant negative correlation between RD and the bulbar sub-scores of the ALSFRS-R are displayed in red. Green colour indicates white matter regions in the corona radiata where spinal sub-scores show negative correlations with RD ($p < .05$, FWE).

3.4 Discussion

ALS is a phenotypically and genetically heterogeneous condition, showing considerable variation in survival, rate of progression, cognitive and behavioural involvement. In this study, the segmental vulnerability of ALS-associated white matter tracts was examined. Additionally, the sensitivity of the four most widely used diffusivity measures was explored in a relatively homogeneous ALS cohort with considerable disease duration and motor disability. As stated earlier, patients in this cohort did not have co-morbid dementia and tested negative for a comprehensive panel of ALS-associated

mutations including *C9orf72* (Kenna et al., 2013).

The whole-brain analyses identified a core three-dimensional white matter signature which, at stringent statistical thresholds, was confined to the corticospinal tracts and corpus callosum (Figure 3.1). By examining several diffusivity parameters, AD was found of limited sensitivity in comparison to FA and RD.

Automated classifier analyses are increasingly applied to neurodegenerative conditions (Orrù et al., 2012) and have recently been applied to ALS (Welsh et al., 2013). The comprehensive evaluation of the sensitivity profile of various diffusivity indices has important implications for future diagnostic applications. These models aspire to capture early white matter alterations.

While corticospinal degeneration is widely regarded as a hallmark feature of ALS imaging, surprisingly little is known of its segmental diffusivity profile (Wong et al., 2007). The vast majority of ALS imaging papers comment on the CST degeneration in the posterior limb of internal capsule (Menke et al., 2012; Turner et al., 2012). However, the comprehensive segmental analysis of the CST demonstrates that CST measures in the cerebral peduncles and corona radiata also reliably discriminate patients and controls (Figure 3.2 and Figure 3.3).

A hierarchy of segmental degeneration can be outlined based on diffusivity changes, which suggest that changes in the cerebral peduncles and body of the corpus callosum may be more significant than those in the internal capsule. In a condition where diagnosis is mainly clinical and significant pathological change is likely to have already taken place before the diagnosis (Schuster et al., 2015) the discussion of the most established anatomical sites of degeneration and most sensitive imaging markers is particularly timely (Figure 3.4).

The present study focuses on the two main motor phenotypes of ALS, those

with spinal and bulbar onset, in the context of the somatotopic anatomy of the motor system. A dual approach using comparative and correlative analyses to localising pathological change in association to motor phenotypes was adapted. Comparative analysis of phenotypes to controls outlined the core spatial patterns where neurodegeneration occurs (Figure 3.6). Design matrices containing specific clinical variables mapped homunculus-wise degenerative changes in the corona radiata independently from pre-established phenotypes (Figure 3.6). These findings complement previous reports of grey matter alterations in relation to motor disability, by demonstrating focal white matter degeneration subjacent to the motor homunculus (Bede et al., 2012a; Mezzapesa et al., 2013; Schuster et al., 2013).

Decreased FA, increased AD and increased RD are generally interpreted as proxies of impaired fibre integrity. Specific diffusivity variables reflect on various aspects of fibre microstructure. AD (λ_1), the eigenvalue along the direction of maximal diffusivity reflects on axonal integrity (Budde et al., 2009). RD is the mean of the second and third ($\lambda_2 + \lambda_3$)/2) eigenvalues which are orthogonal directions perpendicular to the main diffusion direction. RD is affected by the degree of myelination (Beaulieu, 2002), axon diameter (Pierpaoli et al., 2001) and the extracellular microenvironment such as cell infiltration (Wang et al., 2011). Very few histopathologically validated neuroimaging papers exist in ALS (Abe et al., 1997). Our understanding of the microstructural correlates of DTI metrics derives from pathologically-validated animal imaging studies (Wang et al., 2011; Zhang et al., 2012). It is though that combined axonal and myelin degeneration lead to increased RD and inflammatory changes also contribute to RD alterations (Wang et al., 2011; Zhang et al., 2012). Reports on AD changes in ALS are inconsistent. While some groups report widespread AD alterations (Metwalli et al., 2010), other studies are consistent with our finding of limited axial diffusivity change (Agosta et al., 2010b). DTI studies of relatively long disease duration often report modest AD alterations (Ben Bashat et al., 2011) which may be explained by increased intracellular protein accumulation such as pTDP-43 restricting axonal water diffusivity.

Reports on the diagnostic sensitivity of diffusion-tensor imaging (DTI) data depend on the specific diffusivity parameters utilised. An individual patient data meta-analysis of 11 case-control studies including 221 ALS patients and 187 healthy controls using FA, found that the discriminatory power of CST DTI alone is insufficient for the accurate diagnosis of ALS (Foerster et al., 2013). Other studies however, which included radial diffusivity in their models reported a sensitivity of 87.5% and a specificity of 85.0% (Ben Bashat et al., 2011). Our analysis of individual subject RD in specific white matter segments indicates that inclusion of RD in discriminatory models is likely to increase the diagnostic accuracy (Figure 3.4).

Future studies are needed to investigate possible combinations of MRI derived markers and brain areas to increase diagnostic accuracy (Chapter 5).

One of the limitations of this study lies in its cross-sectional nature, longitudinal data on diffusivity indices (Chapter 4) helps to elucidate the temporal nature of white matter degeneration and clarify if axonal degeneration precedes inflammatory or myelin-associated processes. It is conceivable that various stages of ALS are dominated by stage-specific diffusivity alterations. In this study, a patient sample with relatively long disease duration was characterised. Another limitation is the lack of spinal diffusivity measurements. The spinal portion of the CST is associated with significant diffusivity alterations (El Mendili et al., 2014), but anatomical factors, such as small cross-sectional area, CSF flow and cardiac pulsation make spinal DTI methodologically challenging (Bede et al., 2012b). Finally, novel non-parametric diffusion imaging techniques such as Q-ball imaging and diffusion spectrum imaging and parametric methods such as spherical deconvolution are likely to characterise the degeneration of crossing fibres in more detail.

Notwithstanding these limitations, this study shows that the corticospinal tracts and corpus callosum exhibit phenotype-specific segmental vulnerability in ALS, which manifest in selective alteration of diffusivity parameters.

Chapter 4

Longitudinal brain changes during the course of ALS

4.1 Introduction

Heterogeneity is one of the hallmarks of ALS which includes clinical presentation, progression rates, genetic vulnerability, cognition and poses a major challenge to biomarker development.
Previously in this thesis, cross-sectional analyses were presented. The findings so far confirm widespread ALS-related changes soon after the diagnosis. Similarly to other neurodegenerative conditions such as HD, it is well established that considerable presymptomatic changes occur in ALS (Tabrizi et al., 2013; Benatar and Wuu, 2012).

In order to develop a monitoring biomarker, which would be essential to improve clinical trials, the candidate markers need to detect subtle changes occurring during the course of the disease and the change needs to be measurable within a short period of time. It remains unclear whether current MRI measures can fulfil these requirements. Furthermore, it remains unclear whether early during the course of the disease a floor or ceiling effect is reached, that means, the brain changes are too severe to progress any further. Well-designs longitudinal studies are likely to answer these questions.

There is a scarcity of longitudinal ALS studies, which vary considerably in methods, sample sizes and follow-up intervals (Table 4.1). Therefore, it is not surprising that the results are rather inconsistent (Menke et al., 2017). While some studies describe a significant progressive grey matter change over time (Kwan et al., 2012; Menke et al., 2014), others report no measurable longitudinal change (Verstraete et al., 2012; Schuster et al., 2014b; Cardenas-Blanco et al., 2016). This inconsistency also applies to white matter studies: The studies by Blain et al. (2007); Agosta et al. (2009); Kwan et al. (2012) report no progressive changes, whereas other studies detect significant degeneration (Zhang et al., 2011; Menke et al., 2014; Cardenas-Blanco et al., 2016).

The core ALS-associated pathology has been described in the previous chapter, and includes the precentral gyrus and supplementary motor cortex, the corticospinal tract and the corpus callosum (Schuster et al., 2013, 2016a). These are the most promising anatomical locations for candidate biomarkers. Longitudinal changes within these regions have been previously described by several research groups using different methods (Chiò et al., 2014; Grolez et al., 2016; Menke et al., 2017).

The cerebellum is also involved in ALS. It integrates sensory and predictive inputs to regulate timing, coordination, fine motor control, spatial targeting, preventing undershoot and overshoot, and correct errors. As ALS is a neurodegenerative disease involving the motor system, it is not surprising that the cerebellum also exhibits disease-related changes over time and is therefore another biomarker candidate (Bede et al., 2016). Cerebellar involvement is somewhat understudied (Prell and Grosskreutz, 2013). Prell et al. 2013 reviewed the current literature describing structural and functional changes of the cerebellum arguing for a compensatory mechanism. Cerebellar changes have been linked with a *c9orf72* ALS genotype (Mackenzie et al., 2014). Whereas Walhout et al. (2015) reported no difference in total grey matter volume between *c9orf72*-associated ALS patients and controls, Bede et al. (2015) described extensive cerebellar white matter pathology in

patients with no known pathogenic genetic variants. Longitudinal studies do either overlook the potential cerebellar pathology or do not report any changes (Menke et al., 2014; Cardenas-Blanco et al., 2016; Schuster et al., 2014b).

One of the key differences in the different longitudinal studies is whether a voxel-wise/vertex-wise analysis was performed or whether the authors chose to average the voxels within a certain ROI. The disadvantage of averaging multiple voxels is that valuable focal information may be sacrificed. For example, if only a subsection is affected by the disease it will not affect the average, hence, this information would be lost, but with a voxel-wise/vertex-wise approach this subsection could be identified. Another example is that the precentral gyrus and the internal capsule present with a different pattern of degeneration depending on the disease onset: Bulbar onset patients exhibit thinning of the inferior part of the precentral gyrus and the genu of the internal capsule, whereas spinal onset patients present with thinning of the superior part of the precentral gyrus and the posterior part of the posterior limb of the internal capsule. By averaging, e.g., the entire precentral gyrus, this information may be lost. This is another example how disease heterogeneity in ALS affects the focal brain changes observed.

4.2 Objectives and outline

The objective of this project is to determine whether progressive changes can be captured in ALS using MRI. This would support the role of MRI as a potential monitoring marker in ALS. The analyses were restricted to disease-associated key brain regions. The ROI for the grey matter analyses include the precentral gyrus and supplementary motor cortex and for the white matter analyses the corticospinal tract and corpus callosum.

In order to comprehensively interpret longitudinal changes, it is important to describe the baseline pathology. Therefore, the first comparison is a cross-

Year	**Authors**	**Journal**	**Sample Size**	**Time between baseline and 1st follow-up scan**
2016	Cardenas-Blanco et al.	NeuroImage: Clinical	34	6 months
2015	Westeneng et al.	Neurobiology of Aging	39	5.5 months
2014	El Mendili et al.	PloS One	14	11 months
2014	Menke et al.	Brain	27	16 months
2014	Schuster et al.	J Neurol	51	3-12 months
2014	Verstraete et al.	Hum Brain Mapp	24	5.5 months
2013	Kwan et al.	NeuroImage: Clinical	45	12 months
2012	Keil et al.	BMC Neurosci	24	6 months
2012	Menke et al.	Arch Neurol	21	6 months
2012	Verstraete et al.	J Neurol Neurosurg Psychiatry	45	3-12 months
2011	Senda et al.	ALS	17	6 months
2011	van der Graaff et al.	Brain	48	6 months
2011	Zhang et al.	ALS	17	8 months
2009	Agosta et al.	ALS	17	9 months
2009	Agosta et al.	JNNP	28	6-12 months
2009	Avants et al.	Archives of Neurology	4	5 months
2009	Nickerson et al.	Clin Neuroradiol	2	3 months
2008	Vucic et al.	Brain	74	12 months
2007	Blain et al.	ALS	23	6 months
2007	Unrath et al.	J Neurol	11	3 months
2004	Rule et al.	ALS	45	3 months
2002	Aggarwal et al.	JNNP	31	6 months
2002	Suhy et al.	Neurology	28	1 month
2001	Hecht et al.	JNS	31	12 months
1999	de Carvalho et al.	Muscle Nerve	11	3.7 months
1998	Block et al.	Arch Neurol	33	24 months

Table 4.1: List of longitudinal studies in ALS.

sectional one between the baseline scans of the patients and a large age- and gender-matched group of healthy controls. Secondly, the last follow-up scan of the patients is compared to the same group of healthy controls to establish if progressive change can be detected. It is hypothesised that pathological degeneration is measurable within the ROI at both time points.

Subsequently, as the main objective, neurodegenerative change within 4 and within 8 months was explored. It is hypothesised that a 4-month follow-up interval is sufficient to detect significant changes measured by MRI.

Next, the cerebellum was selected as ROI to explore longitudinal changes in ALS.

Additionally, whole-brain longitudinal analyses were conducted to explore whether changes within the motor areas are dominant and whether other brain areas are also affected over time.

A final objective was to explore whether longitudinal degeneration corresponds to physical disability. To this aim, brain areas were evaluated in patients with no corresponding functional disability based on self-reported sub-scores of the ALSFRS-R. These patients can be described as presymptomatic. The change within 4 or 8 months within the motor regions (i.e. the ROI described above) was explored. It was hypotheses that structural brain changes are detectable prior to symptom onset.

4.3 Methods

4.3.1 Sample

For this analysis, the sample was limited to patients with at least 2 follow-up scans. Participating patients were diagnosed according to the revised El Escorial criteria (Brooks et al., 2000). In an attempt to control for some aspects

of disease heterogeneity, patients with a co-morbid diagnosis of frontotemporal dementia according to the Rascovsky Criteria were excluded (Rascovsky et al., 2011). It has been shown that this patient cohort present with additional extra-motor brain changes which may have implication for longitudinal analyses (Chang et al., 2005; Lillo et al., 2012). Sixty-nine age- and gender matched healthy controls were included in this study. The clinical and demographical details are reported in Table 4.2.

	HC	**ALS patients baseline**	**p-value** - baseline compared to HC	**ALS patients 1st follow-up**	**p-value** – compared to baseline	**ALS patients 2nd follow-up**	**p-value** - compared to baseline
N	69	32		32		32	
Male	34	23	$p = .06$				
Handedness (r/ l)	64/5	26/6	$p = .17$				
Age (yrs, SD)	59.97 (9.9)	61.02 (9.21)	$p = .61$				
Site of onset (bulbar, spinal, respiratory)		6/26					
Disease duration onset until baseline scan (mo, SD)		27.19 (19.77)					
ALSFRS-R (mean, SD)		39.31 (6.38)		36.37 (7.94)	$p < .01$	33.88 (7.78)	$p < .01$
ALSFRS-R bulbar score (max 12)		10.06 (2.49)		9.38 (2.95)	$p < .01$	8.97 (3.15)	$p < .01$
ALSFRS-R upper limb score (max 12)		6.16 (2)		5.75 (2.29)	$p < .05$	5 (2)	$p < .01$
ALSFRS-R lower limb score (max 8)		5.47 (2.36)		4.75 (2.82)	$p < .01$	4.34 (2.89)	$p < .01$
Time passed since baseline scan (d, SD)				132.16 (17.03)		273.16 (35.33)	

Table 4.2: Demographical and clinical details of the sample. r = right, l = left, yrs = years, mo =months, d = days, SD = standard deviation

4.3.2 Imaging data pre-processing and analyses

Cortical Thickness

Cortical thickness was analysed using FreeSurfer (version 5.3.0).[1] Cortical thickness has been defined as the distance (vertex) from the white matter surface to the nearest point on the pial surface. The automated processing stream comprises skull-stripping, registration, intensity normalization, Talairach transformation, tissue segmentation, which determines the boundaries between the white and grey matter (white matter surface), the grey matter and the cerebrospinal fluid (pial surface), as well as surface parcellation. Tissue segmentation was individually reviewed, if necessary errors were corrected and the segmentation step was repeated.

The longitudinal processing steam of FreeSurfer (Reuter et al., 2012) was used. Based on all MRI scans available using a robust inverse consistent registration, an individual unbiased within-subject template space and image (temporal average) was created. Next, skull-stripping, Talairach transformation, spherical maps, and parcellation were initialised from the within-subject template for each subject's time point, utilising common information, thereby increasing reliability and statistical power.

For each vertex-wise analysis (cross-sectional or longitudinal), the cortical thickness data were smoothed using a 10 mm full-width/half-maximum Gaussian kernel on the surface in standardised space. If not reported otherwise, the results are significant at $p < 0.5$, corrected for multiple comparisons using false discovery rate method (FDR) implement in FreeSurfer.

Grey matter density

In addition to analysing cortical thinning, progressive change in the grey matter density was also explored. Therefore, the T1-weighted images were

[1] http://surfer.nmr.mgh.harvard.edu/

bias-field corrected, brain-extracted, tissue-types were segmented and aligned to Montreal Neurological Institute 152 standard space using non-linear registration. These processing steps are part of the FSL imaging suite (Smith et al., 2004) A study-specific template was created using the scans relevant for the specific analyses. In the next step, the segmented grey matter images were non-linearly registered to the study-specific template and modulated to correct for local contraction or enlargement due to the non-linear component of the spatial transformation. To smooth the modulated grey matter images, an isotrophic Gaussian kernel of $\sigma = 3$ mm was used.

Voxel-wise generalised linear models were applied and permutation-based non-parametric testing (10,000 permutations) correcting for age. The reported results are, if not stated otherwise, significant at $p < .05$, corrected for multiple comparisons using family-wise error (FWE).

Diffusion tensor imaging

Diffusion-weighted images were also analysed with FMRIB's imaging suite (Smith et al., 2004). The datasets were pre-processed as described previously including eddy current corrections, motion correction and brain-tissue extraction. After this, a diffusion tensor model was fitted at each voxel, generating maps of FA, MD, AD and RD. Voxel-wise statistical analysis of the FA data was carried out using TBSS (Smith et al., 2006). Each dataset was aligned to the FMRIB58a FA standard-space images. Subsequently, a mean FA image was created and thinned to create a mean FA skeleton which represents the centres of all tracts common to the sample (FA < 0.2). Each subject's aligned FA data was then projected onto this skeleton and the resulting data fed into voxel-wise cross-subject statistics. For each analysis a study-specific mean FA skeleton was created. For the longitudinal analysis, the skeleton was based on all available scans.
The tool 'randomise' was used for non-parametric permutation inference with 10,000 permutations and corrections for age. The threshold-free cluster en-

hancement (TFCE) method was applied (Smith and Nichols, 2009). If not stated otherwise, the significance level was set at $p < .05$, corrected for multiple comparisons using family-wise error (FWE) method.

4.4 Statistical analyses and results

Due to the large number of different analyses, this section describes the evaluation of each hypothesis as described in section 4.2 separately. Cortical thickness, grey matter density and diffusion tensor imaging analyses are described separately for clarity.

4.4.1 Cross-sectional analysis of baseline scans

The aim of this analysis is to establish a baseline measurement to later interpretable the results in context of a possible floor or ceiling effect. The hypothesis is that patients exhibit considerable brain changes already at the first scan in comparison to healthy controls (Figure 4.1, Comparison 1). Using the same group of controls, a second cross-sectional analysis is undertaken to investigate whether these changes are more pronounced 8 months later (Figure 4.1, Comparison 2). Both comparisons focus on the region of interest only.

The baseline scan of patients was compared to a group of age- and gender-matched healthy controls scan using age as a covariate of no interest. The ROI for the cortical thickness analysis consisted of the precentral gyrus and supplementary motor cortex. For grey matter density analyses, the ROI included the precentral gyrus and supplementary motor cortex according to the Harvard-Oxford atlas (FSL Harvard-Oxford atlas, Desikan et al. (2006)). The ROI for the white matter analysis consisted of the corticospinal tract and corpus callosum (Chapter 3).

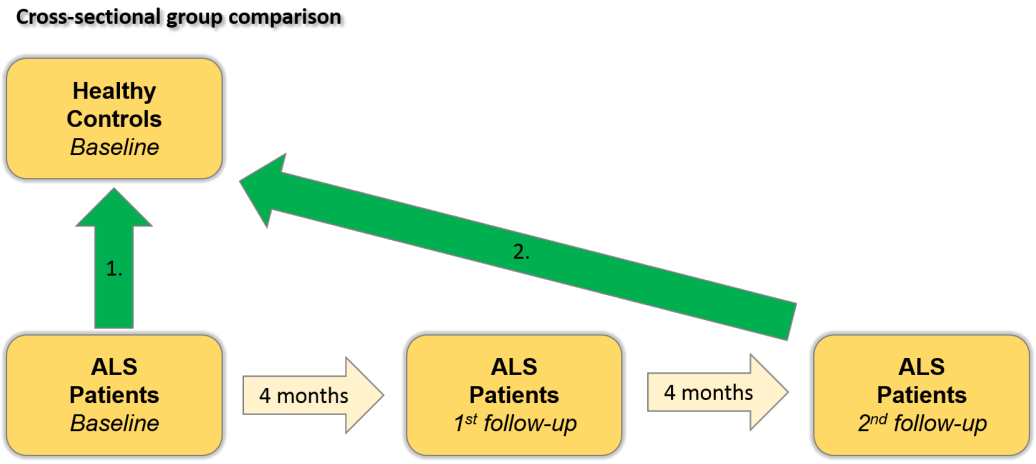

Figure 4.1: Cross-sectional analyses. Green arrows indicated the group comparisons.

Cortical thickness

The vertex-wise group ROI comparison between the baseline scan of patients and age- and gender-matched healthy controls correcting for age did not reveal significant differences.

Next, the scans conducted 8 months later were compared to the same group of healthy controls using the same ROI and age as nuisance variable. Significant cortical thinning of the entire precentral gyrus and supplementary motor cortex was found $p < .05$ (FDR), Figure 4.2.

Grey matter density

A voxel-based ROI group comparison between the baseline scan of the patient with healthy controls showed changes predominately within the right superior (MNI: x = 14, y = -12, z = 72) and inferior precentral gyrus (MNI: x = 62, y = 10, z = 20), $p < .05$ (FWE), Figure 4.3.

The results of comparing the same group of healthy controls to the 2nd follow-up scan of the patients are shown in Figure 4.3. The patients exhibit de-

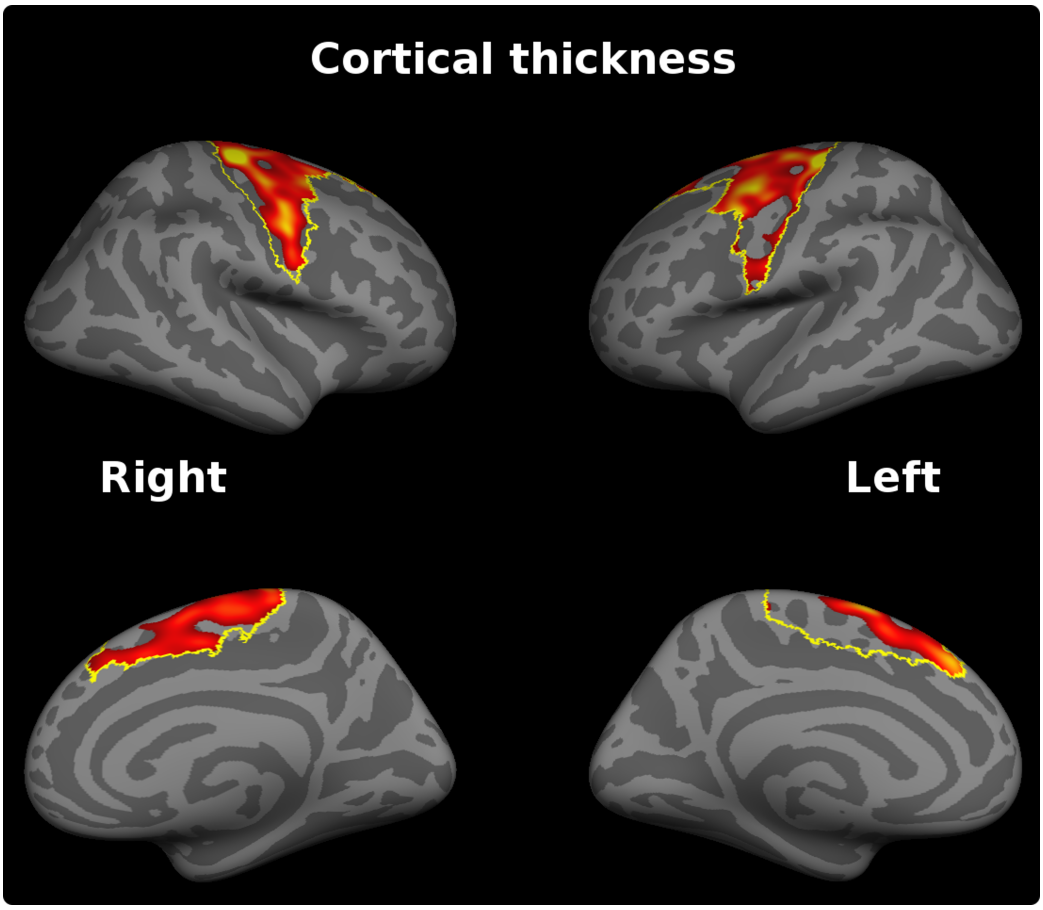

Figure 4.2: Cortical thinning - cross-sectional analysis. Group comparison of the 2nd follow-up scan with healthy controls, $p < .05$ (FDR). The ROI is outlined in yellow.

creased grey matter density in almost the entire ROI, $p < .05$ (FWE).

White matter integrity

A tract-based group ROI comparison between the baseline scan of the patients and healthy controls was performed using age as nuisance variable. Analyses of FA, RD, MD or AD changes were done separately. FA and RD highlighted degeneration of the entire ROI ($p < .05$ (FWE), Figure 4.4); whereas no significant difference was found using MD or AD.

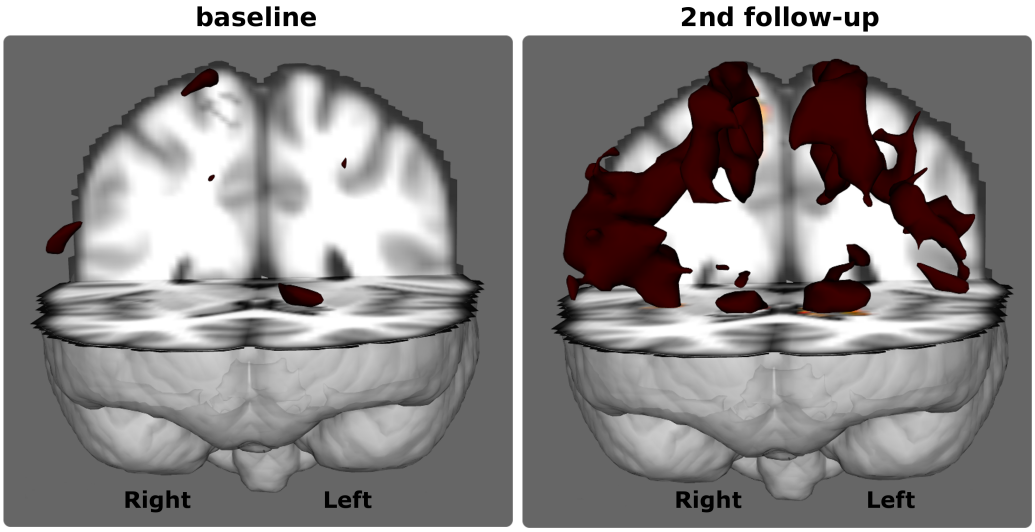

Figure 4.3: Grey matter degeneration - cross-sectional ROI analysis. Group comparison of grey matter density between baseline scan of the patients with healthy controls on the left and between 2nd follow-up scan of the patients and healthy controls on the right, $p < .05$ (FWE).

Comparing the 2nd follow-up scan of the patients with healthy controls revealed significant FA alterations in the bilateral corticospinal tract and RD changes within the right ME, inferior and superior part of the corona radiata, at $p < .05$ (FWE, Figure 4.5). MD did not reveal significant differences. Unexpectedly, patients showed significant decrease of AD in the superior part of the corona radiata, $p < .05$ (FWE).

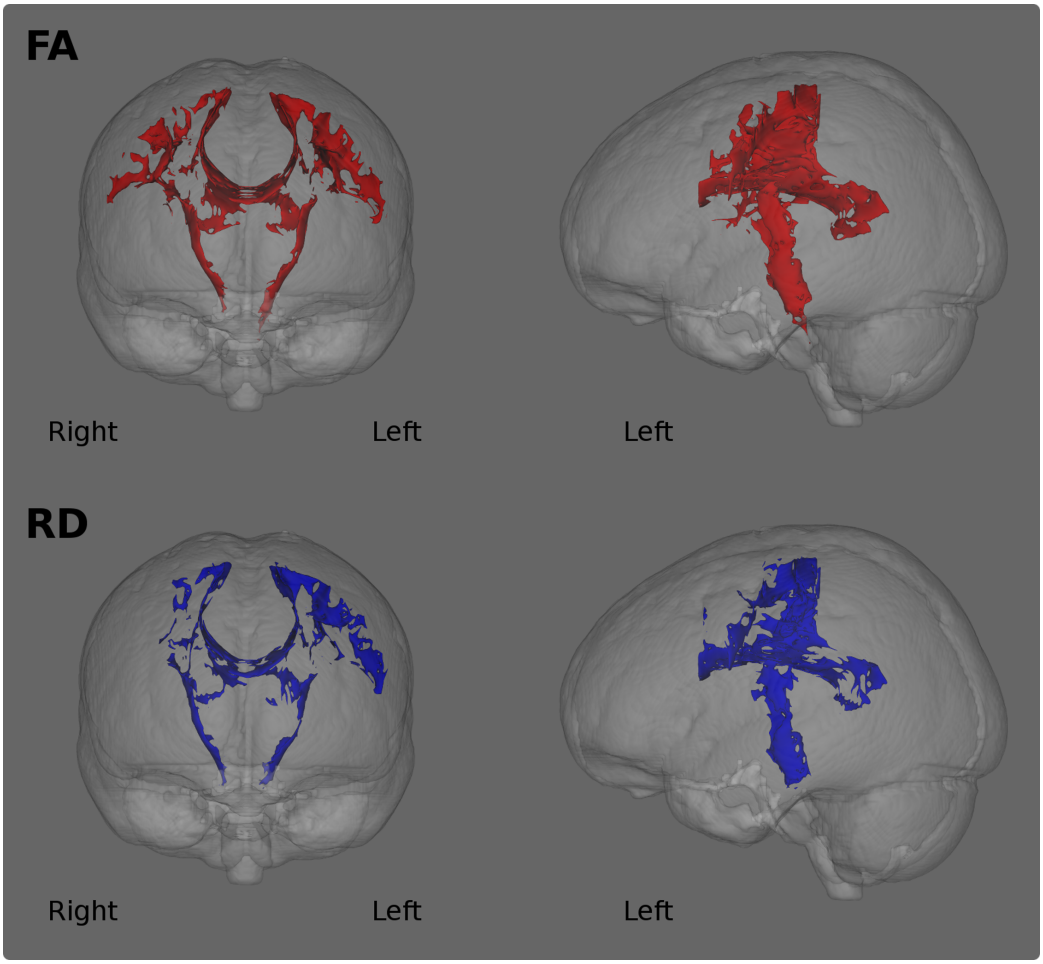

Figure 4.4: White matter degeneration - cross-sectional ROI analysis of baseline scans. Group comparison of white matter degeneration between baseline scans of the patients with healthy controls, $p < .05$ (FWE). FA in red, RD in blue.

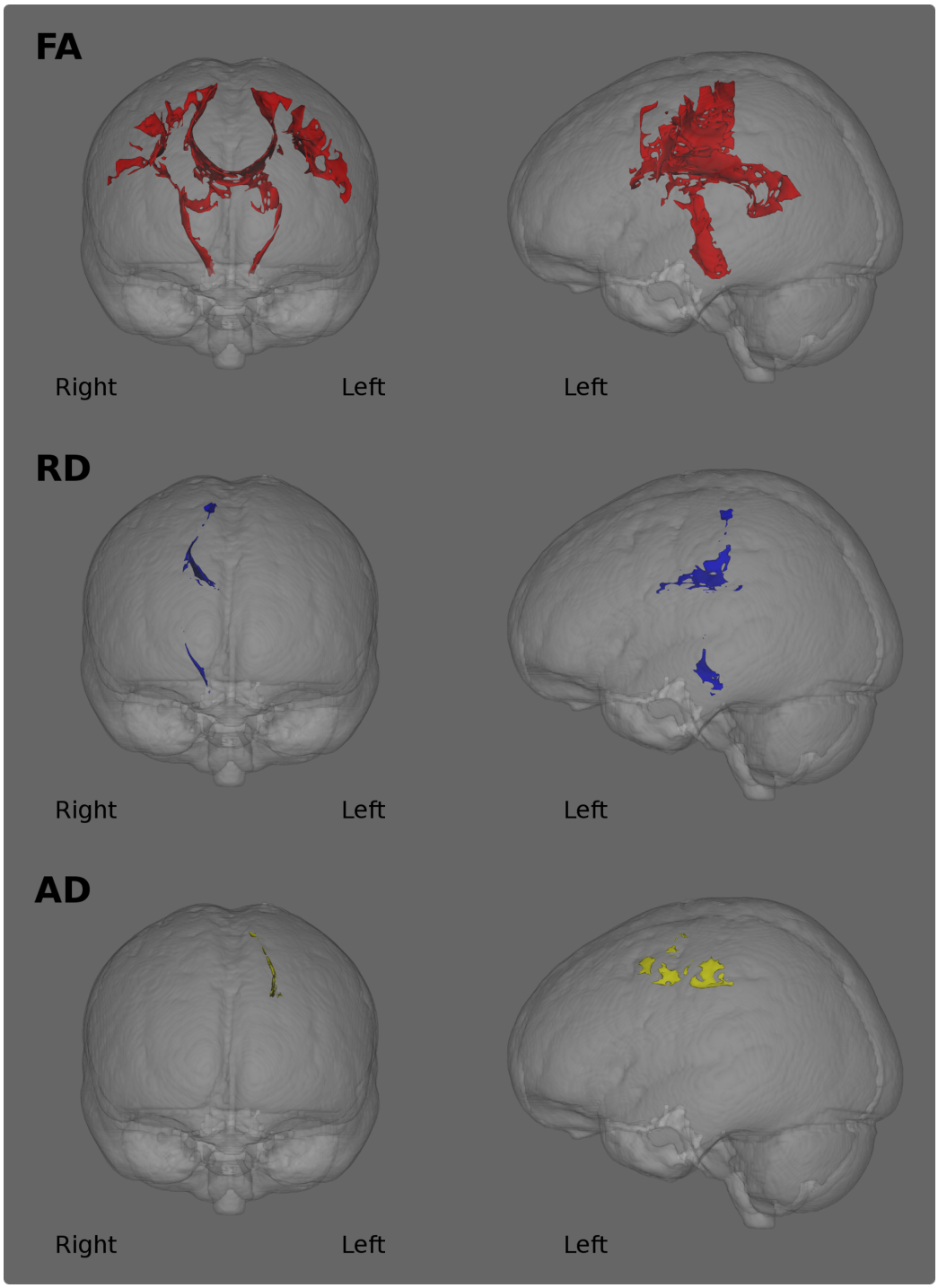

Figure 4.5: White matter degeneration - cross-sectional ROI analysis of 2nd follow-up scans. Group comparison of white matter degeneration between the 2nd follow-up scans of the patients with healthy controls, $p < .05$ (FWE). FA in red, RD in blue, AD in yellow. Note for AD: ALS < HC.

4.4.2 Longitudinal ROI analyses

The baseline scans of the patients were compared with the 1st follow-up or the 2nd follow-up scans (Figure 4.6, Comparison 3 and 4).
For the cortical thickness analyses, paired t-tests were performed using age and time between scans as covariates. The dependent variable was the images pre-processed using the longitudinal stream described above.

In FSL, the difference between the baseline and follow-up scan was calculated and the single group average ('one-sample t-test' as implemented in FSL) was determined using age and the time interval between scan as covariates.

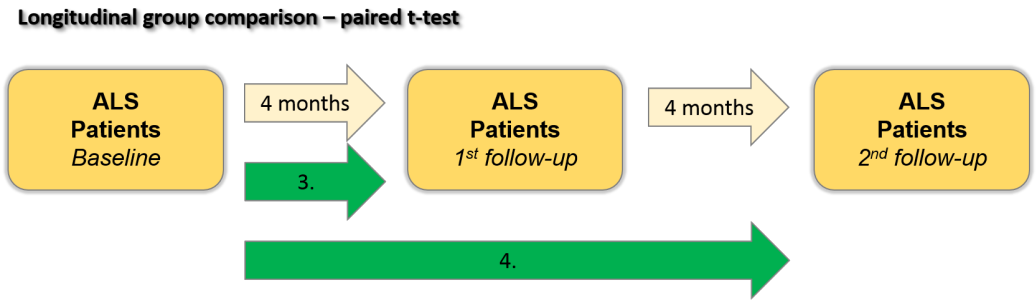

Figure 4.6: Longitudinal comparisons.

Cortical thickness

There was no significant difference with the ROI when comparing the baseline scan to the 1st follow-up scan (4 months follow-up).

The evaluation of longitudinal change in 8-month revealed extensive cortical thinning in the ROI, Figure 4.7. The results are significant at $p < .05$ (FDR), the ROI is outlined in yellow.

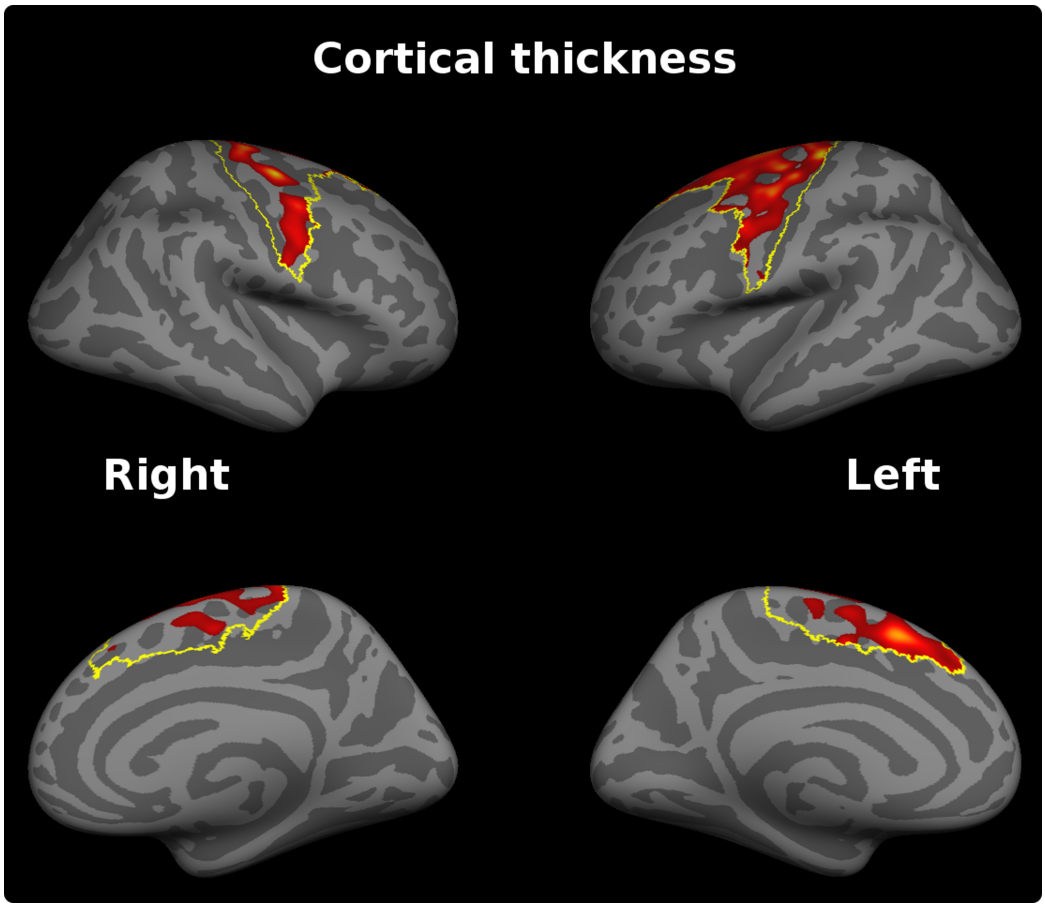

Figure 4.7: Cortical thinning within 8 months, $p < .05$ (FDR). The ROI is outlined in yellow.

Grey matter density

Figure 4.8 shows the results of paired t-tests between the baseline scan and the 1st follow-up scans of ALS patients and the 2nd follow-up scans.
Within the first 4 months the change is confined to the medial part of the motor cortex (MNI: x = -14, y = -28, z = 46; x = -18, y = -28, z = 54; x = 38, y = -26, z = 18) and subsequently spreads over the entire ROI (within 8 months).

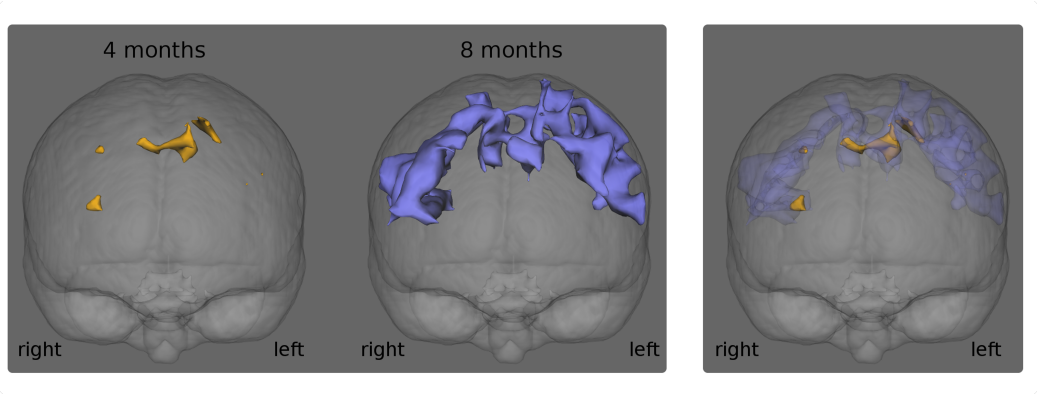

Figure 4.8: Reduction in grey matter density within 4 months in yellow, within 8 months in purple, $p < .05$ (FWE).

White matter integrity

None of the white matter indices highlighted changes within the first 4 months using age and scan interval as covariates in the corticospinal tract ROI.

Within 8 months each index captured significant changes at $p < .05$ (FWE) in the left superior part of the corona radiata (RD, MD, AD) and the posterior limb of the internal capsule (FA, MNI: x = -23, y = -9, z = 14). For illustration purposes, a significant trend at $p < .1$ is also shown in Figure 4.9.

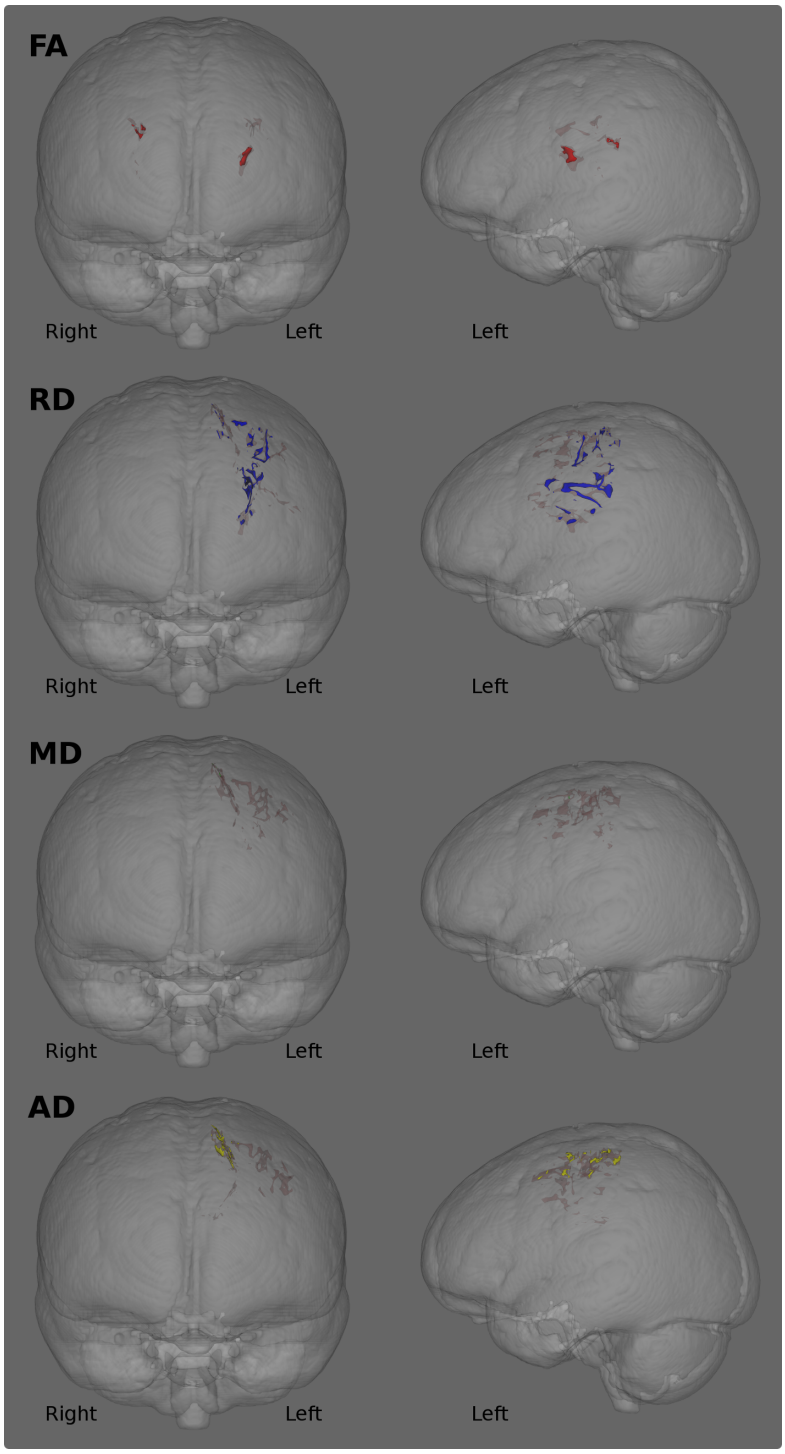

Figure 4.9: Longitudinal ROI white matter changes at $p < .05$ (FWE). FA in red, RD in blue, MD in green, AD in yellow. The results at $p < .1$ (FWE) are added in light brown.

4.4.3 Longitudinal analyses of cerebellar changes

Grey matter density

Within 4-month of the initial scan, significant changes were identified in the right V. lobe, vermis VI, left crus II, left VIIb.
Within 8-month interval, the reduced grey matter density reductions were identified additionally in the bilateral VI. lobe, right V, bilateral crus I and II, bilateral VIIb, VIIIa and VIIb, at $p < .05$ (FWE), Figure 4.10 and Figure 4.11. There areas are labelled according to the Diedrichsen cerebellar atlas (Diedrichsen et al., 2009).

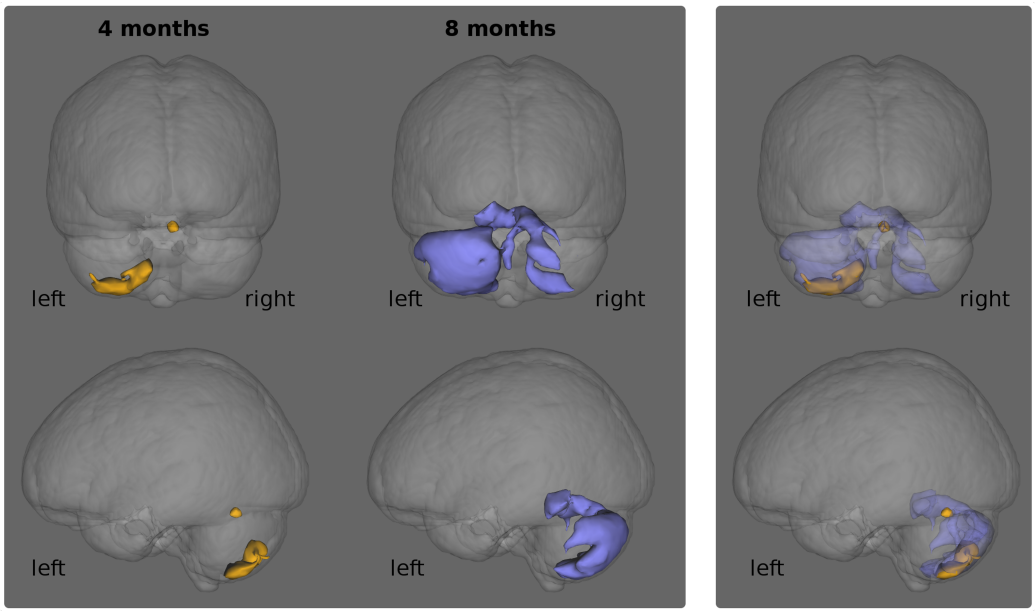

Figure 4.10: Cerebellum – extent of grey matter density loss at $p < .05$ (FWE).

White matter integrity

No statistically significant change was found between the baseline and the 1st or 2nd follow-up scans for any of the DTI indices in the cerebellar ROI.

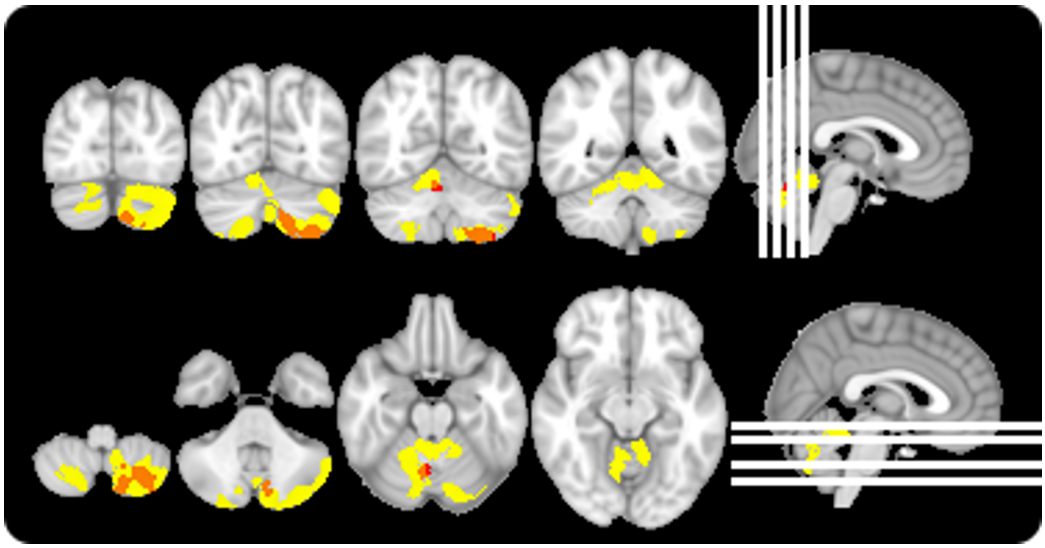

Figure 4.11: Cerebellum – localisation of grey matter density loss at $p <$ .05 (FWE); Top: coronal view, MNI: y = -78, y = -68, y = -58, y = -48. Bottom: axial view, MNI: z = -50, z = -38, z = -20, z = -10. Change within 4 months in red, change within 8 months in yellow, their overlap in orange.

4.4.4 Longitudinal whole-brain analyses

The analyses described under 4.4.2. were repeated focusing on a whole–brain level. The aim was to explore whether change within the motor areas would dominate over extra-motor areas. The objective was to characterise progressive extra-motor changes in ALS.

Cortical thickness

While there was no significant cortical thinning detected within 4 months of the initial scan, within 8-month follow-up, significant thinning was identified within both motor and extra-motor areas.

Adjacent to the precentral and supplementary motor cortices, parietal and temporal lobe thinning was highlighted at $p < .001$ (uncorrected), Figure 4.12. After applying a correction for multiple comparisons ($p < .05$, FDR), the changes were limited to the right hemisphere, Figure 4.13.

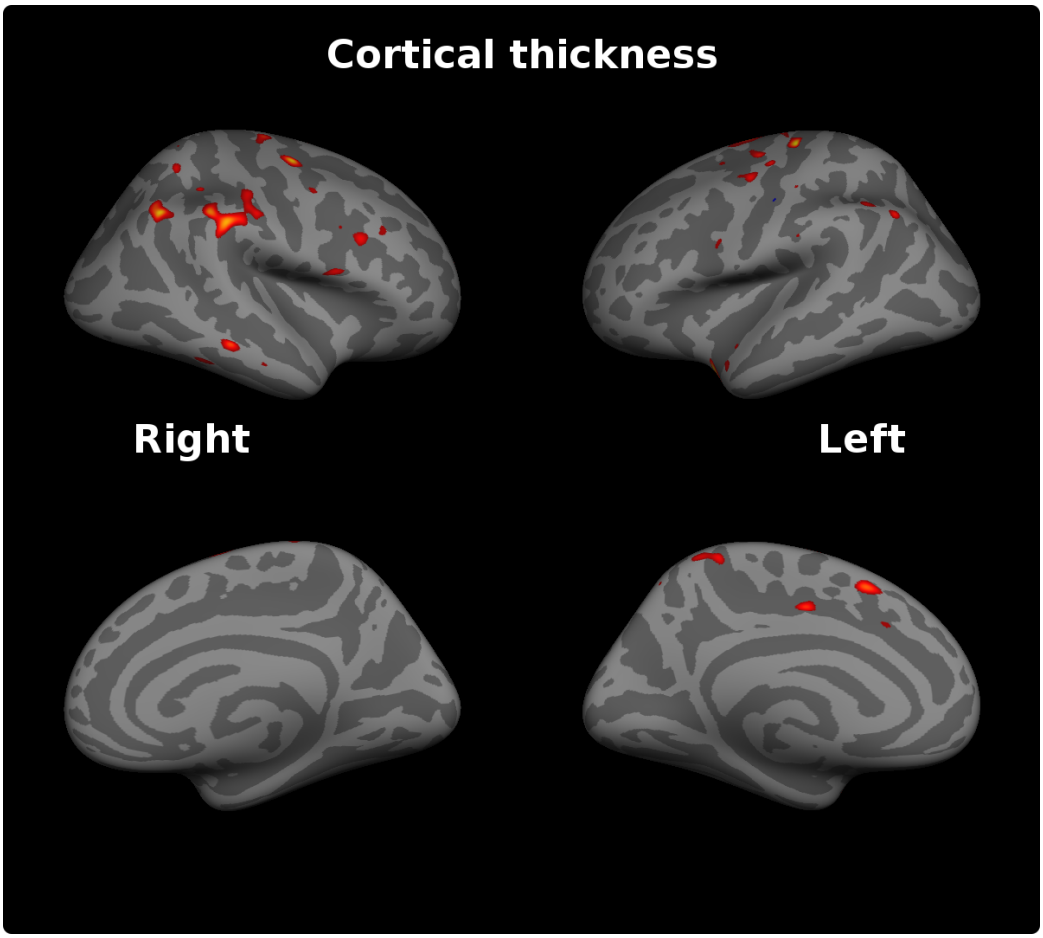

Figure 4.12: Whole brain cortical thinning within 8 months, $p < .001$ (uncorrected).

Grey matter density

Within 4 months of the initial scan, a reduction in grey matter density was detected in the right insular cortex (MNI: x = 38, y = -26, z = 18), right hippocampus (MNI: x = 32, y = -38, z = -10), left superior precentral gyrus (MNI: x = -18, y = -28, z = 54) and the cerebellum (MNI: x = 6, y = -62, z = -22). Figure 4.14 shows the extent of the degeneration and Figure 4.15 provides information about the localisation.

Within 8 months, grey matter degeneration spreads considerably involving

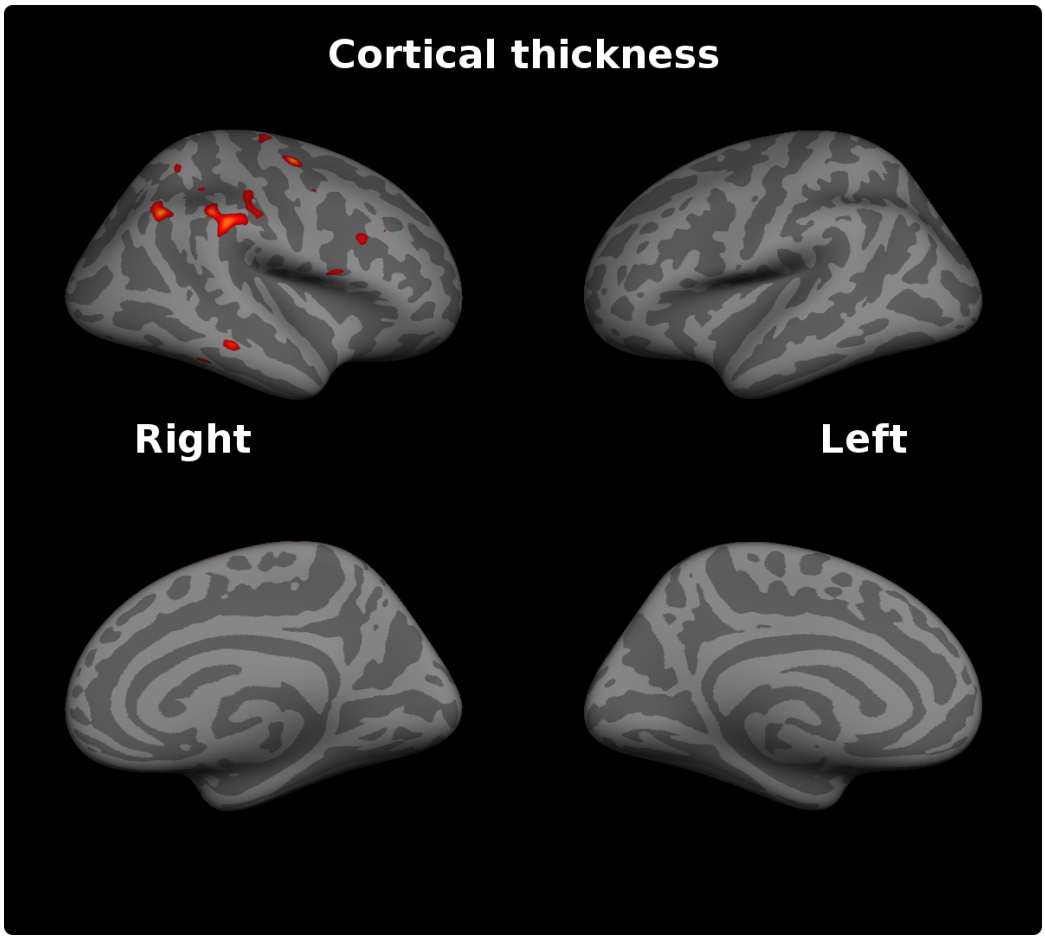

Figure 4.13: Whole brain cortical thinning within 8 months, $p < .05$ corrected using FDR.

the bilateral frontal, temporal and parietal lobes and the cerebellum. The bilateral precentral gyrus showed significant progressive changes, all $p < .001$ (FWE). Figure 4.16 displays the extent of degeneration and the exact location is shown in Figure 4.17 using a multi-slice view.

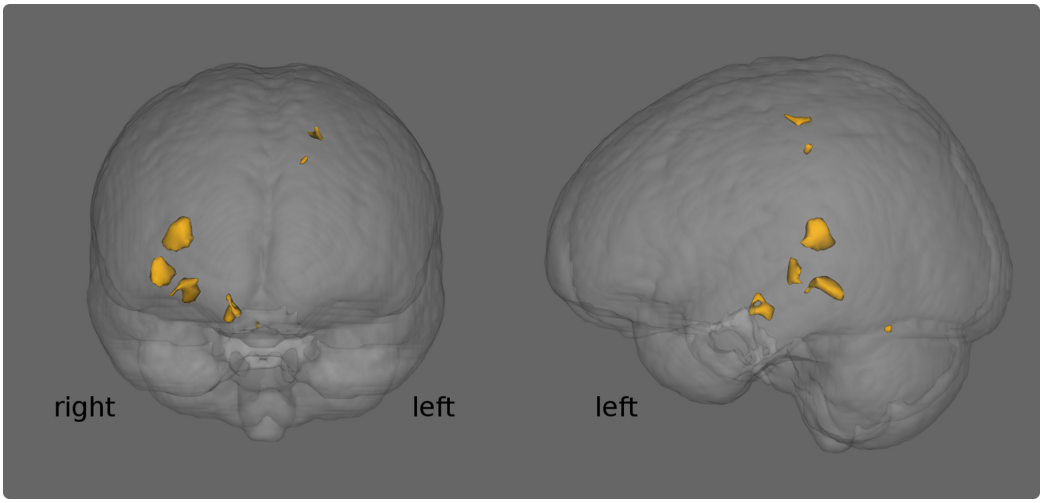

Figure 4.14: Whole-brain grey matter density loss within 4 months, $p < .05$ (FWE).

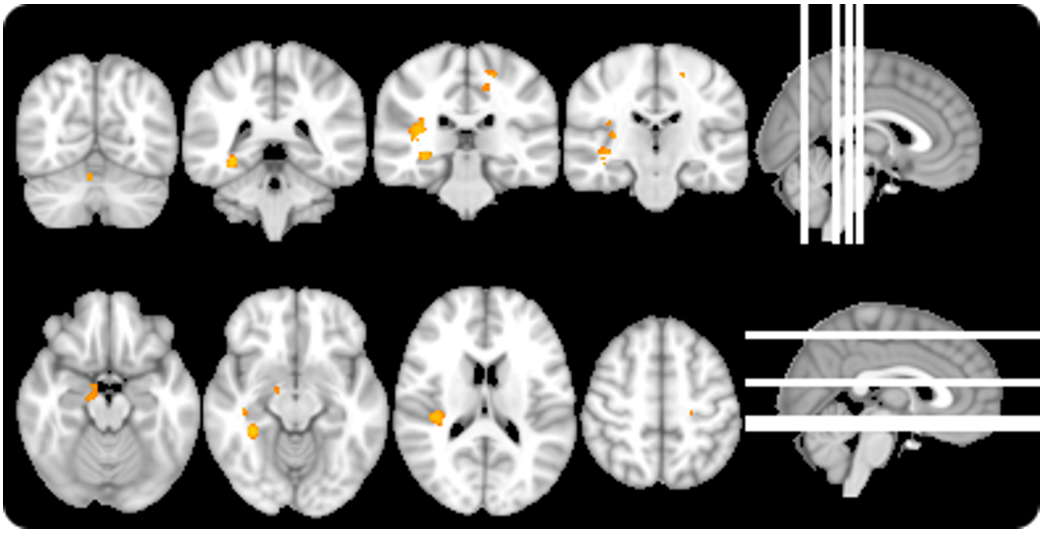

Figure 4.15: Localisation of whole-brain grey matter density loss within 4 months, $p < .05$ (FWE). Top: coronal view, MNI: y = -62, y =-38, y = -28, y = -20. Bottom: axial view, MNI: z = -22, z = -10, z = 18, z = 46. Note: The images are shown according to radiological orientation – right is on the left side.

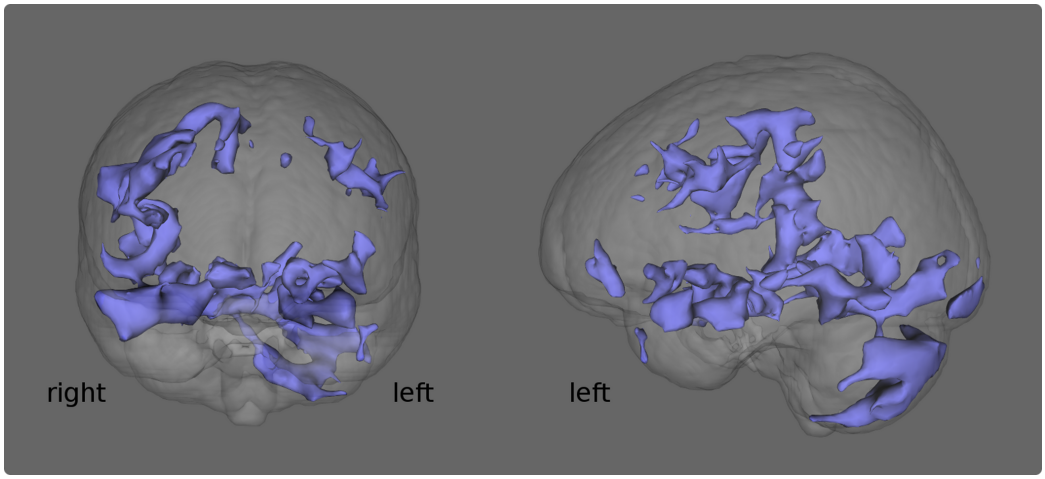

Figure 4.16: Whole-brain grey matter density loss within 8 months, $p < .001$ (FWE).

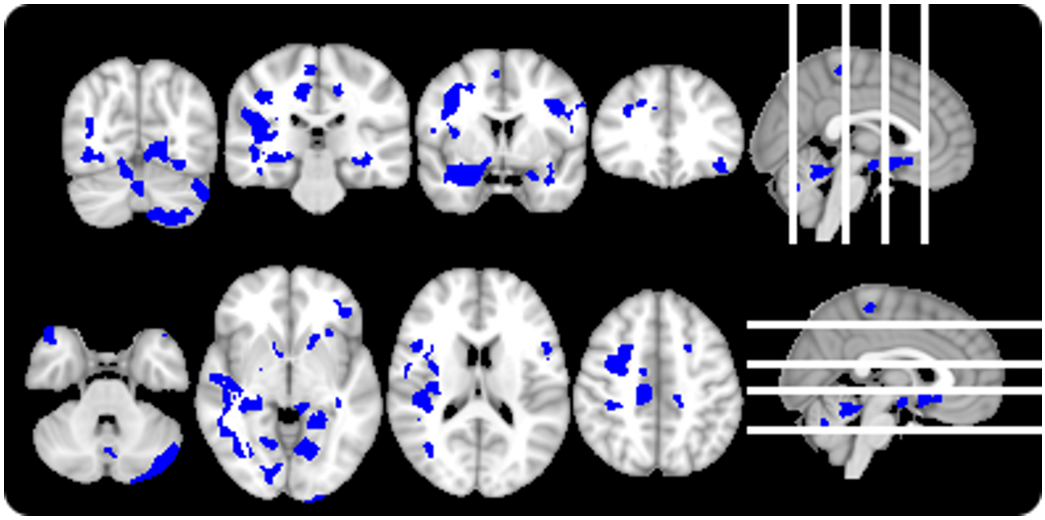

Figure 4.17: Localisation of whole-brain grey matter density loss within 8 months, $p < .001$ (FWE). Top: coronal view, MNI: y = -66, y = -26, y = 4, y = 34. Bottom: axial view, MNI: z = -32, z = -2, z = 18, z = 48. Note: The images are shown according to radiological orientation – right is on the left side.

White matter integrity

There was no significant difference between baseline and the 1st follow-up scans in any of the DTI indices.

Significant white matter degeneration was identified within 8 months after the initial scans. FA showed unilateral change within the right hemisphere: within the corona radiata, the longitudinal fasciculus, posterior thalamic radiation, and the splenium of the corpus callosum $p < .05$ (FWE). RD, MD and AD highlighted progressive unilateral change within the left hemisphere $p < .05$ (FWE). RD displayed changes within the superior and inferior corona radiata, posterior part of the superior longitudinal fasciculus and the posterior limb of the internal capsule; MD within the superior corona radiata, posterior part of the superior longitudinal fasciculus; and AD within the superior and inferior corona radiata, posterior part of the superior longitudinal fasciculus, and body of the corpus callosum (Figure 4.18 and Figure 4.19).

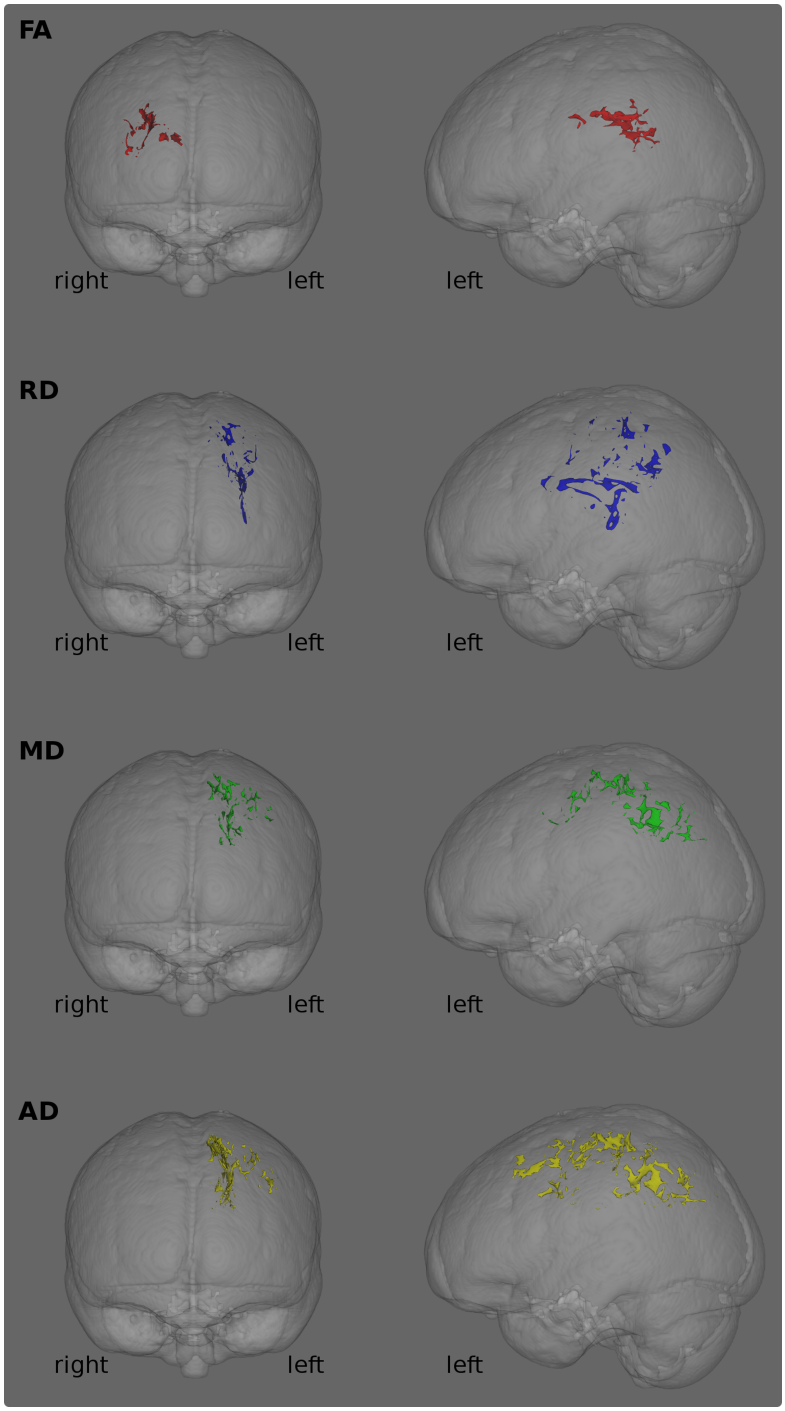

Figure 4.18: Longitudinal whole-brain white matter degeneration within 8 months at $p < .05$ (FWE). FA in red, RD in blue, MD in green, AD in yellow.

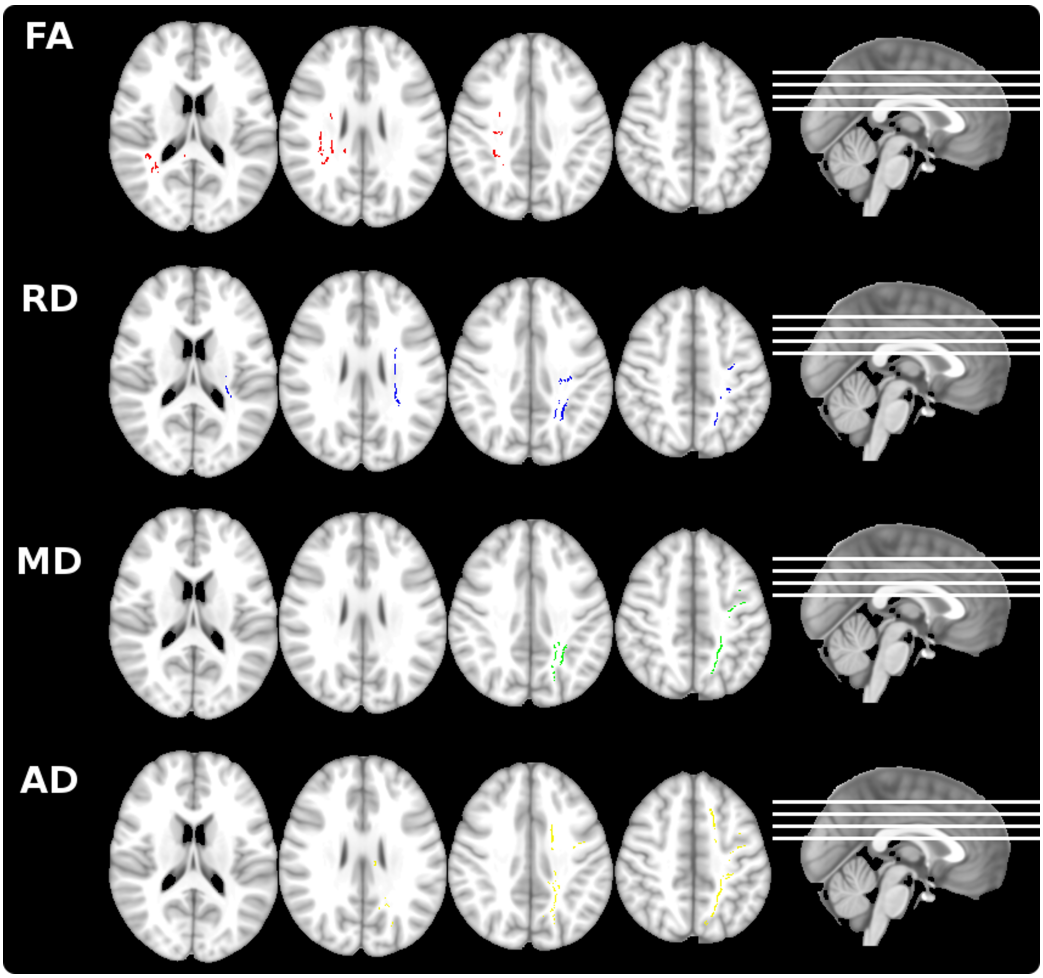

Figure 4.19: Localisation of whole-brain white matter degeneration at $p < .05$ (FWE). Order starting from the first row: FA in red, RD in blue, MD in green, AD in yellow.

4.4.5 Longitudinal analyses of presymptomatic changes

In an attempt to model pre-symptomatic change, brain areas were evaluated in patients with no corresponding functional disability. Accordingly, the patient sample was stratified based on the ALSFRS-R sub-scores; and study groups were limited to patients who did not report any bulbar impairment during any of the visits or any impairment in their lower limbs. There was no patient without upper limbs symptoms; therefore, there is no such subgroup could be created. The analysis was restricted to (1) patients without bulbar impairment and (2) patients without lower limb involvement. Table 4.3 describes the clinical and demographical profile of these subgroups.

The hypothesis was that patients without bulbar symptoms would still exhibit some structural brain changes within the bulbar representation of their motor homunculus in the inferior section of the precentral gyrus and the underlying white matter fibres, as well as in the genu of the internal capsule where the corticobulbar tracts are located. Similarly, it was hypothesised that the patients without lower limb involvement would still exhibit brain changes in the lower limb segment of their motor strips, the white matter regions subjacent to that, and the posterior limb of the internal capsule. For these ROI analyses, age and time between scans were used as covariates of no interest.

	ALS patients pre-symptomatic for bulbar involvement			**ALS patients pre-symptomatic for lower limb involvement**		
N	8			8		
Male	7			5		
Handedness (right/ left)	6/ 2			7/ 1		
Age, y (mean, SD)	56.03 (11.62)			56.63 (6.69)		
Site of onset (bulbar, spinal, respiratory)	0/ 8/ 0			3/ 5/ 0		
Disease duration onset until baseline scan, mo (mean, SD)	25.75 (29.68)			20 (13.11)		
	Baseline	**1st follow-up**	**2nd follow-up**	**Baseline**	**1st follow-up**	**2nd follow-up**
ALSFRS-R at baseline (mean, SD, max 48)	43.12 (2.7)	41.12 (3.81)	38.12 (4.48)	42.25 (1.28)	40.62 (2.45)	38.62 (3.89)
ALSFRS-R bulbar score (mean, SD, max 12)	12	12	12	9.25 (2.82)	8.5 (3.3)	8.12 (3.8)
ALSFRS-R upper limb score (mean, SD, max 12)	9.5 (1.93)	9.12 (2.23)	7.12 (2.53)	9.5 (.2)	8.75 (2.31)	7.62 (2.5)
ALSFRS-R lower limb score (mean, SD, max 8)	6.38 (2.2)	5.38 (2.92)	4.62 (3.11)	8	8	8
Time since baseline, d (mean, SD)	133 (15.52)	279.25 (34.94)	133.75 (21.25)	280.75 (42.41)		

Table 4.3: Demographic and clinical details of the presymptomatic subgroups. y = years, mo = months, d = days

Cortical thickness

None of the results in the ROI survived correction for multiple comparisons at $p < .05$ (FDR). Considering the exploratory nature of this analysis and the small size, results at $p < .01$ (uncorrected) are reported.

Patients without bulbar symptoms exhibited significant cortical thinning within 4 months in the inferior part of the right precentral gyrus corresponding to the bulbar representation of the motor homunculus. Within 8 months, thinning of the left supplementary motor cortex was also identified, Figure 4.20.

Patients without lower limb symptoms showed thinning of the superior part of the precentral gyrus within the right hemisphere throughout 4 months, and bilateral throughout 8 months was found. Throughout 8 months, thinning of the inferior part of the precentral gyrus was affected as well, Figure 4.21.

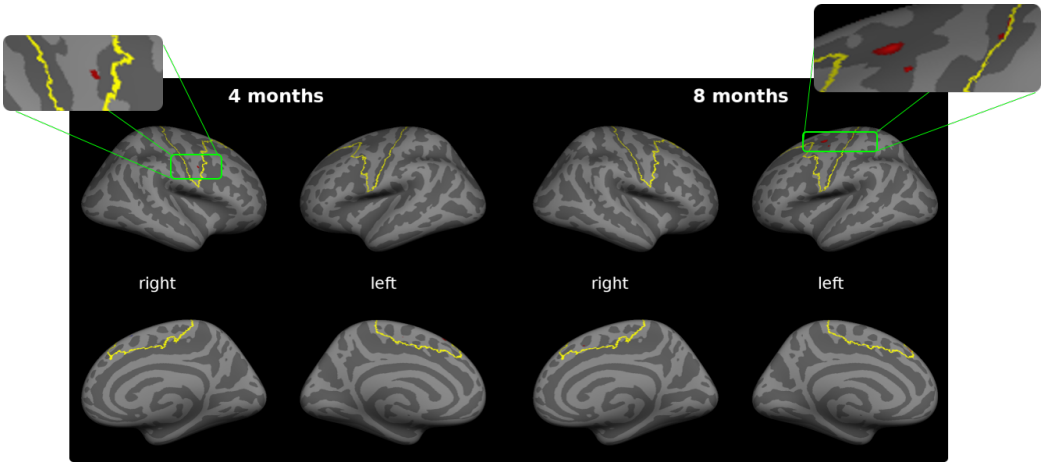

Figure 4.20: Presymptomatic cortical thinning exhibited by the patient group without bulbar symptoms.. Left: thinning within 4 months. Right: thinning within 8 months. ROI is outlined in yellow. Results are significant at $p < .01$ (uncorrected).

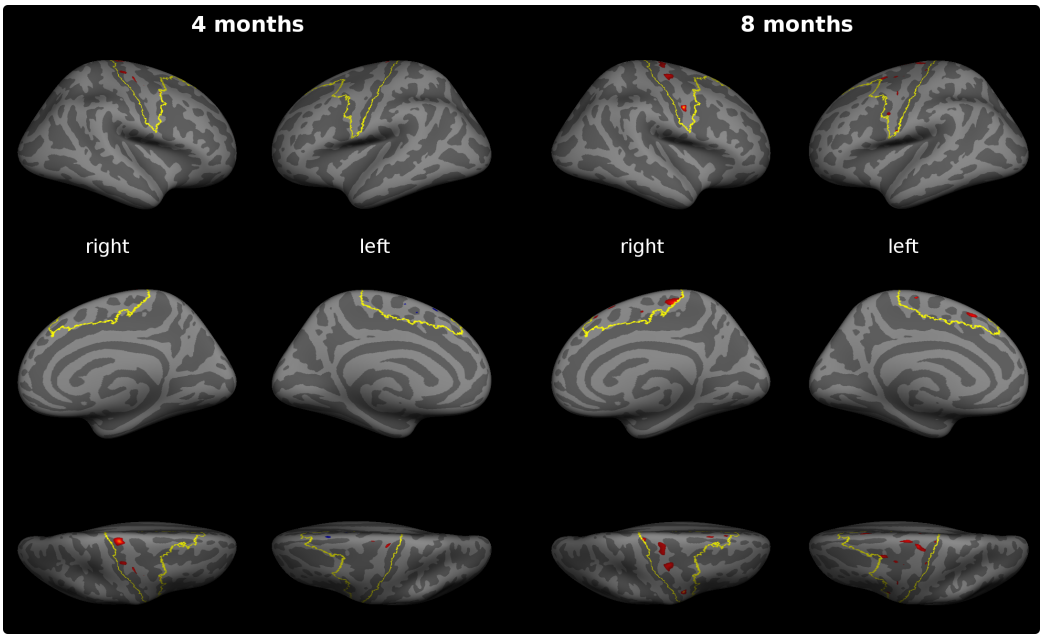

Figure 4.21: Presymptomatic cortical thinning exhibited by the patient group without lower limb symptoms. Left: thinning within 4 months. Right: thinning within 8 months. ROI is outlined in yellow. Results are significant at $p < .01$(uncorrected).

Grey matter density

Only comparing the baseline scans to the 1st follow-up scans of the bulbar subgroup revealed a significant result in the ROI. A small region of significant loss of grey matter density was found within the right precentral gyrus representing the arm muscles (MNI: x = 44, y = -30, z = 62) at $p < .05$ (FWE).
No significant difference was found between the baseline scans and any other follow-up scans for the bulbar or lower limb subgroups.

White matter integrity

Patients without bulbar impairment showed progressive change between baseline and follow-up scans within the left lateral fibres of the corona radiata including the inferior fibres innervating the precentral gyrus highlighted by

RD, MD and AD, Figure 4.22. Using MD the effect was found bilateral between baseline and 1st follow-up. Figure 4.24 and 4.25 show the extent and localisation of these changes. FA highlighted no differences between the baseline scans and any of the follow-up scans in the ROI. Progressive RD and MD alterations were identified in the genu of the left internal capsule between the baseline and the 2nd follow-up scan ($p < .05$ (FWE), Figure 4.23).

Patients without lower limb involvement did not show longitudinal changes between their baseline scans and any of the follow-up scans ($p > .05$, FWE).

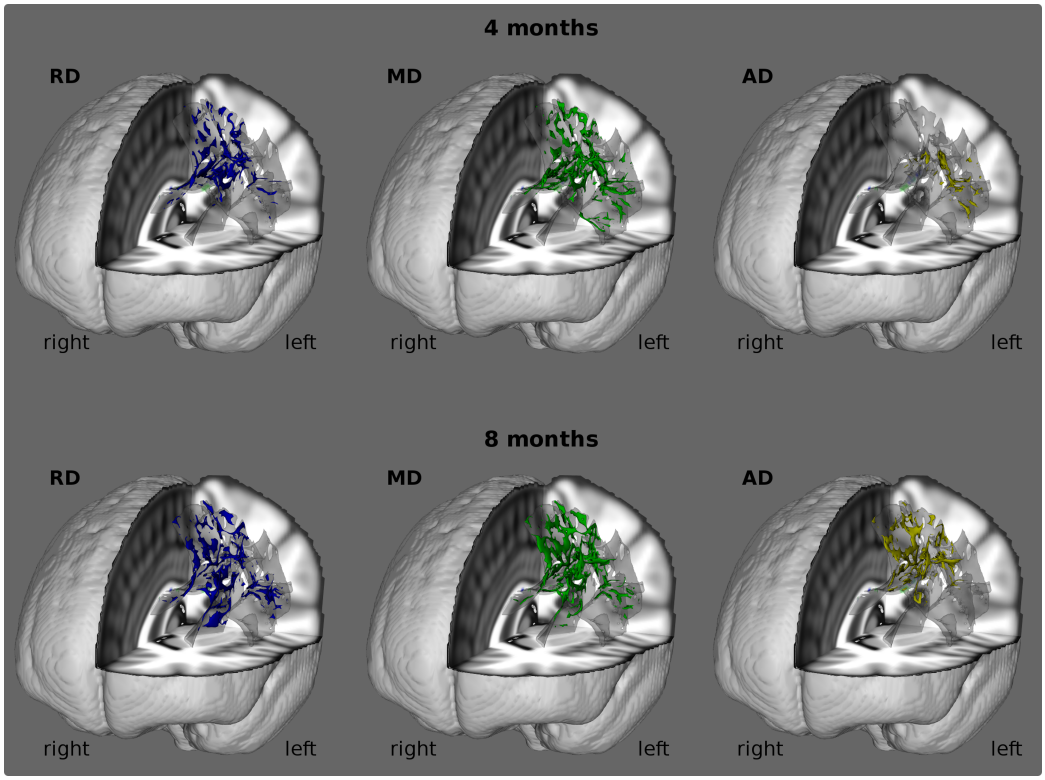

Figure 4.22: Presymptomatic white matter degeneration within 4 months (top) and 8 months (bottom) exhibited by the patient subgroup without bulbar symptoms, $p < .05$ (FWE). Blue = RD, Green = MD, Yellow = AD.

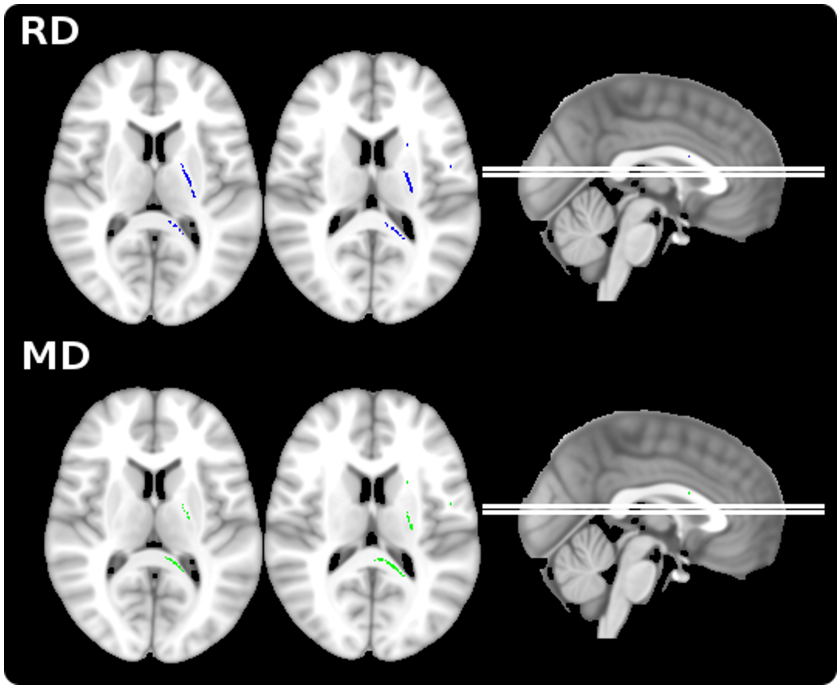

Figure 4.23: Presymptomatic white matter degeneration within the genu internal capsule within 8 months exhibited by the patient subgroup without bulbar symptoms, $p < .05$ (FWE), Axial view: MNI: z = 11, z = 15.

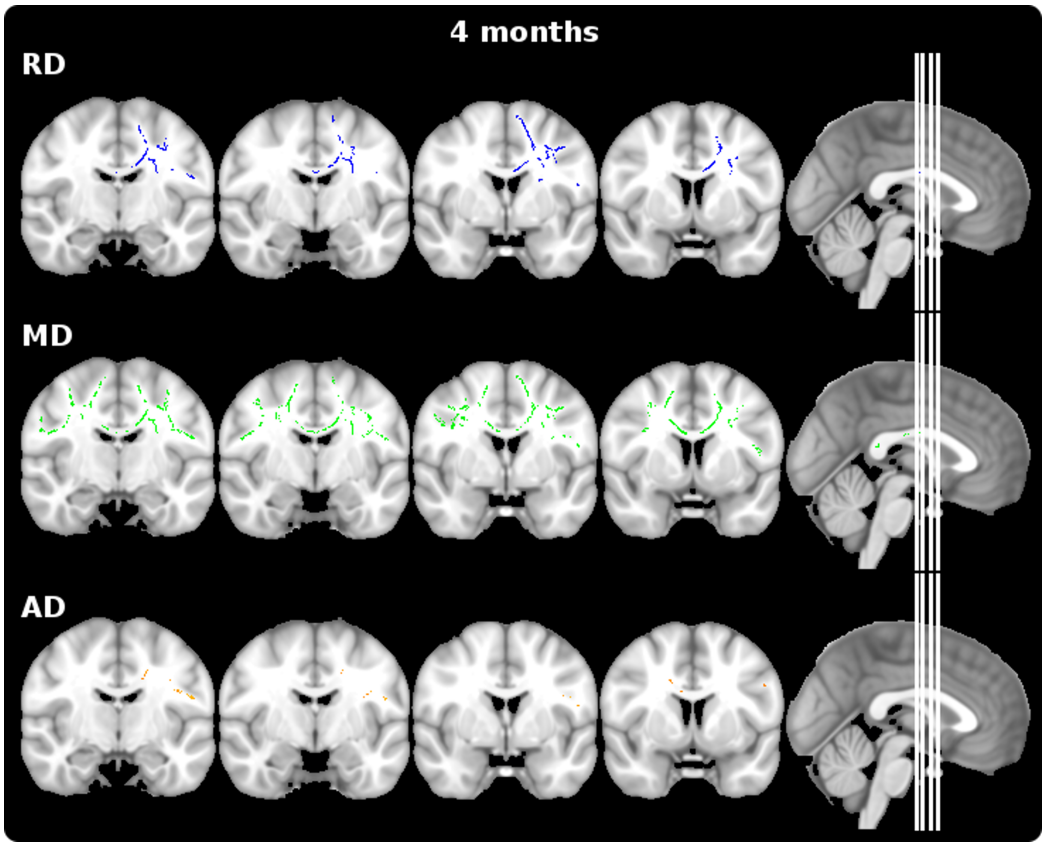

Figure 4.24: Localisation of presymptomatic white matter degeneration within 4 months exhibited by the subgroup without bulbar symptoms, $p <$ .05 (FWE). Coronal view: y = -9, y = -5, y = 1, y = 6. RD in blue, MD in green, AD in yellow.

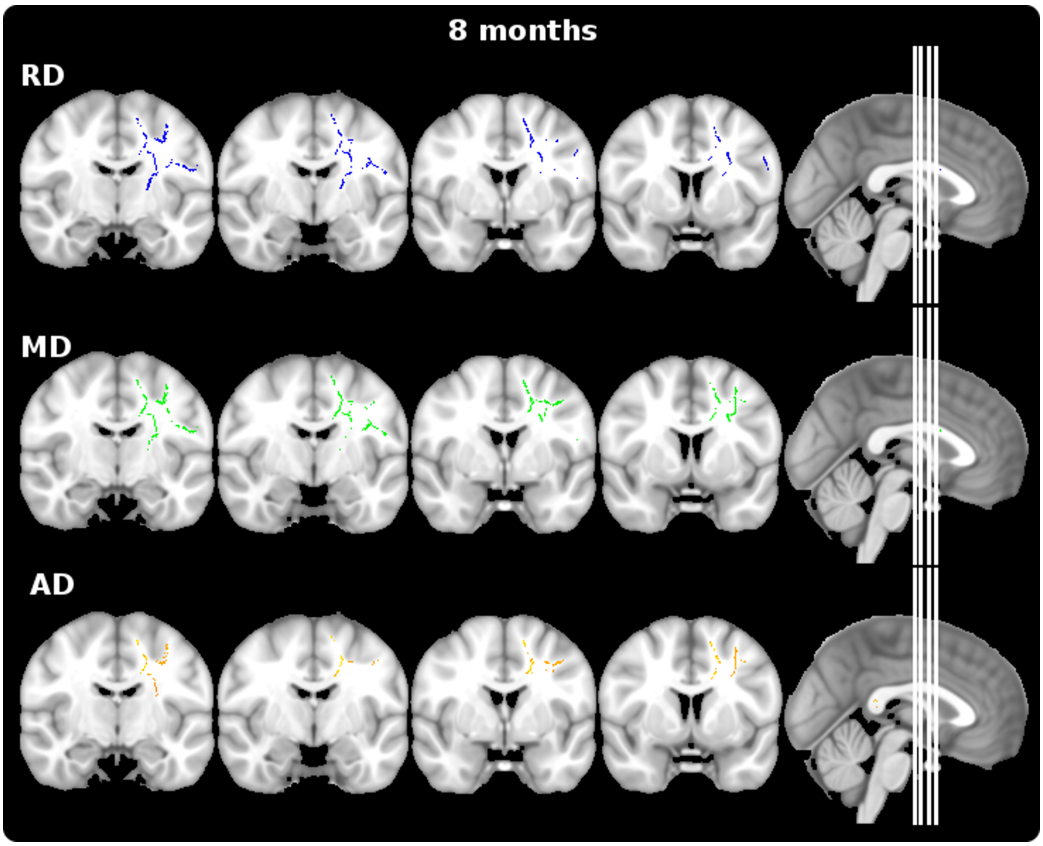

Figure 4.25: Localisation of presymptomatic white matter degeneration within 8 months displayed by the subgroup without bulbar symptoms, $p <$ .05 (FWE). Coronal view: y = -9, y = -5, y = 1, y = 6. RD in blue, MD in green, AD in yellow.

4.5 Discussion

The aim of this chapter was to explore the role of MRI as a disease monitoring biomarker. Validated monitoring markers are indispensable for clinical trials to objectively evaluate response to therapy.

Only voxel-based morphometry was able to detect neurodegenerative change within 4 months. This change was located within the medial precentral gyrus. In 8 months from the initial scan, each method was able to highlight significant progressive changes. Cortical thinning and a reduction of grey matter density occurred throughout the bilateral precentral gyrus and supplementary motor cortex. FA decreased within the posterior limb of the internal capsule, and RD, MD and AD increased within left lateral fibres of the superior corona radiata. One could conclude that for an 'average' patient a 4-month follow-up period is not enough to exhibit degenerative change measurable with current technology.

In their baseline scans, ALS patients already showed significant changes in their white matter integrity. Consequently, it is not surprising that no significant further change was detected throughout the 4-month follow-up period and only a small additional change was detected throughout the 8-month period. White matter loss likely exhibited a ceiling effect early during the disease course.
The baseline scans on the other hand revealed only limited grey matter loss and no significant cortical thinning, which explains the considerable progressive changes throughout the 8-month period.
Comparing the 2nd follow-up to the healthy control group further supports the notion of ceiling effect for white matter changes. At the 2nd follow-up loss of white matter integrity is severe, and loss of grey matter integrity and cortical thickness has become more pronounced. In conclusion, most segments of the corticospinal tract display a ceiling effect.
These findings suggest that radiologically detectable white matter degenerations occur earlier than grey matter pathology during the course of the

disease. Accordingly, white matter may be a superior diagnostic biomarker whereas grey matter may be more useful as a monitoring biomarker.
This is further supported by the results of the "presymptomatic" sample. Patients were selected based on the absence of bulbar or lower limb disability. Considering the natural course of ALS, these patients can be regarded as presymptomatic for the involvement of those domains as they are more than likely to experience some degree of bulbar or lower limb symptoms and anatomically corresponding brain alterations at a later stage of their disease.

DTI and the cortical thickness analyses were able to capture degeneration in these regions before clinical disability. ALSFRS-R has its limitations as a clinical proxy, as it is a self-reported questionnaire. It may be affected by psychological factors, insight, personality and mood
Despite its limitation, ALSFRS-R is currently the gold standard instrument used in clinical trials.[2] While trained clinicians may detect subtle impairment before patients report a specific symptom, the findings suggest that MRI may be used as a useful objective measure, capturing degeneration earlier than ALSFRS-R.

Whilst white matter analyses were only able to capture presymptomatic bulbar involvement, cortical thinning was found in both subgroups. A drawback of the present sample is that, even though these subgroups are likely to lose the function of their bulbar or lower limb muscles, it is unknown when the first symptoms may appear.

There are multiple ways to measure cortical morphology: cortical thickness, cortical surface, cortical volume and grey matter density or concentration (Ashburner and Friston, 2000; Fischl and Dale, 2000). By nature, these measures are related to each other. Cortical volume is the product of cortical thickness and cortical surface (Winkler et al., 2010). The current project focused on cortical thickness as it has been successfully shown to capture precentral gyrus thinning in ALS (Roccatagliata et al., 2009; Agosta et al., 2012;

[2]http://www.als.net/als-research/als-clinical-trials/

Kwan et al., 2012; Verstraete et al., 2012; Schuster et al., 2013, 2014a,b). Furthermore, the results are independent of the folding pattern in a biological meaningful metric, i.e. thickness in mm.
Grey matter density reflects difference in cortical thickness and the amount of cortical folding. A meta-analysis of studies on whole-brain grey matter density revealed that only 24%-50% of the considered studies were able to highlight precentral gyrus atrophy (Chen and Ma, 2010). Even in the whole-brain analysis, atrophy of the precentral gyrus was measureable with both methods within 8 months. But only analysing grey matter density, a significant loss was measured within 4 months.
Due to the heterogeneity of the sample, the relationship between disease stage, grey matter brain changes and analysis technique remains unclear. Future research is needed to disentangle which technique is most sensitive during which stage of the disease.

Based on the present results, it appears that the most vulnerable brain regions are the lateral fibres of the corona radiata. Several MRI indices detected degeneration in the lateral fibres of the corona radiate both cross-sectionally and longitudinally.
Grey matter measures of the cerebellum may also be a good biomarker candidate. Overall, the cerebellum is less studied in ALS (Prell and Grosskreutz, 2013). Even though this study did not find significant white matter pathology in the cerebellum over time, grey matter changes were significant and warranting further studies.

The whole brain analyses readily confirmed precentral gyrus atrophy and the superior corticospinal tract pathology. Moreover, frontal, temporal, parietal lobe and the cerebellar changes were detected. The corona radiata, the superior longitudinal fasciculus and the posterior limb of the internal capsule also showed changes. It is striking that the degeneration is limited to one hemisphere. Whereas grey matter atrophy is more pronounced in the right hemisphere based on both the cortical thickness analysis and the voxel-based morphometry, white matter degeneration was limited to the left hemisphere

measured by radial, mean and axial diffusivity.

It is established that cortical thickness differs between the hemispheres in healthy individuals: The average cortical thickness of the right hemisphere is smaller than in the left hemisphere (Salat et al., 2004). This may suggest a more vulnerable right hemisphere regarding disease related changes, and may be reflected in these results.

Patients typically report unilateral symptom onset and symptoms subsequently spread to the contralateral side (Ravits and La Spada, 2009; Ravits et al., 2007). This observation may have implications to longitudinal analyses. The brain changes in the hemisphere corresponding to the side of onset may initially be more pronounced, but as the disease progresses this difference may decrease.

A key question of longitudinal ALS studies is what time interval is necessary to identify progressive pathological change. Whether or not significant progressive change is detectable is a function of the time interval between scans and sample size. It is furthermore affected by the pulse sequence parameters. If either the time interval or the sample size is increased the likelihood of finding a significant changes increases as well. Most published longitudinal studies in ALS have a limited sample sizes. It is clear that a longer time interval is associated with more significant findings. For example, focusing only on longitudinal ALS study which evaluated multiple MRI measurements: Cardenas-Blanco et al. (2016) concluded, based on a sample of 34 ALS patients with an average ALSFRS-R of 40.2 at baseline which were scanned three times within 6 months, that DTI was successful to track degenerative change, whereas cortical thickness and VBM was not. This is in contrast to Menke et al. (2014) who, based on 27 patients with an average ALSFRS-R of 35 at baseline which were scanned twice within 6 months to 2 years, concluded that only grey matter degeneration was detectable over time. Finally, Kwan et al. (2012) based on 9 ALS patients with an average ALSFRS-R score of 40.2 at baseline who were scanned $\sim$1.5 years apart, reported cor-

tical thinning and grey matter volume loss of the precentral gyri, whereas fractional anisotropy of the corticospinal tract remained stable.

There may be no simple answer which time interval is optimal; it depends on the specific research question and should be adjusted accordingly. If the focus is on patients with fast progression rates the interval has to be much shorter. These present findings need to be interpreted with care as in this sample, the baseline scans were acquired on average 2 years after the initial symptoms. A larger sample may be needed, preferably scanned shortly after the diagnosis, to elucidate whether the sensitivity of the various MRI measures depends on disease stage.

4.5.1 Limitations

The present sample was diagnosed 2 years prior to their initial scans and was too small to subdivide into further subgroups. For this reason, no conclusions can be drawn regarding slow and fast progressors and phenotype- or genotype-specific patterns of progression.

4.5.2 Future directions

Future research need to focus on the timeline when the changes occur within each segment of the brain. It needs to be further evaluated which method is the most sensitive to detect early changes.

4.6 Conclusions

In conclusion, this study captured longitudinal changes in disease-specific brain regions. The main research question was to determine whether MRI could be used as a monitoring marker for clinical trials by exploring the time

course of ALS-related brain changes. A clinical trial would be similar to this study including patients at various stages of the disease. The biomarker would have to be useful for an average patient. Based on the presented results, grey matter density of the precentral gyrus or the cerebellum may be the most likely monitoring biomarker candidate. White matter changes occur earlier in the course of the disease and consequently are better suited as diagnostic markers.

Chapter 5

Development of an imaging based automatic diagnostic protocol for ALS using disease-specific pathognomonic features

The research study described below has been published in the peer reviewed Journal PloS One (Schuster et al., 2016b).

5.1 Introduction

5.1.1 Diagnostic delay

The initial presentation of ALS varies substantially making an early diagnosis and accurate prediction of prognosis difficult (Kraemer et al., 2010). The average diagnostic delay between symptom onset and definite diagnosis is 9 - 16 months, and this is independent of the health system in place (Chiò, 1999; Cellura et al., 2012). A number of barriers for a timely diagnosis have been identified including delayed referral to specialist neurologists, misdiagnosis

of the symptoms to other conditions and consequently unnecessary interventions (Househam and Swash, 2000; Donaghy et al., 2008). Carpal tunnel syndrome, degenerative spinal conditions are just some of the commonest early misdiagnoses and interventions such as lumbar laminectomies, carpal tunnel release surgery, immunoglobulin therapy are not uncommon prior to the diagnosis of ALS (Cellura et al., 2012).

More importantly, diagnostic uncertainty delays the introduction of neuroprotective therapy and recruitment to pharmaceutical trials (Wokke, 2009). In clinical practice MRI is mainly used to exclude intracranial and spinal pathologies which may mimic ALS. Cross-sectional studies of ALS have consistently confirmed extensive grey and white matter degeneration at a group-level including the precentral gyrus and frontal cortex, the basal ganglia, the corticospinal tracts and the corpus callosum (Chiò et al., 2014). The evaluation of these structures at an individual-level has proven more challenging and research-based MRI biomarkers are not readily applicable to clinical practice (Bede and Hardiman, 2014). Until recently, it has been challenging to confirm ALS-specific patterns of neurodegeneration in a single MRI scan as part of the diagnostic process.

5.1.2 Classification in Neurodegeneration

In recent years, several attempts have been made to reliably discriminate various neurological and psychiatric conditions from healthy controls based on imaging data from single individuals. The most commonly used statistical methods include support-vector machines or receiver-operator-curves for categorical binary classification of single individuals often based on a single imaging marker. These studies pave the way for the development of diagnostic MRI biomarkers (Orrù et al., 2012; Teipel et al., 2015a).

Computer aided diagnostic tools have been previously proposed for neurodegenerative conditions. Table 5.1 lists ALS-related classification studies pub-

lished before November 2015 (Filippini et al., 2010; Bashat et al., 2015; Gupta et al., 2012; Foerster et al., 2013; Welsh et al., 2013; Pagani et al., 2014; Van Laere et al., 2014). Foerster et al. (2013) performed an individual patient data meta-analysis evaluating the diagnostic accuracy of diffusion tensor imaging (DTI). The assessment of one brain region and one imaging measure from pooled data of 11 studies suggested limited discriminative power. Smaller studies on the other hand, reported relatively good specificity and sensitivity. Welsh et al. (2013) report 71% accuracy for disease state classification based on resting-state functional MRI data. The study provided a proof of concept and highlights that a single imaging measure of the single technique may not be reliably sufficient to separate ALS from healthy ageing.

With few exceptions, the commonest shortcomings of classification studies in ALS include reliance on a single imaging measure, evaluation of a single anatomical structure and a categorical classification outcome instead of probability values. Additionally, classification studies often restrict their discriminating features to significant voxels only, rendering their model sample-specific i.e. 'over-fitting' and hindering model generalisability. Moreover, classification models are seldom cross-validated in an independent sample.

Authors	**Year**	**Journal**	**Model size**	**Features**	**Sensitivity**	**Specificity**
Filippini et al.	2010	Neurology	24 ALS, 24 HC	FA, RD, GM	92%	88%
Ben Bashat et al.	2011	ALS	26 ALS, 22 HC	DTI	87.7%	85%
Gupta et al.	2012	Journal of Neurological Sciences	44 ALS, 29 HC	demographic, biochemical variables	93.2%	86.2%
Foerster et al.	2013	Acad Radiol	221 ALS, 187 HC	FA	68%	73%
Welsh et al.	2013	Frontiers in Human Neuroscience	32 ALS, 31 HC	rs-MRI	NA	NA
van Laere et al.	2014	JAMA Neurol	59 c9orf72 neg, 11 c9orf72 pos, 7 PLS, 4 PMA, 20 HC	PET	89.8%	85%
Pagani et al.	2014	Neurology	195 ALS, 40 HC (control group with a PET scan negative for ontological disease)	PET	88.7%	82.5%

Table 5.1: Classification studies in ALS.

5.1.3 Objective

The objective of this study was to develop a robust, imaging based automatic diagnostic protocol for ALS, which determines the probability of a single MRI data set representing changes consistent with ALS based on multiple imaging indices of multiple 'disease-defining' anatomical structures.

Based on the available literature, it was hypothesised that the diagnostic accuracy of a classification models may be increased by incorporating multiple imaging indices of multiple disease-defining brain regions, and that instead of binary categorical classification, it is feasible to provide more meaningful diagnostic probability scores.

5.2 Methods

Figure 5.1 outlines the methodology. First, imaging data were divided into a training sample to develop the probability algorithm, and a validation sample to access its generalisability. Discriminating input features were selected based on group comparisons between the patients and controls of the training sample. The selected features were adjusted for age-related differences (Koikkalainen et al., 2012). Subsequently, a binary logistic regression was conducted. The resulting algorithm was then validated in the independent validation sample and further assessed based on the follow-up scans of these participants. The sensitivity, specificity and accuracy of this approach were evaluated in each sub-cohort separately.

5.2.1 Participants

The study is based on 147 participants, i.e. 81 patients with classical ALS and 66 HC. Participating patients were diagnosed according to the revised El Escorial criteria (Brooks et al., 2000). Patients with a co-morbid diagnosis of frontotemporal dementia according to the Rascovsky Criteria (Rascovsky

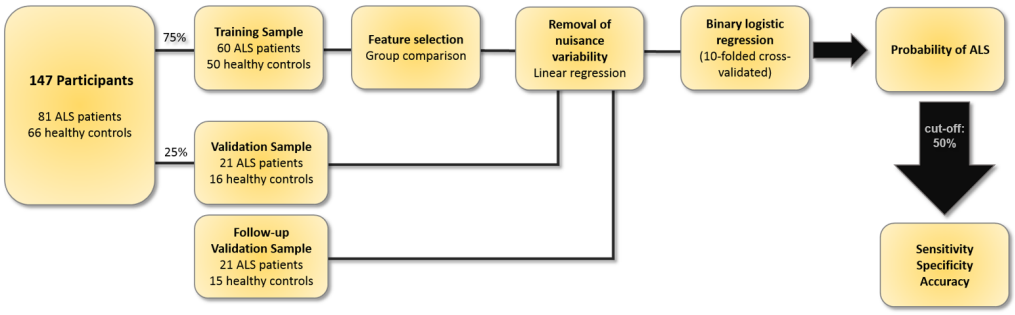

Figure 5.1: Flowchart of the study method.

et al., 2011) were excluded because of the confounding effects of imaging changes (Chang et al., 2005; Lillo et al., 2012).

The classification model is validated with an independent sample to assess generalisability of the approach, therefore, 75% of the data was allocated to the training sample and 25% as the validation sample. For a subset of the sample, the scans were repeated after at least 4 months. It was hypothesised that on follow-up, patients are more likely to be correctly classified, since ALS-related degeneration is expected to be more pronounced. The control sample allows to further evaluate the reliability of the algorithm. The specificity should be in a similar range as calculated based on the validation sample.
For 52 patients and 15 HC, follow-up scans were available. Of these, 21 patients for the validation sample and 15 HC were randomly selected (hereafter called follow-up validation sample).

5.2.2 Model Creation

The training sample consists of a group of 60 ALS patients and 50 age- and gender matched healthy controls. Their socio-demographic and clinical details of this cohort is summarised in Table 5.2.

	ALS patients	Healthy controls	p-value
N	60	50	
Male sex, n	39	24	$p = .10$
Age, yrs (mean, SD)	59.9 (10.88)	60.6 (8.8)	$p = .68$
Handedness (r/ l)	52/ 8	47/ 3	$p = .33$
Disease duration, months (mean, SD)*	26.1 (19.5)		
Type of onset (bulbar/ spinal/ respiratory)	19/ 40/ 1		
ALSFRS-R (mean, SD)	38.2 (6.2)		

Table 5.2: Socio-demographic and clinical data of the training sample. *disease duration from symptom onset until data of scan

Selection of Input Variables - Feature reduction

In order to develop a classifier based on neuroimaging data, one has to face the curse-of-dimensionality (Bellman, 1961). It refers to the fact that the number of variables (in this case voxels) used in the classifier outnumber the number of observations (i.e. the sample size). A good generalisation of a model with a large number of variables (also called features) requires a larger number of observations. Otherwise, one runs the risk of overfitting. This implies that the model follows the error or noise within the data too closely and is, therefore, not able to make reliable prediction for new data. To reduce the risk of overfitting a model, one can apply one of various feature reduction techniques prior to the model creation.

I selected the most relevant features by identifying brain changes which precede the diagnosis of ALS. This was done conducting a group comparison between ALS patients and healthy controls using age, gender and disease duration (from the date of their diagnosis until the date of the scan) as covariates of no interest. The objective was to identify brain regions which degenerated prior to the diagnosis of ALS independent of the patient's age and gender. For a diagnostic protocol, it is important to mimic a clinical

setting, thus, to focus on brain changes appearing prior to the definite diagnosis of ALS.

The affected brain areas highlighted by this analysis were divided into subregions according to the underlying anatomical structures. This was done in accordance with different brain atlases and is described in more detail below. The advantage of using an atlas based parcellation is its good interpretability and general versatility. It allows interpreting the results within a clinical framework. It, furthermore, facilitates the generalisation of the approach to different centres and the inclusion of other neurodegenerative diseases which may spare these brain structures. Overall, the model does not reply on the identified pattern of significant change which strongly depends on the training sample.

The average value of the anatomical structures was extracted and used as input features in the classification approach. The masks to extract one single value per structure were stored to be applied to future data (i.e. an independent validation sample).

Grey matter - VBM

A voxel-based morphometry (VBM) analysis of structural imaging data was carried out using FSL. Images were brain-extracted, tissue-types were segmented and aligned to Montreal Neurological Institute 152 standard space using non-linear registration. A study-specific grey matter template was created including 16 randomly selected ALS patients and 16 age- and gender-matched healthy controls (ALS: male = 8, mean age = 62.9 years $\pm$ 9.3; HC: male = 8, mean age = 62.3 years $\pm$ 9.3; p = .85). Next, all native grey matter images were non-linearly registered to the study-specific template and modulated to correct for local contraction or enlargement due to the non-linear component of the spatial transformation. An isotropic Gaussian kernel (σ = 3 mm) was used to smooth the modulated grey matter images.

A voxel-wise generalised linear model was applied to determine differences between ALS patients and healthy controls with age, gender and disease duration as nuisance variable using permutation-based non-parametric testing (10,000 permutations). The significance level was set at $p < .05$, corrected for multiple comparisons using family-wise error (FWE).

A trend for a significant difference between patients and controls was identified within the precentral gyrus based on the Harvard-Oxford atlas (FSL Harvard-Oxford atlas, Desikan et al. (2006), at $p < .15$ (FWE). Figure 5.2 shows statistically significant regions and the corresponding brain mask. The average grey matter density was extracted using FSLUTILS (fslmeants). In summary, two GM features were selected – the left and right precentral gyrus.

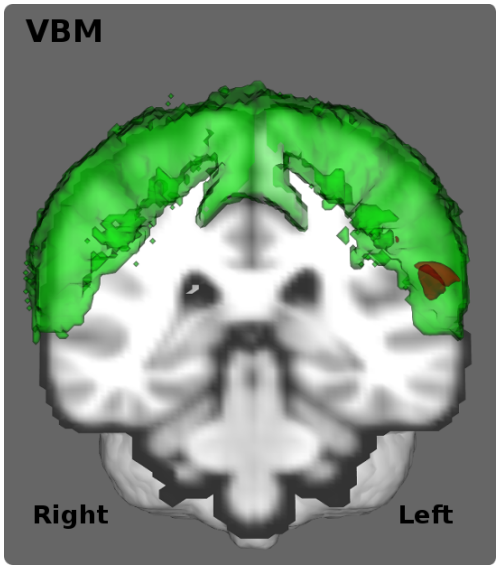

Figure 5.2: VBM - Grey matter feature selection. Grey matter (in red) affected preceding the diagnosis of ALS ($p < .15$, FWE) and the corresponding label for the precentral gyrus (in green).

White matter - DTI

Diffusion weighted images were pre-processed including eddy current corrections, motion correction, brain-tissue extraction using FSL (Smith et al., 2006). A diffusion tensor model was fitted at each voxel, generating maps of FA, RD, MD and AD. Each dataset was aligned to standard-space images and each subject's aligned FA data was projected onto the mean FMRIB58 skeleton representing the common white matter tracts.

ALS patients were compared with healthy controls correcting for age, gender and disease duration using a voxel-based tract-based generalised linear model and permutation-based non-parametric testing with 10,000 permutations. The threshold-free cluster enhancement (TFCE) method (Smith and Nichols, 2009) was applied and the significance level was set at $p < .05$, corrected for multiple comparisons using the family-wise error (FWE) method. Significant differences were detected within the corticospinal tract highlighted by FA or RD at $p < .01$ (FWE), and by MD at $p < .05$ (FWE). There was no significant difference in AD between patients and controls.

Analogue to the GM analysis, features were defined as the brain structures which were significantly different between patients and controls (based on the Johns Hopkins University, FSL JHU atlas: JHU-ICBM-labels-1mm.nii.gz; (Oishi et al., 2008)).

FA and RD were selected, as these are the most recognised markers of white matter change in ALS, using a significance threshold of at $p < .01$, FWE (cf. Chapter 3). The FSL Johns Hopkins University atlas (FSL JHU atlas: JHU-ICBM-labels-1mm.nii.gz) was used for spatial segmentation, which consists of 48 white matter tracts labels created based on the diffusion tensor maps from 81 subjects (Oishi et al., 2008). As it does not include the lateral fibres of the corona radiata, this label was created manually (SUP-CR). The same labels were used in a previous study described in Chapter 3 (Schuster et al., 2016a). The average value was retrieved separately for the left and right

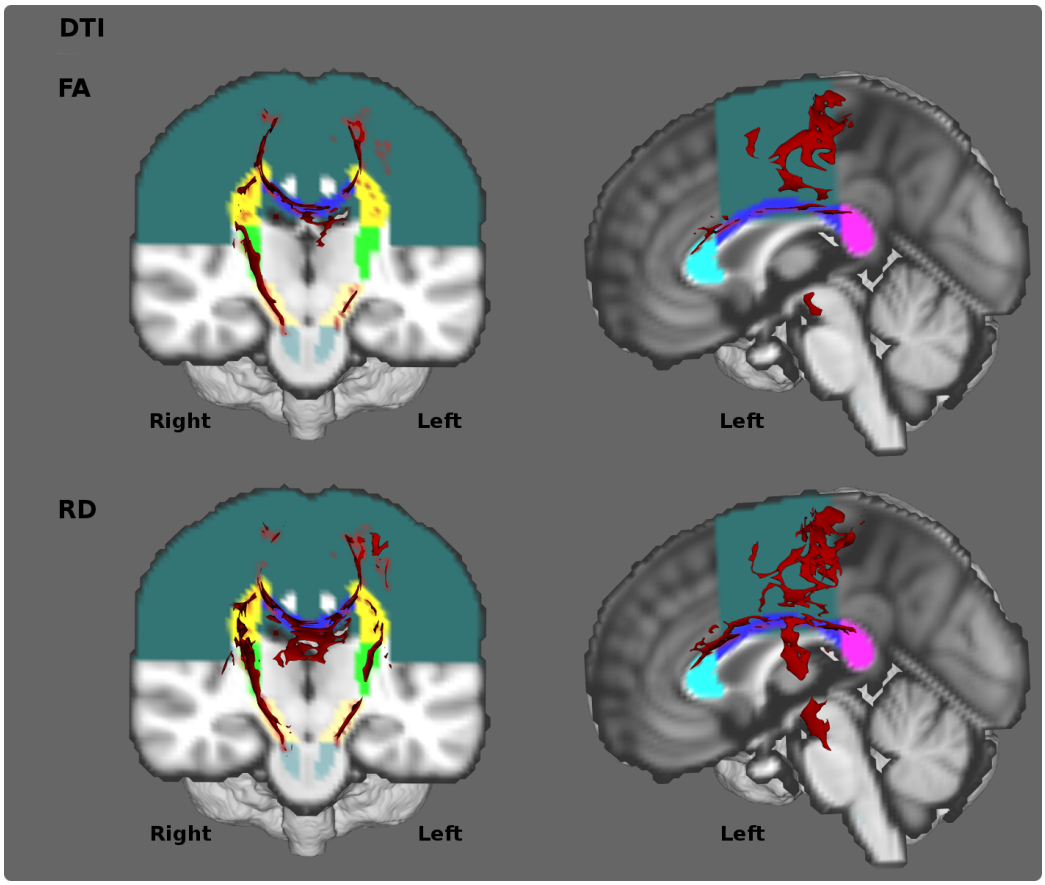

Figure 5.3: DTI - White matter feature selection. Top: Factional anisotrophy (FA) group comparison results are shown in red. Bottom: Radial diffusivity (RD) group comparison results are shown in red. The underlying anatomical labels colour coded as follows: dark green - lateral fibres of the corona radiata, blue - body of the corpus callosum, turquoise - genu of the corpus callosum, pink – splenium of the corpus callosum, yellow – inferior corona radiata, green - the internal capsule, light yellow - bilateral mesencephalic cruri, grey – inferior corticospinal tract.

hemispheres.

The white matter data were reduced to 26 features: average FA and the average RD of the genu (gCC), the body (bCC) and the splenium of the corpus callosum (sCC), the left and right corticospinal tract (CST), mesencephalic cruri (ME), limbs of the internal capsules (IC), the corona radiata (CR) and

the lateral fibres of the corona radiata (SUP-CR).

Figure 5.3 depicts the results and the corresponding brain masks. The average diffusivity value of each brain structures was extracted for each participant using FSLUTILS (fslmeants).

Validation Sample

The demographic and clinical profile of the validation sample is presented in Table 5.3. The pre-processing steps of the independent validation sample were analogous to the pre-processing pipeline of the training sample.
For grey matter analyses, data from each new subject was co-registered to the template created for the training sample. The same smoothing kernel was applied (σ = 3 mm) and the anatomical masks described above were used to extract average grey matter density in the left and right precentral gyrus.

For white matter analyses, the data from new subjects were co-registered to the FMRIB58a FA standard space image. The above described white matter masks were used to extract average FA and average RD values for each pathognomonic white matter region.

Removal of nuisance variability - age effect

Several imaging studies have demonstrated that brain changes occur with healthy ageing (Fjell et al., 2013a). Further studies have suggested that classification accuracy can be improved by removing nuisance variability (Koikkalainen et al., 2012). Accordingly, the age-related variability was removed prior to calculating a binary linear regression.

For each feature, a linear regression model was fitted to the distribution of the values of each feature of the control group using age as independent variable. In order to prevent the removal of disease-specific changes, only

	Validation Sample			Follow-up Validation Sample		
	ALS	**HC**	**p-value**	**ALS**	**HC**	**p-value**
N	21	16		21	15	
Male sex, n	10	6	$p = .74$	12	9	$p = .86$
Age, yrs (mean, SD)	62.5 (10.5)	60.6 (9.4)	$p = .56$	62.9 (10.4)	61.6 (9.2)	$p = .69$
Handedness (r/ l)	19/ 2	14/ 2	$p = .77$	19/ 2	13/ 2	$p = .72$
Disese duration, months (mean, SD) *	20.6 (15.9)			25.8 (15.6)		
Type of onset (bulbar/ spinal/ respiratory)	6/ 15/ 0			6/ 15/ 0		
ALSFRS-R (mean, SD)	39 (7)			35.3 (8.2)		
Time between scans, months (mean, SD)				5.3 (1.5)	4.2 (0.8)	$p < .05$

Table 5.3: Socio-demographic and clinical data of the Validation Sample and their follow-up scans. * disease duration from symptom onset until data of scan

control data was used (Koikkalainen et al., 2012). Based on this equation, each feature was estimated for each subject. These values were then subtracted from the measured values resulting in age-corrected measurements for each feature. This approach has been described in Koikkalainen et al. (2012). As an example, Figure 5.4 and 5.5 illustrates these corrections, by plotting the original and age-corrected FA and RD values of the body of the corpus callosum.

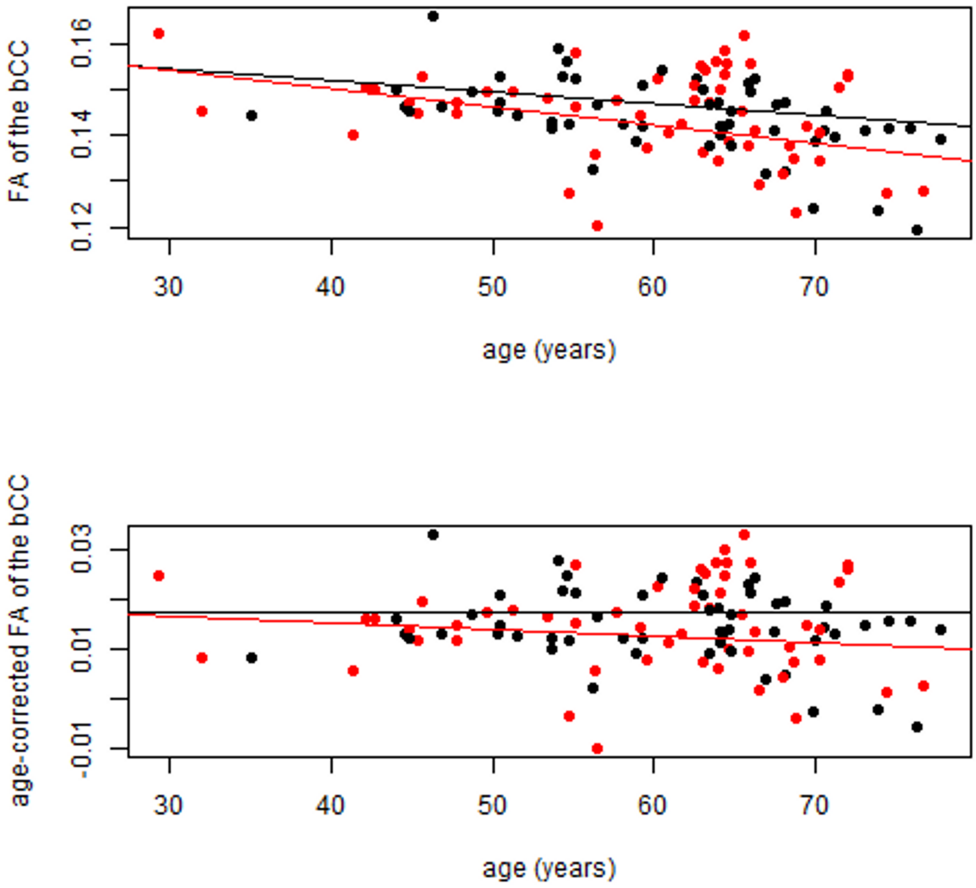

Figure 5.4: Removal of nuisance variance. Top: average FA of the body of the corpus callosum, Bottom: age-corrected FA of the body of the corpus callosum, Red: patients, Black: healthy controls.

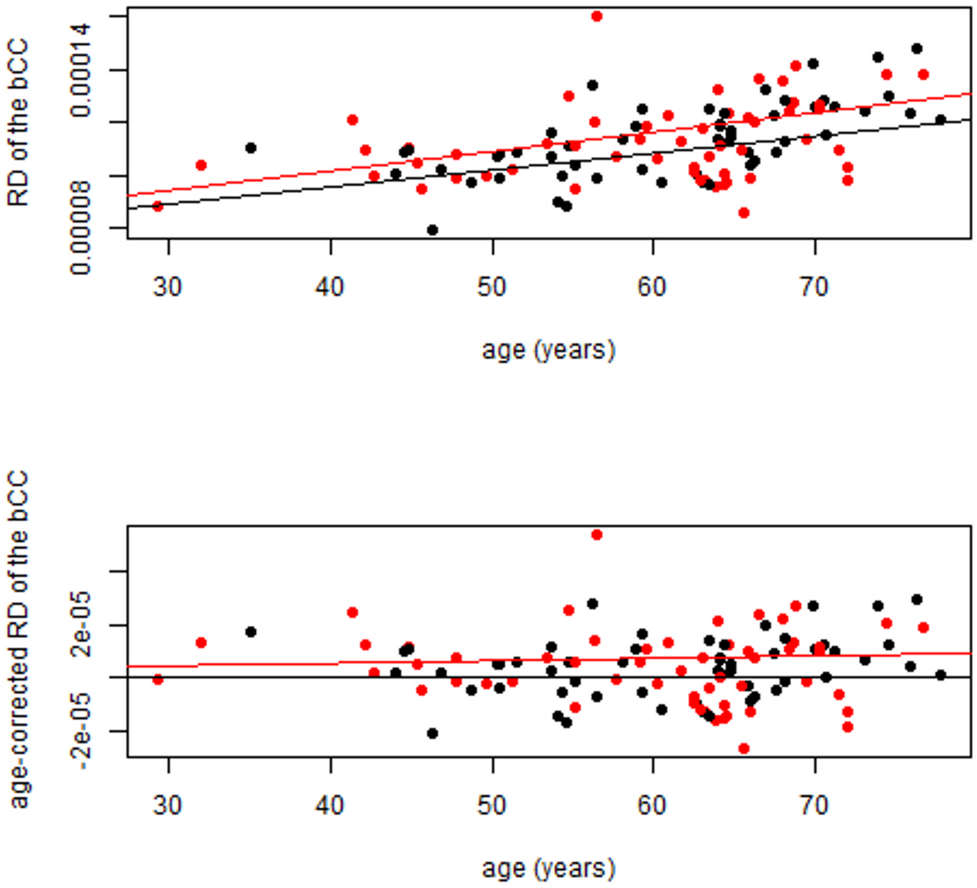

Figure 5.5: Removal of nuisance variance. Top: average RD of the body of the corpus callosum, Bottom: age-corrected RD of the body of the corpus callosum, Red: patients, Black: healthy controls.

Binary logistic regression

There are various classification methods such as binary logistic regression, discriminant analysis or support vector machine (SVM) (Arbabshirani et al., 2016). All of them have been successfully applied to classify groups based on neuroimaging data (e.g. Gupta et al. (2012); Orrù et al. (2012); Pagani et al. (2014); Teipel et al. (2015a,b)). In this study, a binary logistic regression approach was selected for several reasons: It is a relatively simple and well-established classification method which can be easily interpreted. It is as so-called 'white box' method as it allows us to evaluate why a test subject has been assigned to a particular category. Moreover, it provides the probability of a subject belonging to a category. Probability outcomes may be particularly useful in a clinical setting, where a clinician can integrate these values among other diagnostic indicators (Orrù et al., 2012). In contrast, SVM is essentially a 'black box' assigning the new data to one of two categories.

Herein, a binary logistic ridge regression model is fitted using all ALS-specific features and class (patient vs healthy control) as outcome variable using R (R Core Team 2015) and the package 'glmnet' ($\alpha = 0$) (Friedman et al., 2010). The tuning parameter λ was selected based on ten-folded cross-validation which was repeated 100 times. The model with the smallest misclassification error averaged over the 100 estimations was selected.

5.3 Results

Table 5.4 shows the classification results for the training and the validation samples if the probability cut-off is set to 50%. Figure 5.6 plots the probability of each MRI data set of the training sample representing ALS-specific change. The probability of each data of the validation sample is plotted in Figure 5.7 and of the follow-up validation sample in Figure 5.8.

Training Sample

Predicted class \ True class	ALS	HC		
ALS	50	24	**Sensitivity**	83.34%
HC	10	26	**Specificity**	52.00%
			Accuracy	69.09%

Validation Sample

Predicted class \ True class	ALS	HC		
ALS	19	6	**Sensitivity**	90.47%
HC	2	10	**Specificity**	62.50%
			Accuracy	78.37%

Follow-up Validation Sample

Predicted class \ True class	ALS	HC		
ALS	18	5	**Sensitivity**	85.71%
HC	3	10	**Specificity**	66.77%
			Accuracy	77.77%

Table 5.4: Classification results using a 50% probability threshold.

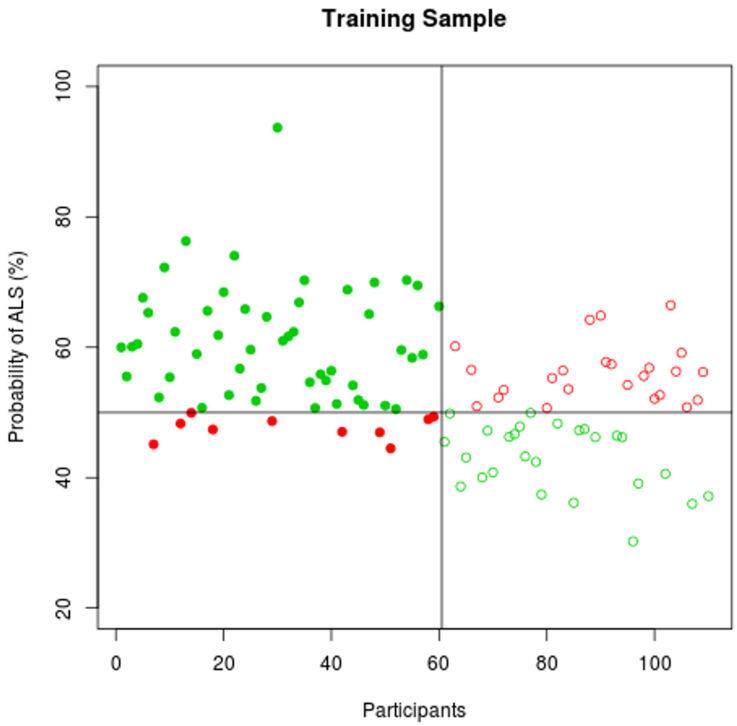

Figure 5.6: Classification accuracy in the training sample. The probability of individual participant's MRI data demonstrating ALS-specific change based on the classification algorithm. Patients with ALS are represented by filled circles, healthy controls by empty circles. Misclassified participants are displayed in red; correctly classified participants in green.

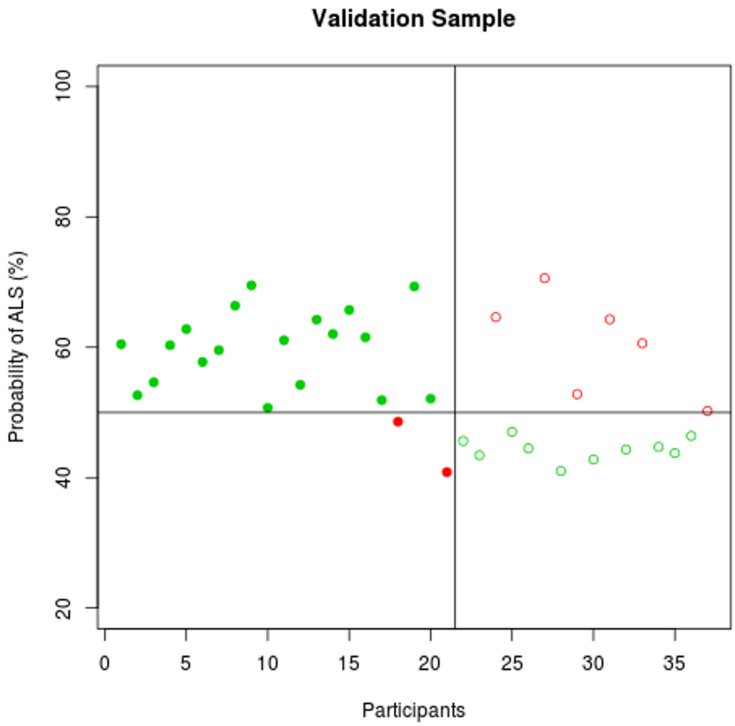

Figure 5.7: Classification accuracy in the validation sample. The probability of individual participant's MRI data demonstrating ALS-specific change based on the classification algorithm. Patients with ALS are represented by filled circles, healthy controls by empty circles. Misclassified participants are displayed in red; correctly classified participants in green.

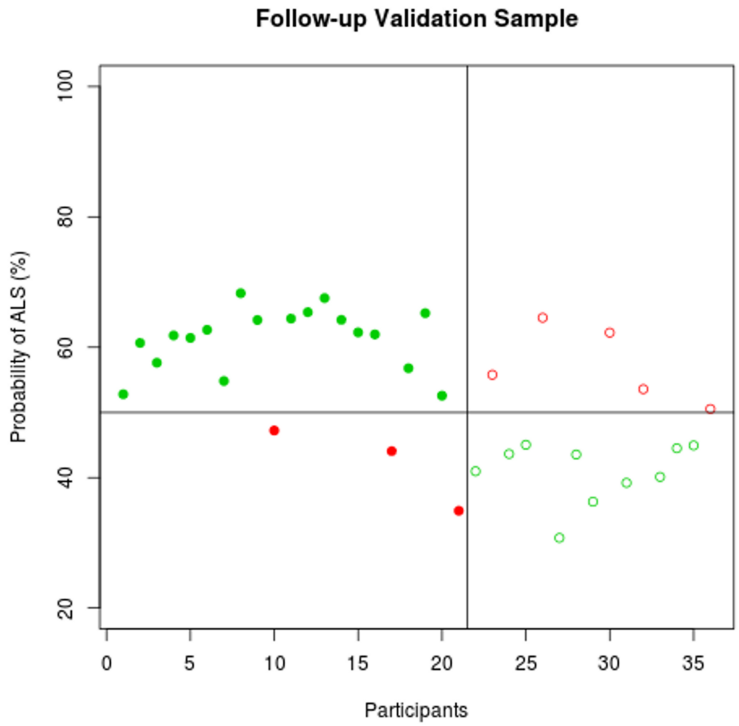

Figure 5.8: Classification accuracy in the follow-up validation sample. The probability of individual participant's MRI data demonstrating ALS-specific change based on the classification algorithm. Patients with ALS are represented by filled circles, healthy controls by empty circles. Misclassified participants are displayed in red; correctly classified participants in green.

5.3.1 Misclassified participants

The basic demographics of the misclassified participants of the training sample are provided in Table 5.5. The corresponding information for the validation sample and their follow-up cohort can be found in Table 5.6 and Table 5.7.

ALS patients

	True Positive	**False Negative**	**p-value**
N	50	10	
Male sex, n	32	7	$p = .72$
Age, yrs (mean, SD)	60.66 (10.46)	56.04 (12.69)	$p = .30$
Handedness (r/ l)	44/ 6	8/ 2	$p = .86$
Disease duration from symptom onset until date of scan, mo (mean, SD)	25.72 (16.07)	28.2 (33.01)	$p = .82$
Type of onset, (bulbar/ spinal/ respiratory)	18/ 31/ 1	1/ 9	$p = .23$
ALSFRS-R (mean, SD)	37.46 (6.57)	42 (4.06)	$p < .01$
Probability of ALS (mean, SD)	61.16 (8.44)	47.63 (1.79)	$p < .01$

Healthy controls

	True Positive	**False Negative**	**p-value**
N	26	24	
Male sex, n	16	8	$p = .08$
Age, yrs (mean, SD)	60.34 (8.48)	60.99 (9.33)	$p = .80$
Handedness (r/ l)	25/ 1	22/ 2	$p = .94$
Probability of ALS (mean, SD)	56.08 (4.39)	43.08 (5.07)	$p < .01$

Table 5.5: Comparison of misclassified and correctly classified ALS patients and HC of the *training sample*.

ALS patients

	True Positive	**False Negative**	**p-value**
N	19	2	
Male sex, n	11	1	$p = .83$
Age, yrs (mean, SD)	62.96 (10.9)	57.85 (1.91)	$p = .10$
Handedness (r/ l)	17/ 2	2/ 0	$p = .63$
Disease duration from symptom onset until date of scan, mo (mean, SD)	21.58 (16.47)	11.5 (4.95)	$p = .12$
Type of onset, (bulbar/ spinal/ respiratory)	6/ 13	0/ 2	$p = .91$
ALSFRS-R (mean, SD)	38.58 (7.27)	43 (1.41)	$p < .05$
Probability of ALS (mean, SD)	59.84 (5.87)	44.73 (5.48)	$p = .13$

Healthy controls

	True Positive	**False Negative**	**p-value**
N	10	6	
Male sex, n	7	3	$p = .42$
Age, yrs (mean, SD)	57.44 (10.07)	65.8 (5.29)	$p < .05$
Handedness (r/ l)	9/ 1	5/ 1	$p = .70$
Probability of ALS (mean, SD)	44.36 (1.76)	60.53 (7.72)	$p < .01$

Table 5.6: Comparison of misclassified and correctly classified ALS patients and HC of the *validation sample*.

ALS patients

	True Positive	False Negative	p-value
N	18	3	
Male sex, n	10	2	$p = .72$
Age, yrs (mean, SD)	63.44 (11.04)	56.67 (0.38)	$p < .05$
Handedness (r/ l)	17/ 1	2/ 1	$p = .65$
Disease duration from symptom onset until date of scan, mo (mean, SD)	22.11 (16.58)	11.67 (8.14)	$p = .14$
Type of onset, (bulbar/ spinal/ respiratory)	5/ 13	1/ 2	$p = .84$
ALSFRS-R (mean, SD)	38.58 (7.27)	43 (1.41)	$p < .05$
Probability of ALS (mean, SD)	61.38 (4.69)	42.08 (6.39)	$p < .05$

Healthy controls

	True Positive	False Negative	p-value
N	10	5	
Male sex, n	7	2	$p = .58$
Age, yrs (mean, SD)	59.35 (10.16)	65.28 (5.74)	$p = .17$
Handedness (r/ l)	9/ 1	4/ 1	$p = .59$
Probability of ALS (mean, SD)	40.91 (4.57)	57.34 (5.89)	$p < .01$

Table 5.7: Comparison of misclassified and correctly classified ALS patients and HC of the *follow-up validation sample*.

5.4 Discussion

Classification methods as well as imaging biomarkers are increasingly used in medicine, and are particularly well integrated into clinical decisions in oncology and Alzheimer's disease. Biomarker development in ALS yielded mostly to descriptive results to date, but the establishment of multi-centre data repositories creates a unique opportunity to test classification models in cross-platform data sets. The main aim of this study was to develop a computer-aided diagnostic tool based on disease-specific pathological signatures and multiple imaging measures. The aim was to assess the discriminative power of these regions in a blinded data set and explore the diagnostic accuracy of an imaging based biomarker. The object was to translate research into clinical use and make interference at the level of the individual.

Based on the multi-modal neuroimaging approach, diagnostic classification accuracy was achieved with good sensitivity and moderate specificity. Previous classification studies of ALS did not use an independent validation sample, instead they solely relied on cross-validation. Consequently, their results correspond to the results based on the present training sample. The training and test data were separated prior the feature reduction technique (feature reduction technique without double-dipping (Mwangi et al., 2013). Furthermore, the test data did not form part of the template created during the pre-processing steps. Such an independent validation is essential to assess the generalisability of the results, and it also paves the way for inclusion of cross-platform data sets.

There are further differences between the methodology of the previous studies and the present one. Previous studies have relied on highly discriminatory voxels of the initial comparisons (Filippini et al., 2010). This tailors the approach to a specific sample. By including an average value per anatomical structure, the generalisability to new data sets was increased. Brain areas which are affected early in the course of ALS were selected by regressing out the effect of disease duration. Thus, a real life clinical application was mimicked. Previous studies succeeded in classifying patients during the later

stages of the disease, when the neurodegenerative change has become pronounced, and controls. This approach represents a proof of concept, but it is less useful to evaluate a potential diagnostic biomarker.

The development of biomarkers needs to be tailored to its primary purpose whether the aim is a diagnostic or a prognostic application. If the aim is to develop a population-base screening tool, it is crucial to have a very high specificity, i.e. no healthy subject is wrongly confronted with the consequences of being ill. Regarding ALS, the application of a biomarker is most likely within a specialized clinic. The sample is pre-selected; it will consist of subjects who have symptoms which made them seek medical attention. A timely diagnosis of ALS is crucial for the patient, for therapy and for clinical trials. For clinical trials, it is crucial to assess the effect of a medication before too much neurodegenerative change has taken place. It is, therefore, important that a potential biomarker for ALS has a high sensitivity. A high specificity is also paramount to prevent patients with mimic neurodegenerative conditions to be misclassified as ALS.
The sensitivity and specificity are based on a binary decision criterion. A 50% cut-off was selected for illustration purposes. The advantage of the binary logistic ridge regression model is that it provides probability outcomes, as opposed to categorical classification. The clinician can integrate this information into his diagnostic decision. For example, if a new patient is classified with 47% probability of suffering from ALS, the binary results would classify him as control. Considering additional diagnostic test results for this patient, the clinician can carefully consider the risks and benefits before prescribing a disease modifying treatment. As discussed above, the need for a biomarker for ALS is clear and the most likely option, to cope with the heterogeneity clinical picture of ALS, is a combination of diagnostic tests including neuroimaging based classifier.

Oncology research established guidelines to facility the development of a biomarker (Pepe et al., 2001). Research in Alzheimer's disease has recognized their value and adapted them to their own effort to translate diagnostic

AD biomarkers from research into clinical practice (The Lancet Neurology, 2014). MND researchers should adapt this framework for their own research. The first phase is pre-clinical exploratory. The aim is to identify potentially useful biomarkers. The second phase evaluates the ability of the candidate markers to distinguish patients and controls. A secondary aim is to assess the reproducibility of the assay within the same and different setting (i.e. different scanners), the relationship between different biomarkers, the association to different factors such as sex, age, environment, lifestyle, disease stage, and prognosis. The third phase determines the capability to detect a prodromal state of the disease. Eventually, the sensitivity and specificity of the biomarker regarding an unselected sample such as tertiary and primary care population has to evaluated (phase 4) and its potential to reduce mortality, morbidity and disability (phase 5).
Phase 1, i.e. the need to establish a characteristic signature of ALS has successfully accomplished (Turner et al., 2012; Chiò et al., 2014). The present study targets the second phase. Next, the relation of different biomarkers needs to be evaluated, i.e. can an imaging biomarker in combination with a physiological diagnostic test make a more accurate diagnosis than the current gold standard?

The analysis of misclassification revealed that patients with a higher ALSFRS-R score where more likely to be misclassified. Within the validation sample, older healthy controls were more likely to be misclassified. ALS is more common in people within 50-70 years of age (Logroscino et al., 2010), but younger and older people can develop the disease as well. It is expected that it becomes increasingly difficult to correctly classify the extrema of this spectrum – young patients who apart from the ALS-related changes have a healthy brain and older controls who may display age-related microangliopathy.

In contrast to the hypothesis, the probability of suffering from ALS did not increase based on the follow-up scan of the patients. One reason may be that by averaging each anatomical structure the change within 4 months was not pronounced enough to influence the average. Ideally, the model should be

developed based on patients who recently received a diagnosis of ALS. Considering the implication of this diagnosis, these patients are not always able to participate in research studies. The present approach, regressing out the time since diagnosis to identify the brain areas which are most likely affected at that stage, tries to overcome this shortcoming.
Regarding the healthy controls, also no change in probability of suffering from ALS was found. This is in line with the hypothesis and supports the validity of this classification approach.

5.4.1 Limitations

The presented study is not without limitations. The study uses a standard single-platform, single-centre approach and is not validated on data acquired from other centres. Despite advances in cross-centre harmonisation (Müller et al., 2016), the effect of pulse sequence differences on spatial statistics is well established (Teipel et al., 2011b). Multicentre MR studies have been successfully conducted in Alzheimer's disease, (Stonnington et al., 2008) and the cross platform calibration of the Alzheimer's Disease Neuroimaging Initiative (ADNI, Mueller et al., 2005) using travelling MRI phantoms has been comprehensively described.

Furthermore, the sample is restricted to patients with classical ALS. Mimic conditions are needed to truly evaluate the generalisability of the results. The study is restricted to the most common phenotype of ALS. Patients with PLS or PMA were not included. Both phenotype present with a different brain signature (Kwan et al., 2012; Schuster et al., 2013) which needs to be considered in the development of a diagnostic biomarker.

The study also did not include ALS patients with an additional diagnosis of FTD. The results are, therefore, not generalizable to this phenotype. A diagnosis of FTD is associated with pronounced brain changes (Lillo et al., 2012; Schuster et al., 2014a). Including ALS patients with a co-morbid diagnosis

of FTD in the training sample would have biased the results in a way that brain areas which deteriorate due to FTD would have been selected as input features. The final probability algorithm would have reflected FTD-specific rather than ALS-specific changes. Restricting the sample to pure ALS patients allowed selecting features which represent the core pathology of ALS. Including ALS patients with a co-morbid diagnosis of FTD to the validation sample would have likely resulted in a correct classification. It would have been unclear whether these is due to the fact that ALS-FTD patients generally present more pronounced brain changes or whether the developed algorithm is truly reliable. To distinguish these reasons, both a validation sample of pure FTD patients is needed.

5.4.2 Future directions

The Neuroimaging Society in ALS (NiSALS) has established a large data repository which is an ideal resource to test classification models in ALS (Turner et al., 2011). The present study is limited to patients with classical ALS and controls. Patients with comorbid frontotemporal dementia and mimic conditions were not included. Notwithstanding the relatively modest specificity results, the data suggest that the inclusion of additional pathognomonic regions such as basal ganglia (Machts et al., 2015), spinal cord (El Mendili et al., 2014), or cerebellar measures (Prell and Grosskreutz, 2013) may increase the diagnostic accuracy of the model further. Moreover, the inclusion of other imaging parameters such as cortical thickness measurements, volumetrics, connectivity measures, or spectroscopy may further enhance diagnostic models (Chiò et al., 2014). From a clinical perspective, urgent work is required to develop classification models which can reliably identify early-stage ALS and distinguish it from mimic conditions and other neurodegenerative conditions. Such models also have to include anatomical regions which are not typically affected in ALS but are implicated in other neurodegenerative conditions (Bede et al., 2016). The accurate classification of overlap syndromes such as ALS-FTD may be particularly challenging.

These conditions have a less distinctive imaging signature with features of both ALS and FTD.

The classification methodology outlined in this study can be used beyond the initial diagnosis to segregate ALS phenotypes. ALS is an outstandingly heterogeneous condition encompassing distinctive motor phenotypes, genotypes, (McLaughlin et al., 2015) cognitive cohorts, (Elamin et al., 2013) slow and fast progressors (Kiernan et al., 2011; McLaughlin et al., 2015). As these phenotypes have distinguishing imaging features, newly diagnosed or suspected patients could potentially be sub-phenotyped for stratification into pharmaceutical trials. Subgroups may respond differently to the medication or randomly allocation of one subgroup to e.g. the placebo group may bias the results (Chapter 6). Finally, classification pipelines developed for ALS are transferable to other neurodegenerative conditions where pathological change also occurs in a unique, disease-specific anatomical pattern.

5.5 Conclusions

The classification approach outlined in this study relies on assessing multiple imaging measures in multiple disease-defining anatomical regions in individual data sets to provide a diagnostic probability score. In an era where cross-platform harmonisation is gaining increasing momentum and acquisition protocols constantly improve, the presented approach is likely to lead to increasingly accurate diagnostic classification. Ultimately, imaging biomarkers in ALS are gradually expanding beyond their descriptive role to be developed into viable diagnostic and prognostic markers.

Chapter 6

Predicting 18-months mortality rate in ALS using structural brain changes and clinical characteristics

6.1 Introduction

While the clinical features of ALS are highly heterogeneous, the overall disease trajectory and life expectancy is relatively uniform, making it a template neurodegenerative condition for the development of diagnostic and prognostic biomarker (Hardiman et al., 2011). It is generally accepted that a long pre-symptomatic phase precedes clinical manifestation (Schuster et al., 2015; Benatar and Wuu, 2012) which may be dominated by bulbar or spinal symptoms at onset, but progresses to respiratory failure over time. The only neuroprotective drug licensed in ALS, Riluzole, offers only modest survival benefit (Miller et al., 2007).

Clinical heterogeneity has multiple dimensions in ALS such as site of onset, coexisting cognitive and behavioural deficits, dominance of upper or lower motor neurodegeneration, variability of progression rates and distinct ALS

phenotypes (Byrne et al., 2012). All of these factors make the accurate prediction of individual prognosis challenging. Clinical heterogeneity precludes smaller clinical trials as a given drug may only be effective in certain ALS phenotypes (Mitsumoto et al., 2014). A prognostic framework would enhance stratification in clinical trials and enable individual patients to make important end-of-life decisions. The planning and timing of supportive interventions such as feeding tube insertion, non-invasive ventilation and palliative measures could also be optimised by accurate prognostic markers (Bede et al., 2011).

Previous studies have successfully linked specific demographic and clinical variables to reduced survival, e.g. older age, bulbar or respiratory onset, short symptom to diagnosis interval and poor motor function. Attendance of a multidisciplinary ALS clinic has been linked to a better prognosis (Chiò et al., 2009; Gordon et al., 2013; Rooney et al., 2015). A recent study focusing on prediction of one-year mortality identified the following factors: age over 75 years, less than 6 months from symptom onset to diagnosis, rapid decline of body weight and advanced functional impairment (Wolf et al., 2014).

MRI has been repeatedly suggested as a prognostic biomarker in ALS (Turner et al., 2009, 2011; Chiò et al., 2014), but has not been convincingly validated to date. As described in in Chapter 3 and 4, structural brain changes during the course of ALS have been well characterised: grey matter atrophy of the precentral gyrus and white matter degeneration of the corticospinal tract (Agosta et al., 2010a; Li et al., 2012; Turner et al., 2012).

Imaging measures in ALS have been previously explored as prognostic indicators. The neuronal integrity of the motor cortex has been directly linked to survival (Kalra et al., 2006); fractional anisotropy (FA) of the corticospinal tract was used to predict survival after 3 years (Agosta et al., 2010b).

6.2 Objectives

The objective of this study was to develop and test a prognostic tool in ALS to predict the probability of 18-month survival based on individual structural MRI data sets. The hypothesis was that structural MRI measures will enhance prediction accuracy compared to clinical variables alone.

6.3 Methods

6.3.1 Overview

The available imaging data were divided into a training sample to perform binary ridge logistic regression to predict the probability of surviving less than 18 months and an independent validation sample to access the generalisability of the approach (Figure 6.1). Clinical characteristics related to survival were selected based on a literature review. MRI measures were defined based on group comparisons between patients and healthy controls. The control group was also used to extract age-related variability of the MRI measurements (Koikkalainen et al., 2012).

A total of three binary ridge regressions were computed with (1) clinical indices alone, (2) MRI features alone and (3) with a combination of both MRI and demographic variables. A cut-off score of 50% probability was selected to evaluate the accuracy, sensitivity and specificity of the models.

6.3.2 Participants

The sample included 60 ALS patients selected from the MRI database for whom a minimum follow-up period of 18-month after their brain scan was available. The census date was the 9^{th} of June 2016. Survival was defined as time between MRI scan and date of death or, for patients who were alive, it was censored. Participating ALS patients were diagnosed with either probable or definite ALS according to the revised El Escorial criteria (Brooks et al.,

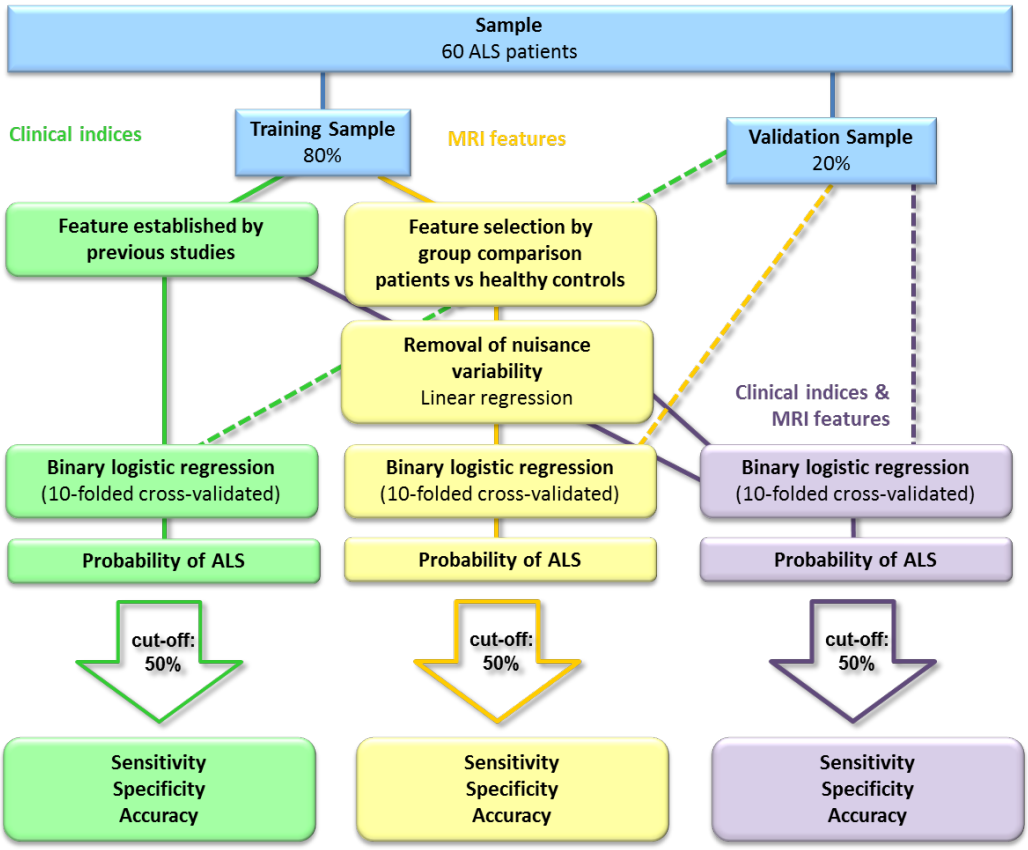

Figure 6.1: Overview of methods.

2000). Patients with a comorbid diagnosis of fronto-temporal dementia according to the Rascovsky Criteria (Rascovsky et al., 2011) were excluded due to the confounding imaging changes associated with this phenotype (Chang et al., 2005; Lillo et al., 2012). Table 6.1 presents clinical and demographic details of the ALS patients. Regarding the site of onset, bulbar and respiratory onset patients are grouped together as non-spinal onset. The sample includes only one patient with respiratory onset, who is part of the validation sample.

Subsequently, 80% of the patient sample was randomly allocated to the training sample and 20% to the validation sample. Of note, there were no significant demographic or clinical differences between the patient groups surviving

shorter or longer than 18-month (with the exception of survival) which is crucial to untangle the influence of demographic, clinical and MRI variables.

To highlight the ALS specific pathology, the training sample was compared to an age- and gender-matched group of 69 healthy controls. The demographic details can be found in Table 6.1.

			Training			Validation		
			ALS patients surviving			ALS patients surviving		
	HC*	p-value	< 18 months	> 18 months	p-value	< 18 months	> 18 months	p-value
N	69		24	24		6	6	
Gender (male/ female)	34/35	$p = .22$	17/7	13/11	$p = .37$	3/3	2/4	$p = 1$
Handedness (r/ l)	64/5	$p = .55$	23/1	20/4	$p = .35$	5/1	5/1	$p = 1$
Age, yrs (mean, SD)	59.97 (9.9)	$p = .17$	63.18 (8)	61.76 (10.73)	$p = .60$	63.96 (8.03)	55.09 (8.82)	$p = .09$
Site of onset (non-spinal/ spinal)			8/16	10/14	$p = .76$	3/3	2/4	$p = 1$
Symptom onset until diagnosis, yrs (mean, SD)			1.2 (0.81)	1.05 (0.75)	$p = .51$	1.28 (1.1)	0.88 (0.3)	$p = .43$
Symptom onset until scan, yrs (mean, SD)			2.17 (1.01)	2.32 (1.34)	$p = .67$	1.94 (1.44)	1.85 (0.54)	$p = .89$
ALSFRS-R (mean, SD)			34.48 (6.84)	37.38 (6.21)	$p = .12$	34.5 (8.34)	39.17 (4.17)	$p = .25$
King's College Staging (1/ 2/ 3/ 4/ NA)			4/ 5/ 3/ 7/ 5	4/ 9/ 5/ 4/ 2		0/ 1/ 2/ 2/ 1	2/ 2/ 1/ 1/ 0	
MITOS (0/ 1/ 2/ 3/ NA)			10/ 8/ 1/ 0/ 5	19/ 2/ 0/ 1/ 2		3/ 1/ 1/ 0/ 1	6/ 0/ 0/ 0/ 0	
Survival from scan, yrs (mean, SD)			0.94 (0.32)	2.26 (1.11)**	$p < .01$	0.92 (0.26)	2.62 (1.32)**	$p < .05$

Table 6.1: Clinical and demographic details. *healthy controls were compared to the training sample of 48 patients. **including only data if the date of death was known - Training Sample: N = 7, mean = 3.31, SD = 1.69; Validation Sample: N = 2, mean = 2.73, SD = 1.03. NA = no available.

6.3.3 MRI pre-processing

Cortical thickness (CT) analysis

The cortical thickness was measured using FreeSurfer (version 5.3.0), an imaging analysis suite which has been both validated using histological (Rosas et al., 2008) and manual measurements (Kuperberg et al., 2003; Salat et al., 2004).[1] The automated processing stream consists of skull-stripping, registration, intensity normalization, Talairach transformation, tissue segmentation, and surface parcellation. Tissue segmentation determines the boundaries between the white and the grey matter (white matter surface) as well as between the grey matter and the cerebrospinal fluid (pial surface). The result of this process was individually reviewed, errors were corrected and the segmentation step was repeated. Cortical thickness has been defined as the distance (vertex) from the white matter surface to the nearest point on the pial surface.

White matter (WM) analysis

As described in the previous chapters, the pre-processing of DTI data included eddy current corrections, motion corrections, and brain-tissue extraction in FSL (Smith et al., 2006). A diffusion tensor model was fitted at each voxel, generating maps of FA, MD, AD and RD. Each dataset was aligned to the FMRIB58a FA standard-space images. Next, the mean FA image was created. Each subject's aligned FA data was then projected onto the FMRIB58a FA standard-space skeleton and the resulting data fed into voxel-wise cross-subject statistics.

6.3.4 Feature selection

In order to identify ALS-specific pathological brain regions, patients of the training sample were compared to healthy controls using age as a nuisance

[1] http://surfer.nmr.mgh.harvard.edu/

variable.

For the cortical thickness analysis, the results are significant at $p < .05$ corrected using for multiple comparisons using false discovery rate (FDR). The selected input variables, also called features, which were selected based on these results and in accordance with the literature, included the precentral gyrus and the paracentral gyrus (Verstraete and Heuvel, 2010; Schuster et al., 2013, 2014a). The Desikan-Killiany atlas (Desikan et al., 2006), Figure 6.2 was used to define the cortical regions and the average cortical thickness was extracted from both regions.

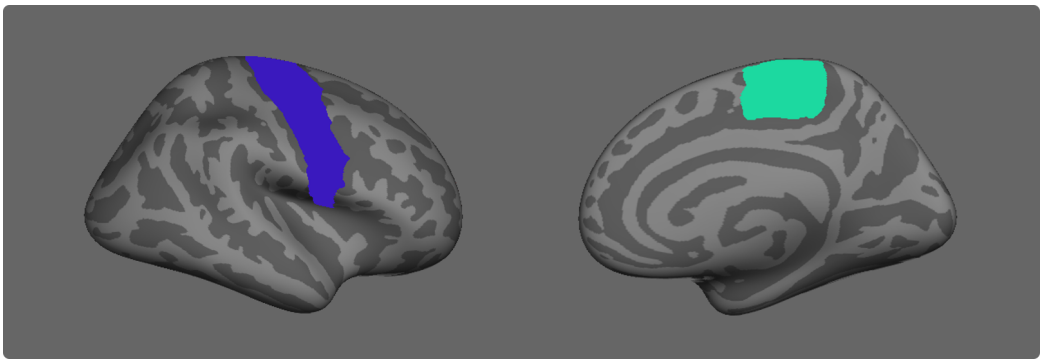

Figure 6.2: Cortical thickness features. Blue: precentral gyrus, Light green: paracentral gyrus. Only the right hemisphere is displayed.

For the comparative white matter analyses, the significance level for the group comparison was set to $p < .01$ corrected using family-wise error (FWE). Similarly to Chapter 3, the following core white matter regions were selected as discriminatory features for the binary regression: the superior corona radiata, inferior corona radiata, anterior and posterior limbs of the internal capsule, cerebral peduncles (mesencephalic crus) and the genu, body and splenium of the corpus callosum (Figure 6.3). These regions were defined using the JHU DTI-based white-matter atlas (Oishi et al., 2008). The average measurement for each DTI index (i.e. FA, RD, MD, AD) for each brain region was extracted.
For all features, the left and right hemisphere were averaged.

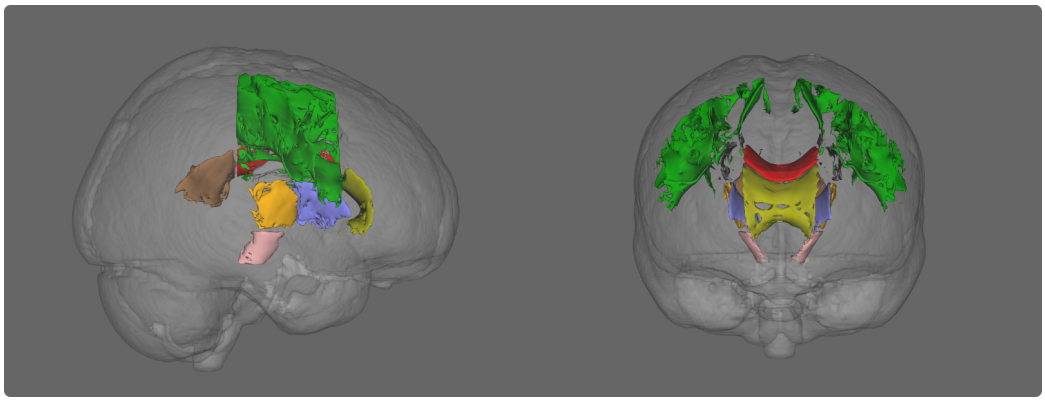

Figure 6.3: White matter features. Green: superior corona radiata, grey: corona radiata, orange: posterior limb of the internal capsule, lilac: anterior limb of the internal capsule, rose: cerebral peduncle, yellow: genu of corpus callosum, red: body of the corpus callosum, brown: splenium of the corpus callosum.

6.3.5 Validation Sample

The pre-processing steps of the independent validation sample were analogous to the pre-processing pipeline of the training sample. The average cortical thickness and diffusivity values were extracted as described in Chapter 5.

6.3.6 Group comparison of selected features

T-tests were conducted using the MRI features as dependent variable and group as independent variable, in order to analyse whether patient groups surviving more or less than 18 months differed regarding the selected MRI features. The significant level was set to $p < .05$.

6.3.7 Reducing age-related variability

The effect of ageing on MRI measures is well established (Fjell et al., 2013a,b) and it has been shown that classification accuracy may be improved by removing this nuisance variable (Koikkalainen et al., 2012). The confounding effect of age is particularly important in ALS which affects a fairly wide age range. From an imaging perspective, a young patient with severe physical disability may exhibit similar brain changes to older patients with less advanced disease. Moreover, age in ALS is considered a prognostic factor (Chiò et al., 2009; Wolf et al., 2014). To account for age-related variability the method of Koikkalainen et al. (2012) was implemented. A linear regression model was fitted to the distribution of the values of each feature of the control group using age as independent variable. Based on this equation, the predicted value for each feature for each individual subject was estimated. These values were then subtracted from the measured values resulting in age-corrected measurement for each feature.

6.3.8 Binary logistic regressions

Three binary ridge logistic regressions were fitted using (1) clinical indices related to shortened survival, (2) MRI features or (3) both. Clinical features included age at disease onset, site of disease onset (bulbar/ spinal), diagnostic delay (time interval from symptom onset to diagnosis), ALSFRS-R at the time of the scan (Table 6.2). MRI features corrected for age-related variability consisted of the average cortical thickness of the precentral gyrus (Figure 6.2), the average FA, RD, MD and AD of the superior corona radiata, inferior corona radiata, anterior and posterior limbs of the internal capsule, cerebral peduncles and the genu, body and splenium of the corpus callosum (Figure 6.3). The outcome variable was patient group stratified surviving more than 18 months or less than 18 months. The statistical software R (R Core Team 2015) and the package 'glmnet' ($\alpha = 0$) (Friedman et al., 2010) was utilised to carry out the logistic regression. The tuning parameter λ was selected based on ten-folded cross-validation which was repeated 100

Clinical indices	MRI features
- Age at disease onset	*Cortical thickness*
- Site of disease onset	- Precentral gyri
- Diagnostic delay	- Paracentral gyri
- Disease severity	*White matter*
	- Superior corona radiata
	- Inferior corona radiata
	- Anterior limbs of the internal capsule
	- Posterior limbs of the internal capsule
	- Cerebral peduncles
	- Genu of the corpus callosum
	- Body of the corpus callosum
	- Splenium of the corpus callosum

Table 6.2: Discriminating features.

times. The model with the smallest misclassification error averaged over the 100 estimations was selected. Subsequently, the regression algorithm was used to estimate the probability of each participant in the validation sample to belong to the group surviving less than 18 months after the brain scan.

6.4 Results

6.4.1 Group comparisons

Comparing ALS patients in the training sample with the control group highlighted the same pathognomonic brain regions as described in Chapter 3. The results are shown in Figure 6.4 for the cortical thickness analyses and in Figure 6.5 for the white matter analyses.
The direct comparison of patients surviving more than 18 months and those surviving less than 18 months, did not reach statistical significance corrected for multiple comparisons.

When comparing the average values of each brain regions within the training sample, the precentral gyrus was the only region showing a trend towards a

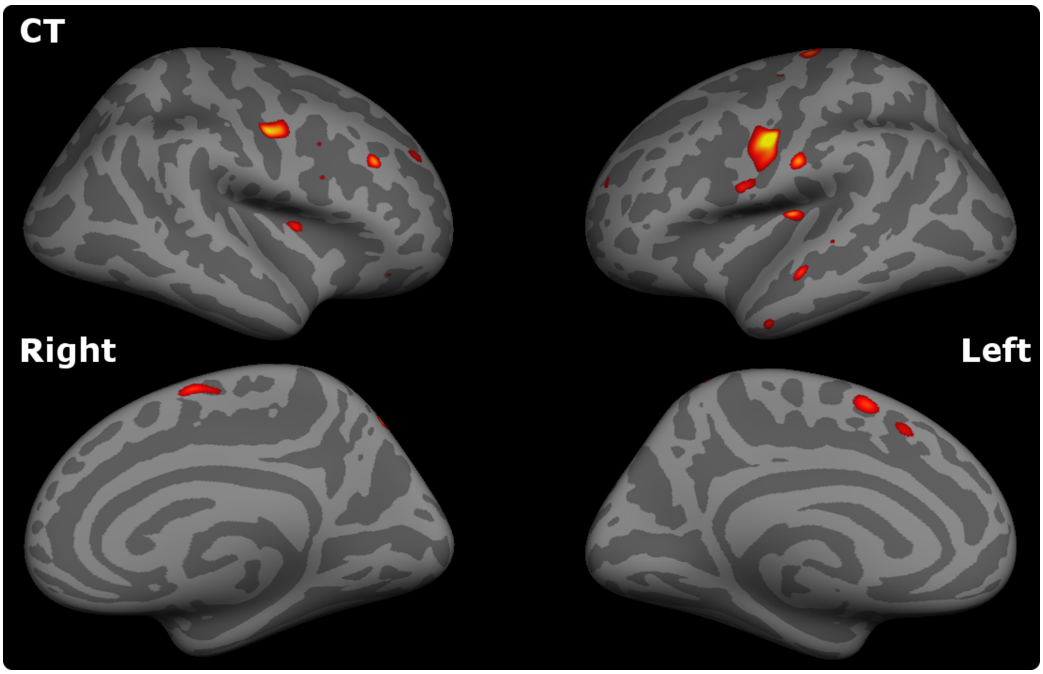

Figure 6.4: Cortical thickness. Group comparison between ALS patients and controls. The significant level is set to $p < .05$ (FDR).

significant difference between patients surviving less than 18 months (M = 2.31 mm, SD = 0.15) and patients surviving more than 18 months (M = 2.39 mm, SD = 0.15, t(45.99) = 1.87, $p = .07$). There was no difference in the other MRI based features.

6.4.2 Binary logistic regression - clinical features alone

Figure 6.6 and Figure 6.7 display the resulting probabilities surviving less than 18-month based on the regression including only clinical characteristics available at the time of the scan.

For illustrative purposes, a cut-off of 50% probability of surviving less than 18 months was selected to evaluate prediction sensitivity, specificity and accuracy. Table 6.3 reports the binary classification results. An analysis of misclassified patients is reported under below (Training sample: Table 6.4:

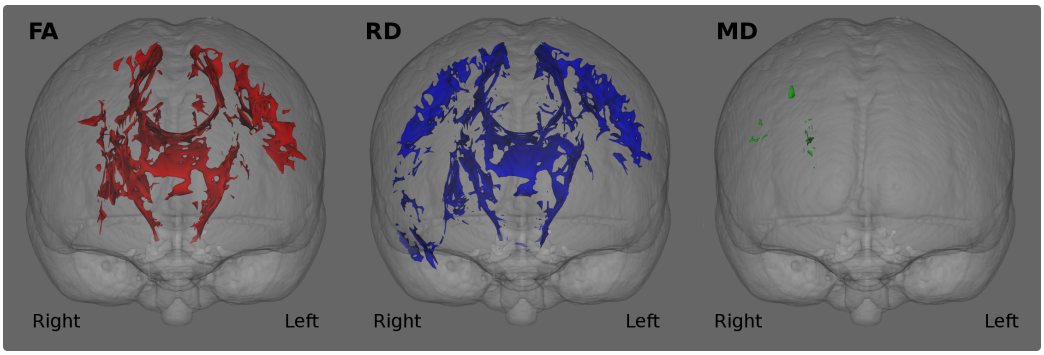

Figure 6.5: White matter analyses. Group comparisons between ALS patients and controls. The significant level is set to $p < .01$ (FWE).

patients surviving < 18 months, Table 6.5: patients surviving > 18 months; Validation sample: Table 6.6: patients surviving < 18 months, Table 6.7: patients surviving > 18 months).

Misclassified patients

Table 6.4 and Table 6.5 shown the demographic and clinical details of the misclassified patients in the training sample surviving less or longer than 18 months, respectively. For the validation sample this information is present in Table 6.6 and 6.7.
Misclassified patients different significantly regarding the ALSFRS-R score.

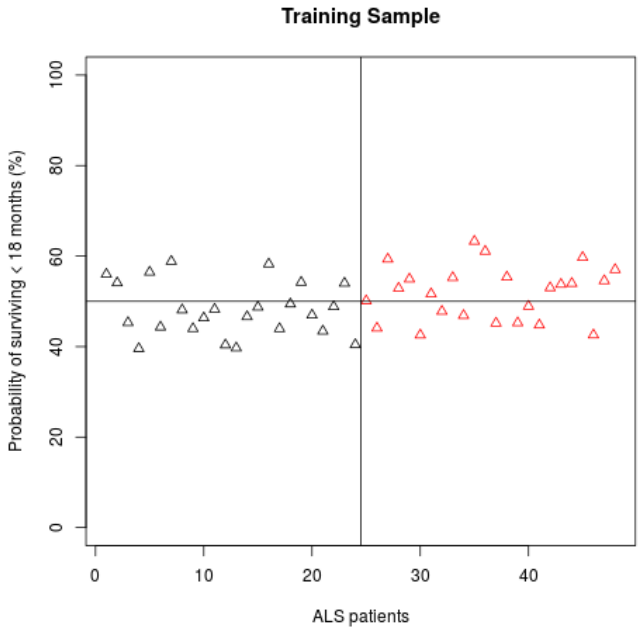

Figure 6.6: Clinical features. Training sample: The probability of surviving less than 18 months. Red: patients surviving < 18 months from the date of their scan; Black: patients surviving > 18 months.

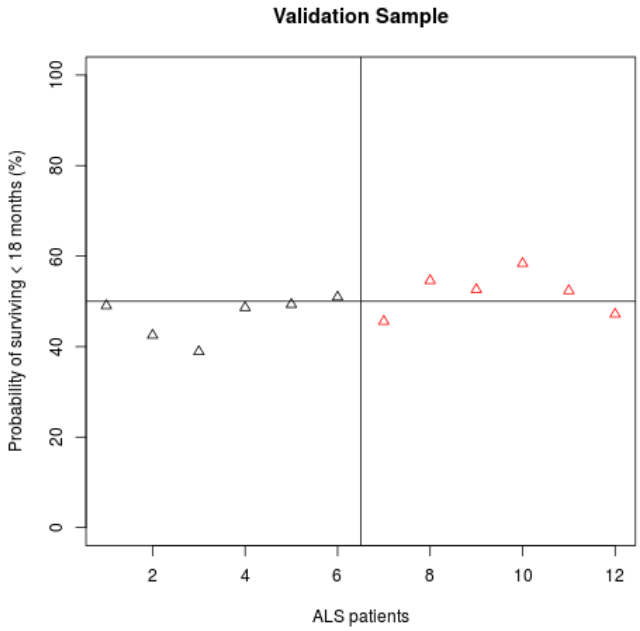

Figure 6.7: Clinical features. Validation sample: The probability of surviving less than 18 months. Red: patients surviving < 18 months from the date of their scan; Black: patients surviving > 18 months.

Training Sample

Predicted group \ True group	Surviving < 18 months	Surviving > 18 months
Surviving < 18 months	17	9
Surviving > 18 months	7	15

Sensitivity	62.50%
Specificity	70.84%
Accuracy	66.67%

Validation Sample

Predicted group \ True group	Surviving < 18 months	Surviving > 18 months
Surviving < 18 months	5	2
Surviving > 18 months	1	4

Sensitivity	66.67%
Specificity	83.34%
Accuracy	75.00%

Table 6.3: Clinical features. Classification results using a cut-off of 50% probability.

Survival < 18 months			
	True Positive	**False Negative**	**p-value**
N	15	9	
Gender (male/ female)	11/ 4	6/ 3	$p = 1$
Age, yrs (mean, SD)	64.58 (9.64)	60.85 (3.38)	$p = .18$
Handedness (r/ l)	14/1	9/ 0	$p = 1$
Site of onset (non-spinal/ spinal)	3/ 12	5/ 4	$p = .18$
Diagnostic delay, yrs (mean, SD)	1.14 (0.8)	1.29 (0.88)	$p = .68$
Disease duration from symptom onset until scan, yrs (mean, SD)	30.93 (6.39)	40.11 (2.03)	$p < .01$
Survival from scan, yrs (mean, SD)	0.86 (0.22)	1.06 (0.44)	$p = .23$

Table 6.4: Clinical features. Demographic and clinical data of correctly and misclassified patients surviving < 18 months of the *training sample*.

Survival > 18 months			
	True Negative	**False Positive**	**p-value**
N	17	7	
Gender (male/ female)	10/ 7	3/ 4	$p = .79$
Age, yrs (means, SD)	67.17 (11.73)	59.52 (9.78)	$p = .16$
Handedness, (r/ l)	14/ 3	6/ 1	$p = 1$
Site of onset (non-spinal/ spinal)	8/ 9	2/ 5	$p = .70$
Diagnostic delay, yrs (mean, SD)	1.1 (0.85)	0.93 (0.45)	$p = .52$
Disease duration from symptom onset until scan, yrs (mean, SD)	2.37 (1.21)	2.2 (1.72)	$p = .83$
ALSFRS-R (mean, SD)	40.06 (2.79)	30.86 (7.56)	$p < .05$
Survival from scan, yrs (mean, SD)	2.01 (0.58)	2.87 (1.79)	$p = .26$

Table 6.5: Clinical features. Demographic and clinical data of correctly and misclassified patients surviving > 18 months of the *training sample*.

Survival < 18 months			
	True Positive	**False Negative**	**p-value**
N	4	2	
Gender (male/ female)	3/ 1	0/ 2	$p = .39$
Age, yrs (means, SD)	60.81 (6.38)	70.25 (9.02)	$p = .35$
Handedness (r/ l)	4/ 0	1/ 1	$p = .69$
Site of onset (non-spinal/ spinal)	1/ 3	2/ 0	$p = .39$
Diagnostic delay, yrs (mean, SD)	1.54 (1.32)	0.75 (0.11)	$p = .32$
Disease duration from symptom onset until scan, yrs (mean, SD)	2.34 (1.67)	1.14 (0.15)	$p = .25$
ALSFRS-R (mean, SD)	30.75 (7.68)	43 (1.41)	$p = .06$
Survival from scan, yrs (mean, SD)	1.01 (0.28)	0.74 (0.08)	$p = .14$

Table 6.6: Clinical features. Demographic and clinical data of correctly and misclassified patients surviving < 18 months of the *validation sample*.

Survival > 18 months			
	True Negative	**False Positive**	**p-value**
N	5	1	
Gender (male/ female)	2/3	0/1	-
Age, yrs (means, SD)	52.64 (7.21)	67.38 (NA)	-
Handedness (r/ l)	4/ 1	1/ 0	-
Site of onset (non-spinal/ spinal)	2/ 3	0/ 1	-
Diagnostic delay, yrs (mean, SD)	0.91 (0.32)	0.75 (NA)	-
Disease duration from symptom onset until scan, yrs (mean, SD)	2.01 (0.41)	1.05 (NA)	-
ALSFRS-R (mean, SD)	38.8 (4.55)	41 (NA)	-
Survival from scan, yrs (mean, SD)	2.83 (1.36)	1.56 (NA)	-

Table 6.7: Clinical features. Demographic and clinical data of correctly and misclassified patients surviving > 18 months of the *validation sample*.

Training Sample

Predicted group \ True group	Surviving < 18 months	Surviving > 18 months
Surviving < 18 months	18	5
Surviving > 18 months	6	19

Sensitivity	79.16%
Specificity	75.00%
Accuracy	77.08%

Validation Sample

Predicted group \ True group	Surviving < 18 months	Surviving > 18 months
Surviving < 18 months	3	2
Surviving > 18 months	3	4

Sensitivity	66.70%
Specificity	50.00%
Accuracy	58.33%

Table 6.8: MRI features. Classification results using a cut-off of 50% probability.

6.4.3 Binary logistic regression - MRI features alone

Figure 6.8 depicts the probability of each patient of the training sample to survive less than 18 months based on MRI features alone. The results for the validation sample are shown in Figure 6.9. Table 6.8 reports the binary classification results and the resulting sensitivity, specificity and accuracy using a cut-off score of 50%.

Survival < 18 months			
	True Positive	**False Negative**	**p-value**
N	19	5	
Gender (male/ female)	14/ 5	3/2	$p = .96$
Age, yrs (means, SD)	62.94 (8.26)	64.12 (7.7)	$p = .77$
Handedness (r/ l)	18/ 1	5/0	$p = 1$
Site of onset(non-spinal/ spinal)	5/14	3/ 2	$p = .38$
Diagnostic delay, yrs (mean, SD)	1.09 (0.71)	1.61 (1.13)	$p = .37$
Disease duration from symptom onset until scan, yrs (mean, SD)	2.14 (1.01)	2.28 (1.1)	$p = .80$
ALSFRS-R (mean, SD)	34.05 (7.26)	35.6 (5.46)	$p = .61$
Survival from scan, yrs (mean, SD)	0.91 (0.34)	1.05 (0.23)	$p = .30$

Table 6.9: MRI features - Demographic and clinical data of correctly and misclassified patients surviving < 18 months of the *training sample*.

Misclassified patients

Misclassified patients of the training sample are described in Table 6.9 and Table 6.10; of the validation sample in Table 6.11 and Table 6.12. There was no significant demographic or clinical difference between correctly and misclassified patients within the training sample or in the validation sample.

Survival > 18 months			
	True Negative	**False Positive**	**p-value**
N	18	6	
Gender (male/ female)	8/ 10	5/ 1	$p = .24$
Age, yrs (means, SD)	62.31 (10)	60.09 (13.61)	$p = .72$
Handedness, (r/ l)	14/ 4	6/ 0	$p = .53$
Site of onset (non-spinal/ spinal)	6/ 12	4/ 2	$p = .34$
Diagnostic delay, yrs (mean, SD)	1.08 (0.79)	0.96 (0.64)	$p = .73$
Disease duration from symptom onset until scan, yrs (mean, SD)	2.42 (1.38)	2.03 (1.27)	$p = .54$
ALSFRS-R (mean, SD)	37.5 (6.05)	37 (7.27)	$p = .88$
Survival from scan, yrs (mean, SD)	2 (0.57)	3.07 (1.87)	$p = .22$

Table 6.10: MRI features - Demographic and clinical data of correctly and misclassified patients surviving > 18 months of the *training sample*.

Survival < 18 months			
	True Positive	**False Negative**	**p-value**
N	4	2	
Gender (male/ female)	2/2	1/1	
Age, yrs (means, SD)	66.4 (8.42)	59.08 (6.18)	$p = .31$
Handedness (r/ l)	3/1	2/0	$p = 1$
Site of onset (non-spinal/ spinal)	3/1	0/2	$p = .38$
Diagnostic delay, yrs (mean, SD)	1.5 (1.34)	0.84 (0.33)	$p = .41$
Disease duration from symptom onset until scan, yrs (mean, SD)	1.84 (1.44)	2.14 (1.99)	$p = .87$
ALSFRS-R (mean, SD)	35.25 (9.46)	33 (8.49)	$p = .79$
Survival from scan, yrs (mean, SD)	0.79 (0.08)	1.19 (0.35)	$p = .34$

Table 6.11: MRI features - Demographic and clinical data of correctly and misclassified patients surviving < 18 months of the *validation sample*.

Survival > 18 months			
	True Negative	**False Positive**	**p-value**
N	3	3	
Gender (male/ female)	2/ 1	0/ 3	$p = .39$
Age, yrs (means, SD)	50.47 (5.83)	59.72 (9.81)	$p = .25$
Handedness (r/ l)	2/ 1	3/ 0	$p = 1$
Site of onset (non-spinal/ spinal)	1/ 2	1/ 2	$p = 1$
Diagnostic delay, yrs (mean, SD)	0.88 (0.26)	0.89 (0.39)	$p = .97$
Disease duration from symptom onset until scan, yrs (mean, SD)	1.97 (0.57)	1.74 (0.6)	$p = .66$
ALSFRS-R (mean, SD)	41.33 (1.15)	37 (5.29)	$p = .29$
Survival from scan, yrs (mean, SD)	2.96 (1.72)	2.28 (1.03)	$p = .59$

Table 6.12: MRI features - Demographic and clinical data of correctly and misclassified patients surviving > 18 months of the *validation sample*.

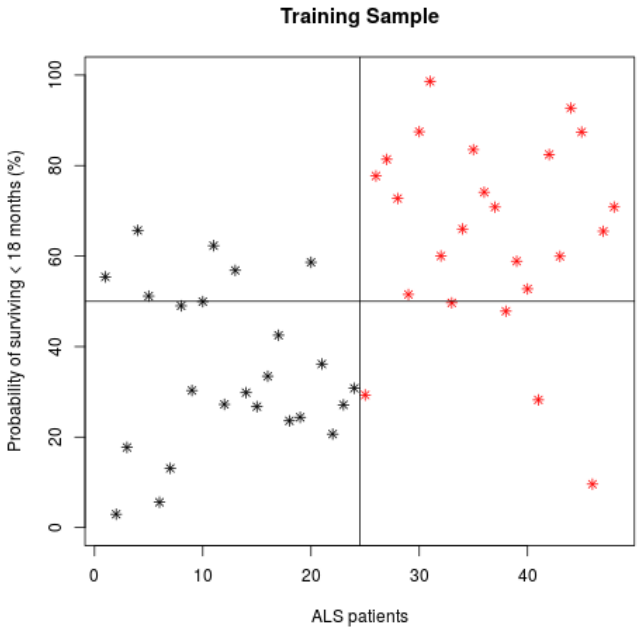

Figure 6.8: MRI features. Training sample: The probability of surviving less than 18 months. Red: patients surviving < 18 months from the date of their scan; Black: patients surviving > 18 months.

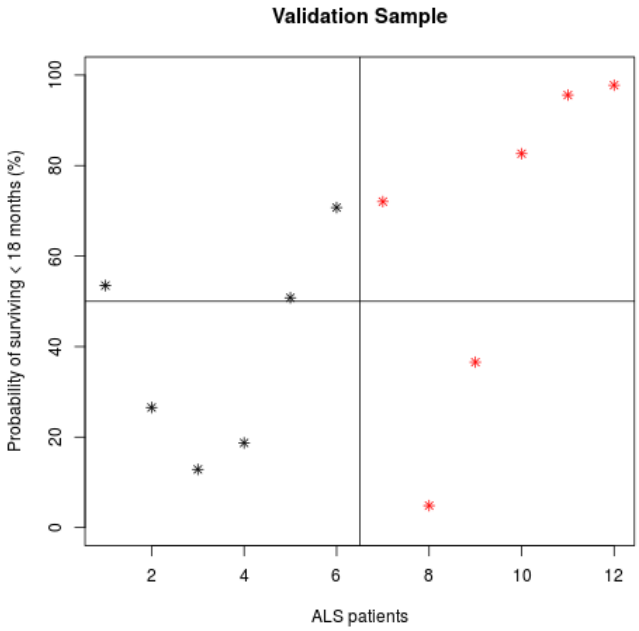

Figure 6.9: MRI features. Validation sample: The probability of surviving less than 18 months. Red: patients surviving < 18 months from the date of their scan; Black: patients surviving > 18 months.

Training Sample

True group / Predicted group	Surviving < 18 months	Surviving > 18 months
Surviving < 18 months	20	6
Surviving > 18 months	4	18

Sensitivity	75.00%
Specificity	83.34%
Accuracy	79.17%

Validation Sample

True group / Predicted group	Surviving < 18 months	Surviving > 18 months
Surviving < 18 months	5	2
Surviving > 18 months	1	4

Sensitivity	66.67%
Specificity	83.34%
Accuracy	75.00%

Table 6.13: Classification results based on both clinical and MRI features using a cut-off of 50% probability.

6.4.4 Binary logistic regression – Combinations of both clinical and MRI features

Figure 6.10 shows the probability of each patient of the training sample to survive less than 18 months based on clinical and MRI features. Figure 6.11 summaries the results for the validation sample. The corresponding classification results are shown in Table 6.13; the cut-off score was set to 50%.

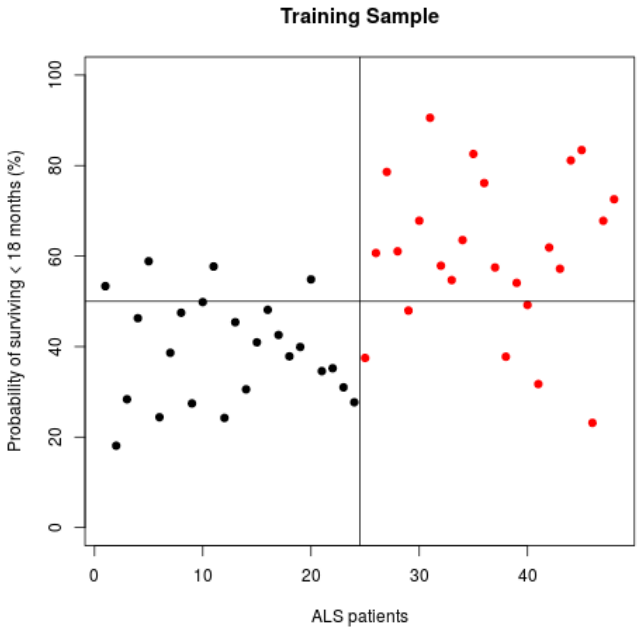

Figure 6.10: Clinical and MRI features. Training sample: The probability of surviving less than 18 months. Red: patients surviving < 18 months from the date of their scan; Black: patients surviving > 18 months.

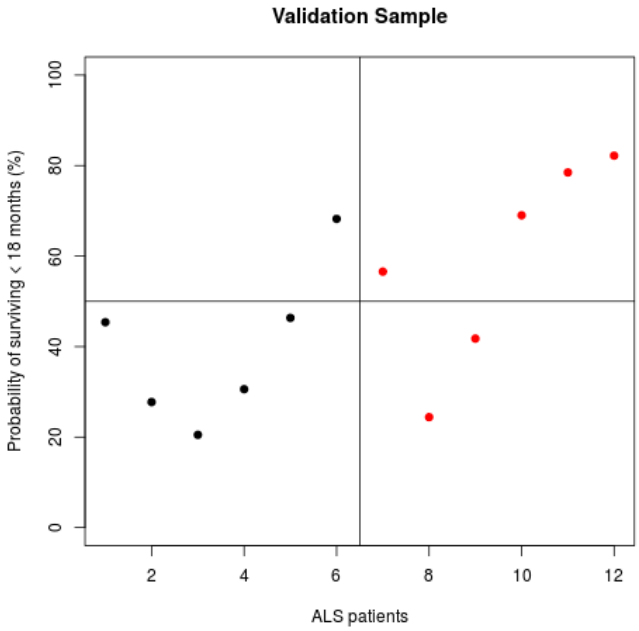

Figure 6.11: Clinical and MRI features. Validation sample: The probability of surviving less than 18 months. Red: patients surviving < 18 months from the date of their scan; Black: patients surviving > 18 months.

Survival < 18 months			
	True Positive	**False Negative**	**p-value**
N	18	6	
Gender (male/ female)	13/ 5	4/ 2	$p = 1$
Age, yrs (means, SD)	63.38 (8.69)	62.59 (6.09)	$p = .81$
Handedness (r/ l)	17/ 1	6/ 0	$p = 1$
Site of onset (non-spinal/ spinal)	6/ 12	2/ 4	$p = 1$
Diagnostic delay, yrs (mean, SD)	1.03 (0.69)	1.71 (1.01)	$p = .17$
Disease duration from symptom onset until scan, years (mean, SD)	1.99 (0.79)	2.71 (1.43)	$p = .29$
ALSFRS-R (mean, SD)	34 (7.21)	35.5 (6.06)	$p = .63$
Survival from scan, yrs (mean, SD)	0.97 (0.3)	0.84 (0.4)	$p = .50$

Table 6.14: Clinical and MRI features - Demographic and clinical data of correctly and misclassified patients surviving < 18 months of the *training sample*.

Misclassified patients

Table 6.14 and Table 6.15 describe the misclassified patients for the training sample; Table 6.16 and Table 6.17 misclassified patients surviving less than 18 months of the validation sample. There was no difference in demographic or clinical details between correctly and misclassified patients within the training sample or the validation sample.

Survival > 18 months			
	True Negative	**False Positive**	**p-value**
N	20	4	
Gender (male/ female)	10/ 10	3/ 1	$p = .71$
Age, yrs (means, SD)	61.82 (10.7)	61.42 (13.72)	$p = .96$
Handedness, (r/ l)	16/ 4	4/ 0	$p = .81$
Site of onset (non-spinal/ spinal)	8/ 12	2/ 2	$p = 1$
Diagnostic delay, yrs (mean, SD)	1.11 (0.77)	0.73 (0.58)	$p = .30$
Disease duration from symptom onset until scan, yrs (mean, SD)	2.46 (1.41)	1.64 (0.65)	$p = .10$
ALSFRS-R (mean, SD)	37.95 (5.9)	34.5 (7.9)	$p = .46$
Survival from scan, yrs (mean, SD)	1.98 (0.54)	3.66 (2.11)	$p = .21$

Table 6.15: Clinical and MRI features - Demographic and clinical data of correctly and misclassified patients surviving > 18 months of the *training sample*.

Survival < 18 months			
	True Positive	**False Negative**	**p-value**
N	4	2	
Gender (male/ female)	2/2	1/ 1	$p = 1$
Age, yrs (means, SD)	66.4 (8.42)	59.08 (6.18)	$p = .32$
Handedness (r/ l)	3/ 1	2/ 0	$p = 1$
Site of onset (non-spinal/spinal)	3/ 1	0 / 2	$p = .39$
Disease delay, yrs (mean, SD)	1.5 (1.34)	0.84 (0.33)	$p = .40$
Disease duration from symptom onset until scan, yrs (mean, SD)	1.84 (1.44)	2.14 (1.99)	$p = .87$
ALSFRS-R (mean, SD)	35.25 (9.46)	33 (8.49)	$p = .79$
Survival from scan, yrs (mean, SD)	0.79 (0.08)	1.19 (0.35)	$p = .35$

Table 6.16: Clinical and features - Demographic and clinical data of correctly and misclassified patients surviving < 18 months of the *validation sample*.

Survival > 18 months			
	True Negative	**False Positive**	**p-value**
N	5	1	
Gender (male/ female)	2/ 3	0/ 1	-
Age, yrs (means, SD)	52.64 (7.21)	67.38 (NA)	-
Handedness (r/ l)	4/ 1	1/ 0	-
Site of onset (non-spinal/ spinal)	2/ 3	0/ 1	-
Diagnostic delay, yrs (mean, SD)	0.91 (0.32)	0.75 (NA)	-
Disease duration from symptom onset until scan, yrs (mean, SD)	2.01 (0.41)	1.05 (NA)	-
ALSFRS-R (mean, SD)	38.8 (4.55)	41 (NA)	-
Survival from scan, yrs (mean, SD)	2.83 (1.36)	1.56 (NA)	-

Table 6.17: Clinical and MRI features - Demographic and clinical data of correctly and misclassified patients surviving > 18 months of the *validation sample*.

6.5 Discussion

The present study explores the role of MRI as prognostic biomarker in ALS. While more and more studies focus on diagnostic and monitoring biomarkers for ALS, there is a scarcity of prognostic studies. The overall objective was to explore the value of structural MRI measures of ALS-related brain changes and clinical characteristics in predicting the probability of 18-month survival. Such a tool could, on the one hand, ensure more appropriate planning of invasive therapeutic interventions and, on the other hand, reduce clinical variability for future clinical trials.

Based on the combination of structural brain measures and clinical characteristics, mortality within 18-month was predicted with relatively high accuracy; 79.17%. Moreover, 83.3% of patients were correctly identified as surviving for longer than 18 months following their brain scan, and 75% of the sample was correctly identified as surviving less than 18-months. Applying the regression algorithm to an independent validation sample further supports the validity of these findings. Despite the relatively small sample size of the validation cohort, the algorithm reached 75% accuracy. 83.34% of patients were correctly identified as surviving more than 18-months and 66.67% of patients were correctly identified as surviving less than 18 months. Based on MRI measures alone, the accuracy and sensitivity of the classification was similar, but the patients surviving more than 18 months were less likely to be identified correctly.

Using clinical and demographic measures alone, without MRI indices, prediction accuracy was considerably lower (66.67%). Similarly, the sensitivity and specificity profile of these predictions were inferior to the ones also incorporating MRI measures. These findings underscore the benefit of MRI measures of pathognomonic brain regions in predicting 18-month survival.

Evaluating misclassified patients based on clinical features alone, the group incorrectly classified surviving less than 18 months was significantly less phys-

ically impaired. They had a higher ALSFRS-R score. In contrast, patients misclassified as surviving longer than 18 months, had significantly longer disease duration. Adding MRI measure, there was no difference found between misclassified patients, again emphasizing the benefit of this additional information.

Previous studies have linked MRI measures to survival. Two-year survival was predicted using motor cortex spectroscopy with a sensitivity of 67% and a specificity of 83% (Kalra et al., 2006). Corticospinal tract diffusivity changes were utilised to predict three-year survival with a specificity of 61.5% and accuracy of 71.0% (Agosta et al., 2010b).
In contrast to previous studies, the present one employs a multi-modal approach assessing cortical thinning in addition to the four most commonly used indices of white matter degeneration. Additionally, the generalisability of this classification method is higher. As discussed in more detail in Chapter 5, the binary ridge regression was cross-validated to increase its generalisability. Additionally, the results were validated with an independent sample.

ALS patients in all stages of the disease are eager to participant in clinical trials and each trial is met with high hopes by patients and clinicians. It is desirable to enrol patients early after diagnosis so that as little as possible neurodegenerative change has taken place. Consequently, an early diagnosis is required. Various trials within the last years have failed (Mitsumoto et al., 2014) which could be attributed to the excitement with which each clinical trial is welcomed. In order to ensure rapid enrolment and to reach targeted sample size of the trial, patients are included regardless of their clinical subtypes (Nicholson et al., 2015). A further possible explanation for the failure is the variability of disease stages of the patients when they are recruited to the study. The heterogeneity of the sample may mask any possible success of the medication. Riluzole remains the only medications proven to extend survival of patients. But even the effectiveness of riluzole failed to be proven in the advanced stages of ALS (Bensimon et al., 2002).
A newly research area is targeted therapy i.e. the focus lies on possible ther-

apeutic approaches for specific ALS subgroups (Nicholson et al., 2015). For example, stem cells therapy is regarded to be less successful in bulbar onset ALS patients as the cells have to be delivered to the most affected regions and it is unlikely to benefit patients in advanced stages as stems cells are not able to replace lost motor neurons (Mitsumoto et al., 2014; Goutman and Feldman, 2015).
de Carvalho and Swash (2006) proposed that the inclusion of patients with rapid progression rates may shorten clinical trials. Nevertheless, one has to keep in mind that certain subtypes might respond differently to therapy (Bakkar et al., 2015). An effective medication for fast progressing patients might not be as successful in slow progressing patients. Overall, it is important that clinical trials include a variety of phenotypes while trying to reduce the variability of the sample by other means. It is necessary to control for confounding variables known to affect the study endpoint (Beghi et al., 2011). If patients drop out due to death it may not be related to the medication effect instead it might be that the disease has progressed too far for the medication to have any effect. Consequently, this represents a potential source of bias. As discussed above, there is no difference between the included patient groups despite their survival is significantly different. Employing the present approach would narrow the variability within the patient sample and could potentially distinguish patient groups for which the medication effect is different.

One may argue that the classification results of three different approaches do not sufficiently differ to only support one single approach. Therefore, one has to take into account the advantages of each approach. Whereas clinical indices are very cost-efficient and easily acquired, the advantage of using solely MRI measures lies in its objectivity. An observer-independent prognostic marker may be helpful for patient stratification into clinical trials. It is also important that study end-points, such as survival are independent from demographic factors.

6.6 Limitations and future directions

The study outlines a prediction method based on single-time point MRI data, which is a snapshot of *in vivo* pathology at specific moment in the patient's disease trajectory. Degeneration is a continuous process. In order to predict survival, one needs to know what brain structures are affect in the late stages of the disease. The current approach to split the patient into two groups is a crude approach. Survival prediction may be more accurate if multiple time-points are included and longitudinal change over time is considered. Moreover, the inclusion of other disease-specific anatomical regions, such as basal ganglia (Machts et al., 2015), spinal cord (El Mendili et al., 2014), cerebellar (Bede et al., 2015) or electrophysiological measures (de Carvalho and Swash, 2006) may improve prognostic categorisation further.

As only patients scanned at least 18 months ago were included, the sample size of the study is relatively limited and 20% of the patients were randomly allocated to the validation sample to demonstrate the generalizability of the methods. Using cross-validation within the training sample renders the results generalizable, and the validation sample supports the findings. Nevertheless, the present pilot study only outlines a proposed prognostic algorithm which should ideally be replicated in larger cohorts or data pooled from multiple centres.

Other future directions include assessment of two-year survival, or other clinical milestones, such as introduction of non-invasive ventilation, walking aids, feeding tubes etc. In this study, the cognitive and behavioural profile of the patients were not considered, despite evidence that executive dysfunction is associated with shorter survival (Elamin et al., 2011) and compliance with assistive devices (Olney et al., 2005). Furthermore, the effect of riluzole could not be assessed due to a lack of corresponding data. The majority of patients were on riluzole at the time of the scan.

6.7 Conclusions

In conclusion, this project outlines a potential approach to reduce clinical variability of ALS. The combination of MRI measures of pathognomonic brain regions and key clinical indices enable the accurate prediction of 18-month survival in ALS. Accurate, objective and validated prognostic markers are urgently required in ALS, and have implications both for clinical trial designs and individualised patient care.

Chapter 7

Summary

ALS is a fatal neurodegenerative condition affecting both upper and lower motor neurons. The initial diagnosis can be challenging and there are currently no disease-modifying treatments available.

The main objective of this thesis was to comprehensively evaluate the role of MRI as a biomarker of ALS. There is currently an urgent and unmet need for viable diagnostic, prognostic and monitoring biomarkers for the management for ALS. A diagnostic biomarker would ideally reduce the diagnostic delay and consequently, belated entry into clinical trials. A prognostic biomarker provides much needed information for patients, caregiver and healthcare professionals which is essential for care-planning, end-of-life decisions and stratification for clinical trials. A monitoring marker is essential for the evaluation of emerging disease modifying-drugs.

In order to thoroughly evaluate MRI as a biomarker the following approach has been adopted: First, an extensive literature review was conducted to identify optimal methodological frameworks. The consequently gathered data was then used to describe key patterns of ALS-associated structural brain changes based on cross-sectional and longitudinal comparisons. Longitudinal brain changes in ALS were discussed from a monitoring perspective. The core disease-related imaging measures were evaluated as diagnostic

biomarkers and used to predict survival.

The reason to conduct a literature review across multiple neurodegenerative conditions is to evaluate imaging methodology, sample size consideration, enrolment bias, follow-up rates and drop-out rates can be gained.
The main methodological lessons learned from the formal literature review is to include incidence and prevalence patients, enrolment patients shortly after their diagnosis, incorporate multiple follow-up assessments, which helps to evaluate the potential of MRI as a monitoring marker. Based on the reviewed literature, a follow-up interval of 4 months seems optimal in ALS. It allows for follow-up data of fast progressing patients, where a comparatively high drop-out rate is expected. It is also clear from the review, that a multimodal imaging approach is advisable to detect the different sensitively thresholds of these techniques to capture disease-related changes.

In general, ALS patients are eager to participate in research. In total, 86 patients were recruited and scanned every 4 months up to three times. The drop-out rate was as expected 23.25% for the 1st follow-up, 26.78% for the 2nd follow-up and 41.46% for the 3rd follow-up which took place a year after the baseline scan. In combination with the existing MRI data included in these studies, the average disease duration was 2.25 years at baseline and the average baseline ALSFRS-R was 37.4/48.

The objective of Chapter 3 was to describe key brain changes associated with ALS. Even though the core pathology, such as the corticospinal tract degeneration has been extensively investigated in the past, the key segments, such as the lateral fibres of the corona radiata, have been surprisingly understudied. From a biomarker perspective, it is crucial to identify which segments of the CST are the most vulnerable as this would be the most likely biomarker candidate. In addition, it is essential to define which diffusion parameter is the most sensitive to capture disease-related change. These questions also apply to the degeneration of the corpus callosum as another key brain region affected by ALS. A simple group comparison was first performed to highlight

ALS-associated change. Next the average white matter integrity of CST and CC segments were calculated. The radial diffusivity within the body of the corpus callosum and the cerebral peduncle best discriminated patients and controls.
The corticospinal tract and the corticobulbar tracts run separately in the internal capsule. In accordance to previous grey matter studies, phenotypic-specific degeneration was successfully highlighted within the white matter by stratifying patients based on their site of onset (bulbar or spinal onset). Additionally, clinical variables mapped homunculus-wise degenerative change in the corona radiata complementing previous grey matter studies. This chapter demonstrated that the corticospinal tracts and corpus callosum exhibit phenotype-specific segmental vulnerability in ALS. Furthermore, it was demonstrated that the diffusivity various parameters have distinct sensitivity profile to capture ALS-related change.

These results have direct implications for the biomarker research, e.g. which brain areas and which diffusivity measures are optimal candidate for a diagnostic biomarker which was further explored in the follow-up chapters.

The next chapter focused on longitudinal MRI changes in ALS from a monitoring biomarker perspective. An ideal monitoring biomarker is expected to capture structural changes within a relatively short period of time.

The inherent heterogeneity in ALS makes the interpretation of longitudinal studies challenging. Patients enrolled in such a study may already differ considerably at baseline. Additionally, longitudinal studies of ALS employ distinctly different study designs and statistical models which makes drawing unifying conclusions on the longitudinal course of ALS difficult. This chapter discusses differences in study design and how it affects study outcomes.
The main aim was to describe the evolution of pathological change over time and explore whether cortical thickness, grey matter density and white matter diffusivity indices can be used to map these longitudinal changes.

First, disease-related changes at baseline were compared to a group of healthy controls. This is essential to evaluate possible floor or ceiling effects. Patients exhibited considerable changes in the fractional anisotropy and radial diffusivity of the corticospinal tract as well as grey matter density alterations in the precentral gyrus. No significant cortical thinning was identified.
The subsequent analyses explored if a 4-month follow-up interval is sufficient to capture progressive radiological changes. This analysis simulated a clinical trial scenario, where patients in different stages of their disease are enrolled. The approach was repeated using a longer follow-up interval of 8 months. Only grey matter density changed significantly within the 4-month interval in the precentral gyrus and the cerebellum. Based on the 8-month follow-up interval, each MRI measure was able to detect progressive degenerative change.

In an additional analysis, presymptomatic patients were selected. These patient subgroups did not report physical disabilities of their lower limbs or their bulbar muscles over the course of the study, but exhibited structural brain change in the corresponding brain regions: patients without bulbar disability exhibited reduced white matter integrity of the inferior lateral corona radiata and patients without physical impairment of their lower limbs present cortical thinning of the superior precentral gyrus.

This chapter concluded that a 4-month interval was not sufficient to capture change for an average patient. Diffusion tensor imaging captured disease-related structural brain changes early during the course of the disease, reaching a floor effect. Grey matter degeneration appeared to start later which could potentially become an objective measurement to track disease progression.

In chapter 5, the findings of chapter 3 were evaluated from a clinical perspective. Even though brain changes due to ALS have been extensively characterised cross-sectionally, few studies capitalised on these results for clinical applications. The difficulties in diagnosing ALS and the pathway how MRI

may be used to decrease diagnostic delay has been established. Referring to oncology research as an example of biomarker development, ALS research needs to focus on discriminating patients from healthy controls and mimics using candidate biomarkers.

In this chapter, a binary logistic ridge regression was performed to determine the probability of an individual brain scan exhibiting ALS-related changes. The advantage of this approach is that the clinician can integrate this information with other clinical markers.

Using multiple MR metrics of multiple brain regions and correcting for age-related brain changes, classification accuracy was achieved with good sensitivity and moderate specificity. The results have been further validated in an independent sample and by their follow-up scans.
Future research needs to focus on discriminating mimic conditions and expand the approach to include different MRI platforms.

Chapter 6 explored MRI measures as possible prognostic biomarkers. The heterogeneity of ALS makes accurate individual prognosis challenging. It, furthermore, precludes smaller clinical trials to demonstrate effectiveness of a medications. A validated prognostic tool could stratify patient subgroups for clinical trials and would enable the planning of supportive interventions for an individual patient. This chapter describes the development and validation of a prognostic tool to predict 18-month survival based on ALS-associated white and grey matter changes. Three binary ridge regressions were performed based on: 1. clinical and demographical variables linked to survival, 2. disease-related MRI measures and 3. both clinical and MRI data.

Combining clinical and MRI variables, high prediction accuracy was achieved with high sensitivity and specificity. Using MRI metrics alone, similar accuracy and sensitivity was reached, but specificity was slightly lower. Using clinical measures alone, accuracy was considerably lower and misclassified patients had significantly less physical disability. The analyses of misclassi-

fied patients based on MRI features or the combined features did not reveal any differences. The advantages of each approach are discussed from a cost-efficiency, practicality, accuracy perspective as well as their utility for clinical trials. Overall, the results support the role of MRI as an objective prognostic tool in ALS.

7.1 Future directions

The overall aim of the thesis was to comprehensively evaluate the role of MRI as a biomarker for ALS. Throughout the chapters, it was demonstrated that MRI has the potential to identify core ALS-related changes, it can be used to predict survival and can capture progressive changes longitudinally. In conclusion, the findings suggest the MRI is indeed a robust surrogate marker of ALS-associated pathology and MRI metrics may be used as diagnostic, prognostic and monitoring markers in ALS. The findings of this large single-centre biomarker study need to be replicated in large, multi-centre, multi-platform studies and tested in real-life clinical applications and clinical trials.

Funding

This work was supported by the Irish Institute of Clinical Neuroscience (IICN) - Novartis Ireland Research Grant, The Iris O'Brien Foundation, The Perrigo Clinician-Scientist Research Fellowship, the Health Research Board and the Research Motor Neuron (RMN-Ireland) foundation. Professor Hardiman's research group has also received funding from the European Community's Seventh Framework Programme (FP7/2007-2013) under grant agreement n° [259867] (EUROMOTOR), the EU-Joint Programme for Neurodegeneration (JPND) SOPHIA project.

Bibliography

Abe, K., Fujimura, H., Kobayashi, Y., Fujita, N., and Yanagihara, T. (1997). Degeneration of the pyramidal tracts in patients with amyotrophic lateral sclerosis. A premortem and postmortem magnetic resonance imaging study. *Journal of neuroimaging : official journal of the American Society of Neuroimaging*, 7(4):208–12.

Abrahams, S., Goldstein, L. H., Suckling, J., Ng, V., Simmons, A., Chitnis, X., Atkins, L., Williams, S. C. R., and Leigh, P. N. (2005). Frontotemporal white matter changes in amyotrophic lateral sclerosis. *Journal of Neurology*, 252(3):321–331.

Acosta-Cabronero, J., Alley, S., Williams, G. B., Pengas, G., and Nestor, P. J. (2012). Diffusion tensor metrics as biomarkers in Alzheimer's disease. *PLoS One*, 7(11):e49072.

Agosta, F., Chiò, a., Cosottini, M., De Stefano, N., Falini, a., Mascalchi, M., Rocca, M. a., Silani, V., Tedeschi, G., and Filippi, M. (2010a). The present and the future of neuroimaging in amyotrophic lateral sclerosis. *AJNR. American journal of neuroradiology*, 31(10):1769–77.

Agosta, F., Pagani, E., Petrolini, M., Caputo, D., Perini, M., Prelle, a., Salvi, F., and Filippi, M. (2010b). Assessment of White Matter Tract Damage in Patients with Amyotrophic Lateral Sclerosis: A Diffusion Tensor MR Imaging Tractography Study. *AJNR. American journal of neuroradiology*, 31(8):1457–61.

Agosta, F., Rocca, M. A., Valsasina, P., Sala, S., Caputo, D., Perini, M.,

Salvi, F., Prelle, A., and Filippi, M. (2009). A longitudinal diffusion tensor MRI study of the cervical cord and brain in amyotrophic lateral sclerosis patients. *J Neurol Neurosurg Psychiatry*, 80(1):53–55.

Agosta, F., Valsasina, P., Riva, N., Copetti, M., Messina, M. J., Prelle, A., Comi, G., and Filippi, M. (2012). The cortical signature of amyotrophic lateral sclerosis. *PLoS One*, 7(8):e42816.

Al-Chalabi, A. and Hardiman, O. (2013). The epidemiology of ALS: a conspiracy of genes, environment and time. *Nature Reviews Neurology*.

Al-Chalabi, A., Hardiman, O., Kiernan, M. C., Chiò, A., Rix-Brooks, B., and van den Berg, L. H. (2016). Amyotrophic lateral sclerosis: moving towards a new classification system. *The Lancet Neurology*, 15(11):1182–1194.

Alonso, a., Logroscino, G., Jick, S. S., and Hernán, M. a. (2009). Incidence and lifetime risk of motor neuron disease in the United Kingdom: a population-based study. *European Journal of Neurology*, 16(6):745–751.

Andersen, P. M. and Al-Chalabi, A. (2011). Clinical genetics of amyotrophic lateral sclerosis: what do we really know? *Nature Reviews Neurology*, 7(11):603–615.

Arbabshirani, M. R., Plis, S., Sui, J., and Calhoun, V. D. (2016). Single subject prediction of brain disorders in neuroimaging: Promises and pitfalls. *NeuroImage*.

Ashburner, J. and Friston, K. J. (2000). Voxel-based morphometry–the methods. *NeuroImage*, 11(6 Pt 1):805–21.

Aylward, E. H., Sparks, B. F., Field, K. M., Yallapragada, V., Shpritz, B. D., Rosenblatt, A., Brandt, J., Gourley, L. M., Liang, K., Zhou, H., Margolis, R. L., and Ross, C. A. (2004). Onset and rate of striatal atrophy in preclinical Huntington disease. *Neurology*, 63(1):66–72.

Bak, T. H. and Chandran, S. (2012). What wires together dies together: verbs, actions and neurodegeneration in motor neuron disease. *Cortex*, 48(7):936–944.

Bakkar, N., Boehringer, A., and Bowser, R. (2015). Use of biomarkers in ALS drug development and clinical trials. *Brain research*, 1607:94–107.

Balendra, R., Jones, A., Jivraj, N., Steen, I. N., Young, C. A., Shaw, P. J., Turner, M. R., Leigh, P. N., Al-Chalabi, A., and UK-MND LiCALS Study Group, Mito Target ALS Study Group, M. T. A. S. G. (2015). Use of clinical staging in amyotrophic lateral sclerosis for phase 3 clinical trials. *Journal of neurology, neurosurgery, and psychiatry*, 86(1):45–9.

Bashat, D. B., Artzi, M., Tarrasch, R., Nefussy, B., Drory, V. E., and Aizenstein, O. (2015). A potential tool for the diagnosis of ALS based on diffusion tensor imaging. *Amyotrophic Lateral Sclerosis*.

Basser, P., Mattiello, J., and Lebihan, D. (1994). Estimation of the Effective Self-Diffusion Tensor from the NMR Spin Echo. *Journal of Magnetic Resonance, Series B*, 103(3):247–254.

Beaulieu, C. (2002). The basis of anisotropic water diffusion in the nervous system - a technical review. *NMR in biomedicine*, 15(7-8):435–55.

Bede, P., Bokde, A., Elamin, M., Byrne, S., McLaughlin, R. L., Jordan, N., Hampel, H., Gallagher, L., Lynch, C., Fagan, A. J., Pender, N., and Hardiman, O. (2012a). Grey matter correlates of clinical variables in amyotrophic lateral sclerosis (ALS): a neuroimaging study of ALS motor phenotype heterogeneity and cortical focality. *Journal of Neurology, Neurosurgery & Psychiatry*, 84(7):766–73.

Bede, P., Bokde, A. L. W., Byrne, S., Elamin, M., Fagan, A. J., and Hardiman, O. (2012b). Spinal cord markers in ALS: Diagnostic and biomarker considerations. *Amyotrophic Lateral Sclerosis*.

Bede, P., Bokde, A. L. W., Byrne, S., Elamin, M., McLaughlin, R. L., Kenna, K., Fagan, A. J., Pender, N., Bradley, D. G., and Hardiman, O. (2013a). Multiparametric MRI study of ALS stratified for the C9orf72 genotype. *Neurology*, 81(4):361–9.

Bede, P., Elamin, M., Byrne, S., McLaughlin, R. L., Kenna, K., Vajda, A., Fagan, A., Bradley, D. G., and Hardiman, O. (2015). Patterns of cerebral and cerebellar white matter degeneration in ALS. *Journal of neurology, neurosurgery, and psychiatry*, 86(4):468–70.

Bede, P., Elamin, M., Byrne, S., McLaughlin, R. L., Kenna, K., Vajda, A., Pender, N., Bradley, D. G., and Hardiman, O. (2013b). Basal ganglia involvement in amyotrophic lateral sclerosis. *Neurology*, 81(24):2107–15.

Bede, P. and Hardiman, O. (2014). Lessons of ALS imaging: Pitfalls and future directions — A critical review. *NeuroImage: Clinical*, 4:436–443.

Bede, P., Iyer, P. M., Schuster, C., Elamin, M., Mclaughlin, R. L., Kenna, K., and Hardiman, O. (2016). The selective anatomical vulnerability of ALS: 'disease-defining' and 'disease-defying' brain regions. *Amyotrophic Lateral Sclerosis and Frontotemporal Degeneration*, 17(7-8):561–570.

Bede, P., Oliver, D., Stodart, J., van den Berg, L., Simmons, Z., O Brannagáin, D., Borasio, G. D., and Hardiman, O. (2011). Palliative care in amyotrophic lateral sclerosis: a review of current international guidelines and initiatives. *Journal of neurology, neurosurgery, and psychiatry*, 82(4):413–8.

Beghi, E., Chiò, A., Couratier, P., Esteban, J., Hardiman, O., Logroscino, G., Millul, A., Mitchell, D., Preux, P.-M., Pupillo, E., Stevic, Z., Swingler, R., Traynor, B. J., Van den Berg, L. H., Veldink, J. H., and Zoccolella, S. (2011). The epidemiology and treatment of ALS: focus on the heterogeneity of the disease and critical appraisal of therapeutic trials. *Amyotrophic lateral sclerosis : official publication of the World Federation of Neurology Research Group on Motor Neuron Diseases*, 12(1):1–10.

Bellman, R. (1961). Adaptive control processes: a guided tour. *pup.princeton.edu*.

Ben Bashat, D., Artzi, M., Tarrasch, R., Nefussy, B., Drory, V. E., and Aizenstein, O. (2011). A potential tool for the diagnosis of ALS based on

diffusion tensor imaging. *Amyotrophic lateral sclerosis : official publication of the World Federation of Neurology Research Group on Motor Neuron Diseases*, 12(6):398–405.

Benatar, M. and Wuu, J. (2012). Presymptomatic studies in ALS: rationale, challenges, and approach. *Neurology*, 79(16):1732–9.

Bensimon, G., Lacomblez, L., Delumeau, J. C., Bejuit, R., Truffinet, P., Meininger, V., and III, f. t. R. S. G. (2002). A study of riluzole in the treatment of advanced stage or elderly patients with amyotrophic lateral sclerosis. *Journal of Neurology*, 249(5):609–615.

Blain, C. R. V., Williams, V. C., Johnston, C., Stanton, B. R., Ganesalingam, J., Jarosz, J. M., Jones, D. K., Barker, G. J., Williams, S. C. R., Leigh, N. P., and Simmons, A. (2007). A longitudinal study of diffusion tensor MRI in ALS. *Amyotrophic lateral sclerosis : official publication of the World Federation of Neurology Research Group on Motor Neuron Diseases*, 8(6):348–355.

Bourke, S. C., Tomlinson, M., Williams, T. L., Bullock, R. E., Shaw, P. J., and Gibson, G. J. (2006). Effects of non-invasive ventilation on survival and quality of life in patients with amyotrophic lateral sclerosis: a randomised controlled trial. *The Lancet Neurology*, 5(2):140–147.

Braak, H. and Braak, E. (1995). Staging of alzheimer's disease-related neurofibrillary changes. *Neurobiology of Aging*, 16(3):271–278.

Brettschneider, J., Del Tredici, K., Toledo, J. B., Robinson, J. L., Irwin, D. J., Grossman, M., Suh, E., Van Deerlin, V. M., Wood, E. M., Baek, Y., Kwong, L., Lee, E. B., Elman, L., McCluskey, L., Fang, L., Feldengut, S., Ludolph, A. C., Lee, V. M.-Y., Braak, H., and Trojanowski, J. Q. (2013). Stages of pTDP-43 pathology in amyotrophic lateral sclerosis. *Annals of Neurology*, 74(1):20–38.

Brooks, B. R., Miller, R. G., Swash, M., and Munsat, T. L. (2000). El Escorial revisited: Revised criteria for the diagnosis of amyotrophic lateral

sclerosis. *Amyotrophic Lateral Sclerosis and Other Motor Neuron Disorders*, 1(5):293–299.

Budde, M. D., Xie, M., Cross, A. H., and Song, S.-K. (2009). Axial diffusivity is the primary correlate of axonal injury in the experimental autoimmune encephalomyelitis spinal cord: a quantitative pixelwise analysis. *The Journal of neuroscience : the official journal of the Society for Neuroscience*, 29(9):2805–13.

Byrne, S., Elamin, M., Bede, P., Shatunov, A., Walsh, C., Corr, B., Heverin, M., Jordan, N., Kenna, K., Lynch, C., McLaughlin, R. L., Iyer, P. M., O'Brien, C., Phukan, J., Wynne, B., Bokde, A. L., Bradley, D. G., Pender, N., Al-Chalabi, A., and Hardiman, O. (2012). Cognitive and clinical characteristics of patients with amyotrophic lateral sclerosis carrying a C9orf72 repeat expansion: a population-based cohort study. *The Lancet Neurology*, 11(3):232–240.

Canu, E., Agosta, F., Rive, N., Sala, S., Prelle, A., Caputo, D., Perini, M., Comi, G., Filippi, M., Riva, N., Sala, S., Prelle, A., Caputo, D., Perini, M., and Comi, G. (2011). The Topography of Brain Microstructural Damage in Amyotrophic Lateral Sclerosis Assessed Using Diffusion Tensor MR Imaging. *AJNR. American journal of neuroradiology*, 32(7):1307–1314.

Cardenas-Blanco, A., Machts, J., Acosta-Cabronero, J., Kaufmann, J., Abdulla, S., Kollewe, K., Petri, S., Schreiber, S., Heinze, H.-J., Dengler, R., Vielhaber, S., and Nestor, P. J. (2016). Structural and diffusion imaging versus clinical assessment to monitor amyotrophic lateral sclerosis. *NeuroImage: Clinical*.

Cedarbaum, J. M., Stambler, N., Malta, E., Fuller, C., Hilt, D., Thurmond, B., and Nakanishi, A. (1999). The ALSFRS-R: a revised ALS functional rating scale that incorporates assessments of respiratory function. *Journal of the Neurological Sciences*, 169(1):13–21.

Cellura, E., Spataro, R., Taiello, A. A. C., Bella, V. L., and La Bella, V. (2012). Factors affecting the diagnostic delay in amyotrophic lateral sclerosis. *Clinical Neurology and Neurosurgery*, 114(6):550–554.

Chang, J. L., Lomen-Hoerth, C., Murphy, J., Henry, R. G., Kramer, J. H., Miller, B. L., and Gorno-Tempini, M. L. (2005). A voxel-based morphometry study of patterns of brain atrophy in ALS and ALS / FTLD. *Neurology*, 65(1):75–80.

Chen, S.-H., Sun, J., Dimitrov, L., Turner, A. R., Adams, T. S., Meyers, D. A., Chang, B.-L., Zheng, S. L., Grönberg, H., Xu, J., and Hsu, F.-C. (2008). A support vector machine approach for detecting gene-gene interaction. *Genetic Epidemiology*, 32(2):152–167.

Chen, Z. and Ma, L. (2010). Grey matter volume changes over the whole brain in amyotrophic lateral sclerosis: A voxel-wise meta-analysis of voxel based morphometry studies. *Amyotrophic Lateral Sclerosis*, 11(June):549–554.

Chiò, A. (1999). ISIS Survey: an international study on the diagnostic process and its implications in amyotrophic lateral sclerosis. *Journal of neurology*, 246 Suppl(S3):III1–5.

Chiò, A., Mora, G., Calvo, A., Mazzini, L., Bottacchi, E., and Mutani, R. (2009). Epidemiology of ALS in Italy: a 10-year prospective population-based study. *Neurology*, 72(8):725–31.

Chiò, A., Pagani, M., Agosta, F., Calvo, A., Cistaro, A., and Filippi, M. (2014). Neuroimaging in amyotrophic lateral sclerosis: insights into structural and functional changes. *The Lancet Neurology*, 13(12):1228–1240.

Ciarmiello, A., Giovacchini, G., Orobello, S., Bruselli, L., Elifani, F., and Squitieri, F. (2012). 18F-FDG PET uptake in the pre-Huntington disease caudate affects the time-to-onset independently of CAG expansion size. *European Journal of Nuclear Medicine and Molecular Imaging*, 39(6):1030–1036.

Ciccarelli, O., Behrens, T. E., Altmann, D. R., Orrell, R. W., Howard, R. S., Johansen-Berg, H., Miller, D. H., Matthews, P. M., and Thompson, A. J. (2006). Probabilistic diffusion tractography: a potential tool to assess the rate of disease progression in amyotrophic lateral sclerosis. *Brain : a journal of neurology*, 129(Pt 7):1859–71.

Cronin, S., Hardiman, O., and Traynor, B. J. (2007). Ethnic variation in the incidence of ALS: A systematic review.

de Carvalho, M. and Swash, M. (2006). Can selection of rapidly progressing patients shorten clinical trials in amyotrophic lateral sclerosis? *Archives of neurology*, 63(4):557–60.

Desiato, M. T., Bernardi, G., Hagi H, A., Boffa, L., and Caramia, M. D. (2002). Transcranial magnetic stimulation of motor pathways directed to muscles supplied by cranial nerves in amyotrophic lateral sclerosis. *Clinical Neurophysiology*, 113(1):132–140.

Desikan, R. S., Ségonne, F., Fischl, B., Quinn, B. T., Dickerson, B. C., Blacker, D., Buckner, R. L., Dale, A. M., Maguire, R. P., Hyman, B. T., Albert, M. S., and Killiany, R. J. (2006). An automated labeling system for subdividing the human cerebral cortex on MRI scans into gyral based regions of interest. *NeuroImage*, 31(3):968–80.

Diedrichsen, J., Balsters, J. H., Flavell, J., Cussans, E., and Ramnani, N. (2009). A probabilistic MR atlas of the human cerebellum.

Donaghy, C., Dick, A., Hardiman, O., and Patterson, V. (2008). Timeliness of diagnosis in motor neurone disease: a population-based study. *The Ulster medical journal*, 77(1):18–21.

Donaghy, C., O'Toole, O., Sheehan, C., Kee, F., Hardiman, O., and Patterson, V. (2009). An all-Ireland epidemiological study of MND, 2004-2005. *European Journal of Neurology*, 16(1):148–153.

Douaud, G., Smith, S., Jenkinson, M., Behrens, T., Johansen-Berg, H., Vickers, J., James, S., Voets, N., Watkins, K., Matthews, P. M., and James,

A. (2007). Anatomically related grey and white matter abnormalities in adolescent-onset schizophrenia. *Brain*, 130(9):2375–2386.

Eisen, A., Kiernan, M., Mitsumoto, H., and Swash, M. (2014). Amyotrophic lateral sclerosis: a long preclinical period? *Journal of neurology, neurosurgery, and psychiatry*, 85(11):1232–8.

El Mendili, M.-M., Cohen-Adad, J., Pelegrini-Issac, M., Rossignol, S., Morizot-Koutlidis, R., Marchand-Pauvert, V., Iglesias, C., Sangari, S., Katz, R., Lehericy, S., Benali, H., Pradat, P.-F., Mendili, M. E., and Cohen-Adad, J. (2014). Multi-parametric spinal cord MRI as potential progression marker in amyotrophic lateral sclerosis. *PloS one*, 9(4):e95516.

Elamin, M., Bede, P., Byrne, S., Jordan, N., Gallagher, L., Wynne, B., O'Brien, C., Phukan, J., Lynch, C., Pender, N., Hardiman, O., O'Brien, C., Phukan, J., Lynch, C., and Pender, N. (2013). Cognitive changes predict functional decline in ALS A population-based longitudinal study. *Neurology*, 80(17):1590–1597.

Elamin, M., Phukan, J., Bede, P., Jordan, N., Byrne, S., Pender, N., and Hardiman, O. (2011). Executive dysfunction is a negative prognostic indicator in patients with ALS without dementia. *Neurology*, 76(14):1263–1269.

Filippini, N., Douaud, G., Mackay, C. E., Knight, S., Talbot, K., and Turner, M. R. (2010). Corpus callosum involvement is a consistent feature of amyotrophic lateral sclerosis. *Neurology*, 75(18):1645–1652.

Fischl, B. and Dale, A. M. (2000). Measuring the thickness of the human cerebral cortex from magnetic resonance images. *Proceedings of the National Academy of Sciences*, 97(20):11050–11055.

Fjell, A. M., McEvoy, L., Holland, D., Dale, A. M., and Walhovd, K. B. (2013a). Brain changes in older adults at very low risk for Alzheimer's disease. *J Neurosci*, 33(19):8237–8242.

Fjell, A. M., Westlye, L. T., Grydeland, H., Amlien, I., Espeseth, T., Reinvang, I., Raz, N., Holland, D., Dale, A. M., and Walhovd, K. B. (2013b). Critical ages in the life course of the adult brain: nonlinear subcortical aging. *Neurobiology of Aging*, 34(10):2239–2247.

Foerster, B. R., Dwamena, B. A., Petrou, M., Carlos, R. C., Callaghan, B. C., Churchill, C. L., Mohamed, M. A., Bartels, C., Benatar, M., Bonzano, L., Ciccarelli, O., Cosottini, M., Ellis, C. M., Ehrenreich, H., Filippini, N., Ito, M., Kalra, S., Melhem, E. R., Pyra, T., Roccatagliata, L., Senda, J., Sobue, G., Turner, M. R., Feldman, E. L., and Pomper, M. G. (2013). Diagnostic accuracy of diffusion tensor imaging in amyotrophic lateral sclerosis: a systematic review and individual patient data meta-analysis. *Academic radiology*, 20(9):1099–106.

Fox, N. and Warrington, E. (1996). Presymptomatic hippocampal atrophy in Alzheimer's disease. *Brain*.

Freund, P., Wheeler-Kingshott, C., Jackson, J., Miller, D., Thompson, A., and Ciccarelli, O. (2010). Recovery after spinal cord relapse in multiple sclerosis is predicted by radial diffusivity. *Mult Scler*, 16(10):1193–1202.

Friedman, J., Hastie, T., and Tibshirani, R. (2010). Regularization Paths for Generalized Linear Models via Coordinate Descent. *Journal of statistical software*, 33(1):1–22.

Frings, L., Mader, I., Landwehrmeyer, B. G., Weiller, C., Hull, M., and Huppertz, H. J. (2012). Quantifying change in individual subjects affected by frontotemporal lobar degeneration using automated longitudinal MRI volumetry. *Hum Brain Mapp*, 33(7):1526–1535.

Gomeni, R., Fava, M., and Consortium, T. P. R. O.-A. A. C. T. (2014). Amyotrophic lateral sclerosis disease progression model. *Amyotrophic Lateral Sclerosis and Frontotemporal Degeneration*, 15(1-2):119–129.

Gordon, P. H., Salachas, F., Lacomblez, L., Le Forestier, N., Pradat, P.-F., Bruneteau, G., Elbaz, A., and Meininger, V. (2013). Predicting survival

of patients with amyotrophic lateral sclerosis at presentation: a 15-year experience. *Neuro-degenerative diseases*, 12(2):81–90.

Goutman, S. A. and Feldman, E. L. (2015). Clinical Trials of Therapies for Amyotrophic Lateral Sclerosis: One Size Does Not Fit All. *JAMA neurology*, 72(7):743–4.

Grolez, G., Moreau, C., Danel-Brunaud, V., Delmaire, C., Lopes, R., Pradat, P. F., El Mendili, M. M., Defebvre, L., and Devos, D. (2016). The value of magnetic resonance imaging as a biomarker for amyotrophic lateral sclerosis: a systematic review. *BMC Neurology*, 16(1):155.

Grothe, M., Heinsen, H., and Teipel, S. (2013). Longitudinal measures of cholinergic forebrain atrophy in the transition from healthy aging to Alzheimer's disease. *Neurobiol Aging*, 34(4):1210–1220.

Gupta, P. K., Prabhakar, S., Sharma, S., and Anand, A. (2012). A predictive model for amyotrophic lateral sclerosis (ALS) diagnosis. *Journal of the neurological sciences*, 312(1-2):68–72.

Hardiman, O., van den Berg, L. H., and Kiernan, M. C. (2011). Clinical diagnosis and management of amyotrophic lateral sclerosis. *Nature reviews. Neurology*, 7(11):639–649.

Hoehn, M. and Yahr, D. (1967). Parkinsonism: onset, progression, and mortality. *Neurology*.

Hong, Y.-H., Lee, K.-W., Sung, J.-J., Chang, K.-H., and Song, I. C. (2004). Diffusion tensor MRI as a diagnostic tool of upper motor neuron involvement in amyotrophic lateral sclerosis. *Journal of the Neurological Sciences*, 227(1):73–78.

Househam, E. and Swash, M. (2000). Diagnostic delay in amyotrophic lateral sclerosis: what scope for improvement? *Journal of the Neurological Sciences*, 180(1-2):76–81.

Jack, C. R., Bernstein, M. A., Fox, N. C., Thompson, P., Alexander, G., Harvey, D., Borowski, B., Britson, P. J., L. Whitwell, J., Ward, C., Dale, A. M., Felmlee, J. P., Gunter, J. L., Hill, D. L., Killiany, R., Schuff, N., Fox-Bosetti, S., Lin, C., Studholme, C., DeCarli, C. S., Gunnar Krueger, H. A., Ward, H. A., Metzger, G. J., Scott, K. T., Mallozzi, R., Blezek, D., Levy, J., Debbins, J. P., Fleisher, A. S., Albert, M., Green, R., Bartzokis, G., Glover, G., Mugler, J., and Weiner, M. W. (2008). The Alzheimer's disease neuroimaging initiative (ADNI): MRI methods. *Journal of Magnetic Resonance Imaging*, 27(4):685–691.

Johnston, C. a., Stanton, B. R., Turner, M. R., Gray, R., Blunt, A. H.-M., Butt, D., Ampong, M.-A., Shaw, C. E., Leigh, P. N., and Al-Chalabi, A. (2006). Amyotrophic lateral sclerosis in an urban setting: a population based study of inner city London. *Journal of neurology*, 253(12):1642–3.

Kalra, S., Tai, P., Genge, A., and Arnold, D. (2006). Rapid improvement in cortical neuronal integrity in amyotrophic lateral sclerosis detected by proton magnetic resonance spectroscopic imaging. *Journal of neurology*.

Kasper, E., Schuster, C., Machts, J., Kaufmann, J., Bittner, D., Vielhaber, S., Benecke, R., Teipel, S., and Prudlo, J. (2014). Microstructural white matter changes underlying cognitive and behavioural impairment in ALS–an in vivo study using DTI. *PloS one*, 9(12):e114543.

Kassubek, J., Müller, H.-P., Del Tredici, K., Brettschneider, J., Pinkhardt, E. H., Lulé, D., Böhm, S., Braak, H., and Ludolph, A. C. (2014). Diffusion tensor imaging analysis of sequential spreading of disease in amyotrophic lateral sclerosis confirms patterns of TDP-43 pathology. *Brain : a journal of neurology*, 137(Pt 6):1733–40.

Kenna, K. P., McLaughlin, R. L., Byrne, S., Elamin, M., Heverin, M., Kenny, E. M., Cormican, P., Morris, D. W., Donaghy, C. G., Bradley, D. G., and Hardiman, O. (2013). Delineating the genetic heterogeneity of ALS using targeted high-throughput sequencing. *Journal of medical genetics*, 50(11):776–83.

Kenna, K. P., van Doormaal, P. T. C., Dekker, A. M., Ticozzi, N., Kenna, B. J., Diekstra, F. P., van Rheenen, W., van Eijk, K. R., Jones, A. R., Keagle, P., Shatunov, A., Sproviero, W., Smith, B. N., van Es, M. A., Topp, S. D., Kenna, A., Miller, J. W., Fallini, C., Tiloca, C., McLaughlin, R. L., Vance, C., Troakes, C., Colombrita, C., Mora, G., Calvo, A., Verde, F., Al-Sarraj, S., King, A., Calini, D., de Belleroche, J., Baas, F., van der Kooi, A. J., de Visser, M., ten Asbroek, A. L. M. A., Sapp, P. C., McKenna-Yasek, D., Polak, M., Asress, S., Muñoz-Blanco, J. L., Strom, T. M., Meitinger, T., Morrison, K. E., D'Alfonso, S., Mazzini, L., Comi, G. P., Del Bo, R., Ceroni, M., Gagliardi, S., Querin, G., Bertolin, C., Pensato, V., Castellotti, B., Corti, S., Cereda, C., Corrado, L., Sorarù, G., Lauria, G., Williams, K. L., Leigh, P. N., Nicholson, G. A., Blair, I. P., Leblond, C. S., Dion, P. A., Rouleau, G. A., Pall, H., Shaw, P. J., Turner, M. R., Talbot, K., Taroni, F., Boylan, K. B., Van Blitterswijk, M., Rademakers, R., Esteban-Pérez, J., García-Redondo, A., Van Damme, P., Robberecht, W., Chio, A., Gellera, C., Drepper, C., Sendtner, M., Ratti, A., Glass, J. D., Mora, J. S., Basak, N. A., Hardiman, O., Ludolph, A. C., Andersen, P. M., Weishaupt, J. H., Brown, R. H., Al-Chalabi, A., Silani, V., Shaw, C. E., van den Berg, L. H., Veldink, J. H., and Landers, J. E. (2016). NEK1 variants confer susceptibility to amyotrophic lateral sclerosis. *Nature Genetics*, 48(9):1037–1042.

Kiernan, M. C., Vucic, S., Cheah, B. C., Turner, M. R., Eisen, A., Hardiman, O., Burrell, J. R., and Zoing, M. C. (2011). Amyotrophic lateral sclerosis. *Lancet*, 377(9769):942–955.

Knopman, D. S., Jack, C., Kramer, J. H., Jack Jr., C. R., Kramer, J. H., Boeve, B. F., Caselli, R. J., Graff-Radford, N. R., Mendez, M. F., Miller, B. L., and Mercaldo, N. D. (2009). Brain and ventricular volumetric changes in frontotemporal lobar degeneration over 1 year. *Neurology*, 72(21):1843–1849.

Koikkalainen, J., Pölönen, H., Mattila, J., van Gils, M., Soininen, H., and

Lötjönen, J. (2012). Improved classification of Alzheimer's disease data via removal of nuisance variability. *PloS one*, 7(2):e31112.

Kraemer, M., Buerger, M., and Berlit, P. (2010). Diagnostic problems and delay of diagnosis in amyotrophic lateral sclerosis. *Clinical Neurology and Neurosurgery*, 112(2):103–105.

Kuperberg, G. R., Broome, M. R., McGuire, P. K., and al., E. (2003). Regionally localized thinning of the cerebral cortex in schizophrenia. *Archives of General Psychiatry*, 60(9):878–888.

Kurtzke, J. F. (1983). Rating neurologic impairment in multiple sclerosis: an expanded disability status scale (EDSS). *Neurology*, 33(11):1444–52.

Kwan, J. Y., Meoded, A., Danielian, L. E., Wu, T., and Floeter, M. K. (2012). Structural imaging differences and longitudinal changes in primary lateral sclerosis and amyotrophic lateral sclerosis. *NeuroImage: Clinical*, 2(0):151–160.

Laakso, M. P., Lehtovirta, M., Partanen, K., Riekkinen, P. J., and Soininen, H. (2000). Hippocampus in Alzheimer's disease: a 3-year follow-up MRI study. *Biol Psychiatry*, 47(6):557–561.

Lam, B. Y. K., Halliday, G. M., Irish, M., Hodges, J. R., and Piguet, O. (2014). Longitudinal white matter changes in frontotemporal dementia subtypes. *Human Brain Mapping*, 35(7):3547–3557.

Lee, D. H., Kwon, Y. H., Hwang, Y. T., Kim, J. H., and Park, J. W. (2012). Somatotopic location of corticospinal tracts in the internal capsule with MR tractography. *European neurology*, 67(2):69–73.

Leung, K. K., Bartlett, J. W., Barnes, J., Manning, E. N., Ourselin, S., and Fox, N. C. (2013). Cerebral atrophy in mild cognitive impairment and Alzheimer disease: rates and acceleration. *Neurology*, 80(7):648–654.

Li, J., Pan, P., Song, W., Huang, R., Chen, K., and Shang, H. (2012). A meta-analysis of diffusion tensor imaging studies in amyotrophic lateral sclerosis. *Neurobiology of aging*, 33(8):1833–1838.

Lillo, P., Mioshi, E., Burrell, J. R., Kiernan, M. C., Hodges, J. R., and Hornberger, M. (2012). Grey and white matter changes across the amyotrophic lateral sclerosis-frontotemporal dementia continuum. *PloS one*, 7(8):e43993.

Logroscino, G., Traynor, B. J., Hardiman, O., Chiò, A., Mitchell, D., Swingler, R. J., Millul, A., Benn, E., and Beghi, E. (2010). Incidence of amyotrophic lateral sclerosis in Europe. *Journal of neurology, neurosurgery, and psychiatry*, 81(4):385–90.

Lu, P. H., Thompson, P. M., Leow, A., Lee, G. J., Lee, A., Yanovsky, I., Parikshak, N., Khoo, T., Wu, S., Geschwind, D., and Bartzokis, G. (2011). Apolipoprotein E Genotype is Associated with Temporal and Hippocampal Atrophy Rates in Healthy Elderly Adults: A Tensor-Based Morphometry Study. *Journal of Alzheimer's Disease*, 23(3):433–442.

Ludolph, A., Drory, V., Hardiman, O., Nakano, I., Ravits, J., Robberecht, W., Shefner, J., and ALS/MND, f. T. W. R. G. O. (2015). A revision of the El Escorial criteria - 2015. *Amyotrophic Lateral Sclerosis and Frontotemporal Degeneration*, 16(5-6):291–292.

Machts, J., Loewe, K., Kaufmann, J., Jakubiczka, S., Abdulla, S., Petri, S., Dengler, R., Heinze, H.-J., Vielhaber, S., Schoenfeld, M. A., and Bede, P. (2015). Basal ganglia pathology in ALS is associated with neuropsychological deficits. *Neurology*, 85(15):1301–9.

Mackenzie, I. R. A., Frick, P., and Neumann, M. (2014). The neuropathology associated with repeat expansions in the C9ORF72 gene. *Acta Neuropathologica*, 127(3):347–357.

McDonald, C. R., McEvoy, L. K., Gharapetian, L., Fennema-Notestine, C., Hagler Jr., D. J., Holland, D., Koyama, A., Brewer, J. B., and Dale, A. M. (2009). Regional rates of neocortical atrophy from normal aging to early Alzheimer disease. *Neurology*, 73(6):457–465.

McLaughlin, R. L., Kenna, K. P., Vajda, A., Bede, P., Elamin, M., Cronin, S., Donaghy, C. G., Bradley, D. G., and Hardiman, O. (2015). A second-generation Irish genome-wide association study for amyotrophic lateral sclerosis. *Neurobiology of Aging*, 36(2):1221.e7–1221.e13.

Menke, R. a. L., Abraham, I., Thiel, C. S., Filippini, N., Knight, S., Talbot, K., and Turner, M. R. (2012). Fractional anisotropy in the posterior limb of the internal capsule and prognosis in amyotrophic lateral sclerosis. *Archives of neurology*, 69(11):1493–1499.

Menke, R. A. L., Agosta, F., Grosskreutz, J., Filippi, M., and Turner, M. R. (2017). Neuroimaging Endpoints in Amyotrophic Lateral Sclerosis. *Neurotherapeutics*, 14(1):11–23.

Menke, R. A. L. R. A. L., Körner, S., Filippini, N., Douaud, G., Knight, S., Talbot, K., and Turner, M. R. (2014). Widespread grey matter pathology dominates the longitudinal cerebral MRI and clinical landscape of amyotrophic lateral sclerosis. *Brain*, 137(Pt 9):2546–55.

Metwalli, N. S., Benatar, M., Nair, G., Usher, S., Hu, X., and Carew, J. D. (2010). Utility of axial and radial diffusivity from diffusion tensor MRI as markers of neurodegeneration in amyotrophic lateral sclerosis. *Brain Research*, 1348:156–164.

Mezzapesa, D. M., D'Errico, E., Tortelli, R., Distaso, E., Cortese, R., Tursi, M., Federico, F., Zoccolella, S., Logroscino, G., Dicuonzo, F., and Simone, I. L. (2013). Cortical Thinning and Clinical Heterogeneity in Amyotrophic Lateral Sclerosis. *PLoS ONE*, 8(11):e80748.

Miller, R. G., Mitchell, J. D., Lyon, M., Moore, D. H., Rg, M., Jd, M., M, L., and Dh, M. (2003). Riluzole for amyotrophic lateral sclerosis (ALS)/motor neuron disease (MND). *Amyotrophic Lateral Sclerosis*, 4(3):191–206.

Miller, R. G. R., Mitchell, J. D., Lyon, M., Moore, D. H. D. D. H., Lyon, M., and Moore, D. H. D. D. H. (2007). Riluzole for amyotrophic lateral sclerosis (ALS)/motor neuron disease (MND). In Miller, R. G., editor, *Cochrane Database of Systematic Reviews*. John Wiley & Sons, Ltd, Chichester, UK.

Mitsumoto, H., Brooks, B. R., and Silani, V. (2014). Clinical trials in amyotrophic lateral sclerosis: why so many negative trials and how can trials be improved? *The Lancet Neurology*, 13(11):1127–1138.

Mueller, S. G., Weiner, M. W., Thal, L. J., Petersen, R. C., Jack, C. R., Jagust, W., Trojanowski, J. Q., Toga, A. W., and Beckett, L. (2005). Ways toward an early diagnosis in Alzheimer's disease: The Alzheimer's Disease Neuroimaging Initiative (ADNI). *Alzheimer's & Dementia*, 1(1):55–66.

Müller, H.-P., Turner, M. R., Grosskreutz, J., Abrahams, S., Bede, P., Govind, V., Prudlo, J., Ludolph, A. C., Filippi, M., Kassubek, J., and Neuroimaging Society in ALS (NiSALS) DTI Study Group (2016). A large-scale multicentre cerebral diffusion tensor imaging study in amyotrophic lateral sclerosis. *Journal of neurology, neurosurgery, and psychiatry*, 87(6):570–9.

Müller, H.-P., Unrath, A., Huppertz, H.-J., Ludolph, A. C., and Kassubek, J. (2012). Neuroanatomical patterns of cerebral white matter involvement in different motor neuron diseases as studied by diffusion tensor imaging analysis. *Amyotrophic lateral sclerosis : official publication of the World Federation of Neurology Research Group on Motor Neuron Diseases*, 13(3):254–64.

Mwangi, B., Tian, T. S., and Soares, J. C. (2013). A Review of Feature Reduction Techniques in Neuroimaging. *Neuroinformatics*, 12(2):229–244.

Nicholson, K. A., Cudkowicz, M. E., and Berry, J. D. (2015). Clinical Trial Designs in Amyotrophic Lateral Sclerosis: Does One Design Fit All? *Neurotherapeutics : the journal of the American Society for Experimental NeuroTherapeutics*, 12(2):376–83.

Nowrangi, M. A., Lyketsos, C. G., Leoutsakos, J.-M. S., Oishi, K., Albert, M., Mori, S., and Mielke, M. M. (2013). Longitudinal, region-specific course of diffusion tensor imaging measures in mild cognitive impairment and Alzheimer's disease. *Alzheimer's & Dementia*, 9(5):519–528.

Oishi, K., Zilles, K., Amunts, K., Faria, A., Jiang, H., Li, X., Akhter, K., Hua, K., Woods, R., Toga, A. W., Pike, G. B., Rosa-Neto, P., Evans, A., Zhang, J., Huang, H., Miller, M. I., van Zijl, P. C. M., Mazziotta, J., and Mori, S. (2008). Human brain white matter atlas: identification and assignment of common anatomical structures in superficial white matter. *NeuroImage*, 43(3):447–57.

Olney, R. K., Murphy, J., Forshew, D., Garwood, E., Miller, B. L., Langmore, S., Kohn, M. A., and Lomen-Hoerth, C. (2005). The effects of executive and behavioral dysfunction on the course of ALS. *Neurology*, 65(11):1774–1777.

Orrù, G., Pettersson-Yeo, W., Marquand, A. F., Sartori, G., and Mechelli, A. (2012). Using Support Vector Machine to identify imaging biomarkers of neurological and psychiatric disease: A critical review. *Neurosci. Biobehav. Rev.*, 36(4):1140–1152.

Pagani, M., Chiò, A., Valentini, M. C., Öberg, J., Nobili, F., Calvo, A., Moglia, C., Bertuzzo, D., Morbelli, S., De Carli, F., Fania, P., and Cistaro, A. (2014). Functional pattern of brain FDG-PET in amyotrophic lateral sclerosis. *Neurology*, 83(12):1067–74.

Pavese, N., Moore, R. Y., Scherfler, C., Khan, N. L., Hotton, G., Quinn, N. P., Bhatia, K. P., Wood, N. W., Brooks, D. J., Lees, A. J., and Piccini, P. (2010). In vivo assessment of brain monoamine systems in parkin gene carriers: A PET study. *Experimental Neurology*, 222(1):120–124.

Pea-Casanova, J. (1997). Alzheimers Disease Assessment ScaleCognitive in Clinical Practice. *International Psychogeriatrics*, 9(S1):105–114.

Pepe, M. S., Etzioni, R., Feng, Z., Potter, J. D., Thompson, M. L., Thornquist, M., Winget, M., and Yasui, Y. (2001). Phases of biomarker development for early detection of cancer. *Journal of the National Cancer Institute*, 93(14):1054–61.

Phukan, J., Elamin, M., Bede, P., Jordan, N., Gallagher, L., Byrne, S., Lynch, C., Pender, N., and Hardiman, O. (2012). The syndrome of cognitive impairment in amyotrophic lateral sclerosis: a population-based study. *Journal of Neurology, Neurosurgery & Psychiatry*, 83(1):102–108.

Pierpaoli, C., Barnett, A., Pajevic, S., Chen, R., Penix, L. R., Virta, A., and Basser, P. (2001). Water diffusion changes in Wallerian degeneration and their dependence on white matter architecture. *NeuroImage*, 13(6 Pt 1):1174–85.

Pierpaoli, C., Jezzard, P., Basser, P. J., Barnett, A., and Di Chiro, G. (1996). Diffusion tensor MR imaging of the human brain. *Radiology*, 201(3):637–48.

Prell, T. and Grosskreutz, J. (2013). The involvement of the cerebellum in amyotrophic lateral sclerosis. *Amyotrophic Lateral Sclerosis and Frontotemporal Degeneration*, 14(7-8):507–515.

Prell, T., Hartung, V., Tietz, F., Penzlin, S., Ilse, B., Schweser, F., Deistung, A., Bokemeyer, M., Reichenbach, J. R., Witte, O. W., and Grosskreutz, J. (2015). Susceptibility-weighted imaging provides insight into white matter damage in amyotrophic lateral sclerosis. *PloS one*, 10(6):e0131114.

Radue, E.-W., O'Connor, P., Polman, C. H., Hohlfeld, R., Calabresi, P., Selmaj, K., Mueller-Lenke, N., Agoropoulou, C., Holdbrook, F., de Vera, A., Zhang-Auberson, L., Francis, G., Burtin, P., Kappos, L., and Group, f. t. F. R. E. E. o. D. O. T. i. M. S. F. S. (2012). Impact of Fingolimod Therapy on Magnetic Resonance Imaging Outcomes in Patients With Multiple Sclerosis. *Archives of Neurology*, 69(10):1259.

Rajagopalan, V., Liu, Z., Allexandre, D., Zhang, L., Wang, X.-F., Pioro, E. P., and Yue, G. H. (2013). Brain white matter shape changes in amyotrophic lateral sclerosis (ALS): a fractal dimension study. *PloS one*, 8(9):e73614.

Rascovsky, K., Hodges, J. R., Knopman, D., Mendez, M. F., Kramer, J. H., Neuhaus, J., van Swieten, J. C., Seelaar, H., Dopper, E. G. P., Onyike,

C. U., Hillis, A. E., Josephs, K. a., Boeve, B. F., Kertesz, A., Seeley, W. W., Rankin, K. P., Johnson, J. K., Gorno-Tempini, M.-L. L., Rosen, H., Prioleau-Latham, C. E., Lee, A., Kipps, C. M., Lillo, P., Piguet, O., Rohrer, J. D., Rossor, M. N., Warren, J. D., Fox, N. C., Galasko, D., Salmon, D. P., Black, S. E., Mesulam, M., Weintraub, S., Dickerson, B. C., Diehl-Schmid, J., Pasquier, F., Deramecourt, V., Lebert, F., Pijnenburg, Y., Chow, T. W., Manes, F., Grafman, J., Cappa, S. F., Freedman, M., Grossman, M., and Miller, B. L. (2011). Sensitivity of revised diagnostic criteria for the behavioural variant of frontotemporal dementia. *Brain : a journal of neurology*, 134(Pt 9):2456–77.

Ravits, J., Paul, P., and Jorg, C. (2007). Focality of upper and lower motor neuron degeneration at the clinical onset of ALS. *Neurology*, 68(19):1571–1575.

Ravits, J. M. and La Spada, A. R. (2009). ALS motor phenotype heterogeneity, focality, and spread: deconstructing motor neuron degeneration. *Neurology*, 73(10):805–811.

Renton, A. E., Chiò, A., and Traynor, B. J. (2014). State of play in amyotrophic lateral sclerosis genetics. *Nat. Neurosci.*, 17(1):17–23.

Reuter, M., Schmansky, N. J., Rosas, H. D., and Fischl, B. (2012). Within-subject template estimation for unbiased longitudinal image analysis. *NeuroImage*, 61(4):1402–1418.

Roccatagliata, L., Bonzano, L., Mancardi, G., Canepa, C., and Caponnetto, C. (2009). Detection of motor cortex thinning and corticospinal tract involvement by quantitative MRI in amyotrophic lateral sclerosis. *Amyotrophic lateral sclerosis : official publication of the World Federation of Neurology Research Group on Motor Neuron Diseases*, 10(1):47–52.

Rohrer, J. D. J., Ridgway, G. R. G., Modat, M., Ourselin, S., Mead, S., Fox, N. C., Rossor, M. N., and Warren, J. D. (2010). Distinct profiles of brain atrophy in frontotemporal lobar degeneration caused by progranulin and tau mutations. *Neuroimage*, 53(3):1070–1076.

Rooney, J., Byrne, S., Heverin, M., Corr, B., Elamin, M., Staines, A., Goldacre, B., Hardiman, O., Cox, D., Royston, P., Lambert, P., Cleves, M., Gould, W., Gutierrez, R., Marchenko, Y., and StataCorp, L. (2013). Survival Analysis of Irish Amyotrophic Lateral Sclerosis Patients Diagnosed from 1995–2010. *PLoS ONE*, 8(9):e74733.

Rooney, J., Byrne, S., Heverin, M., Tobin, K., Dick, A., Donaghy, C., Hardiman, O., Kiernan, M., Vucic, S., Cheah, B., Bensimon, G., Lacomblez, L., Meininger, V., Bourke, S., Tomlinson, M., Williams, T., Newsom-Davis, I., Lyall, R., Leigh, P., Chiò, A., Logroscino, G., Hardiman, O., Traynor, B., Alexander, M., Corr, B., Rooney, J., Byrne, S., Heverin, M., den Berg, J. V., Kalmijn, S., Lindeman, E., Zoccolella, S., Beghi, E., Palagano, G., Aridegbe, T., Kandler, R., Walters, S., Donaghy, C., O'Toole, O., Sheehan, C., Donaghy, C., Clarke, J., Patterson, C., Andersen, P., Borasio, G., Dengler, R., StataCorp, Creemers, H., Veldink, J., Grupstra, H., UK, C. R., HSE, Keren, N., Scott, K., Tsuda, M., Elamin, M., Phukan, J., and Bede, P. (2015). A multidisciplinary clinic approach improves survival in ALS: a comparative study of ALS in Ireland and Northern Ireland. *Journal of neurology, neurosurgery, and psychiatry*, 86(5):496–501.

Rosas, H. D., Salat, D. H., Lee, S. Y., Zaleta, A. K., Pappu, V., Fischl, B., Greve, D., Hevelone, N., and Hersch, S. M. (2008). Cerebral cortex and the clinical expression of Huntington's disease: complexity and heterogeneity. *Brain : a journal of neurology*, 131(Pt 4):1057–68.

Rothstein, J. D. (1996). Therapeutic horizons for amyotrophic lateral sclerosis. *Current Opinion in Neurobiology*, 6(5):679–687.

Ruocco, H. H., Bonilha, L., Li, L. M., Lopes-Cendes, I., and Cendes, F. (2008). Longitudinal analysis of regional grey matter loss in Huntington disease: effects of the length of the expanded CAG repeat. *Journal of neurology, neurosurgery, and psychiatry*, 79(2):130–5.

Sabuncu, M. R., Desikan, R. S., Sepulcre, J., Yeo, B. T., Liu, H., Schmansky, N. J., Reuter, M., Weiner, M. W., Buckner, R. L., Sperling, R. A., and

Fischl, B. (2011). The dynamics of cortical and hippocampal atrophy in Alzheimer disease. *Arch Neurol*, 68(8):1040–1048.

Salat, D. H., Buckner, R. L., Snyder, A. Z., Greve, D. N., Desikan, R. S. R., Busa, E., Morris, J. C., Dale, A. M., and Fischl, B. (2004). Thinning of the Cerebral Cortex in Aging. *Cerebral Cortex*, 14(7):721–730.

Salimi-Khorshidi, G., Smith, S. M., and Nichols, T. E. (2011). Adjusting the effect of nonstationarity in cluster-based and TFCE inference. *NeuroImage*, 54(3):2006–2019.

Sarro, L., Agosta, F., Canu, E., Riva, N., Prelle, a., Copetti, M., Riccitelli, G., Comi, G., and Filippi, M. (2011). Cognitive Functions and White Matter Tract Damage in Amyotrophic Lateral Sclerosis: A Diffusion Tensor Tractography Study. *AJNR. American journal of neuroradiology*, 32(10):1866–72.

Schuster, C., Elamin, M., Hardiman, O., and Bede, P. (2015). Presymptomatic and longitudinal neuroimaging in neurodegeneration—from snapshots to motion picture: a systematic review. *Journal of Neurology, Neurosurgery & Psychiatry*, 86(10):1089–1096.

Schuster, C., Elamin, M., Hardiman, O., and Bede, P. (2016a). The segmental diffusivity profile of amyotrophic lateral sclerosis associated white matter degeneration. *European Journal of Neurology*, 23(8):1361–1371.

Schuster, C., Hardiman, O., and Bede, P. (2016b). Development of an Automated MRI-Based Diagnostic Protocol for Amyotrophic Lateral Sclerosis Using Disease-Specific Pathognomonic Features: A Quantitative Disease-State Classification Study. *PLOS ONE*, 11(12):e0167331.

Schuster, C., Kasper, E., Dyrba, M., Machts, J., Bittner, D., Kaufmann, J., Mitchell, A. J., Benecke, R., Teipel, S., Vielhaber, S., and Prudlo, J. (2014a). Cortical thinning and its relation to cognition in amyotrophic lateral sclerosis. *Neurobiology of Aging*, 35(1):240–246.

Schuster, C., Kasper, E., Machts, J., Bittner, D., Kaufmann, J., Benecke, R., Teipel, S., Vielhaber, S., and Prudlo, J. (2013). Focal thinning of the motor cortex mirrors clinical features of amyotrophic lateral sclerosis and their phenotypes: a neuroimaging study. *J Neurol*, 260(11):1–9.

Schuster, C., Kasper, E., Machts, J., Bittner, D., Kaufmann, J., Benecke, R., Teipel, S., Vielhaber, S., and Prudlo, J. (2014b). Longitudinal course of cortical thickness decline in amyotrophic lateral sclerosis. *Journal of Neurology*, 261(10):1871–1880.

Simon, N. G. N., Turner, M. M. R., Vucic, S., Al-Chalabi, A., Shefner, J., Lomen-Hoerth, C., and Kiernan, M. C. (2014). Quantifying disease progression in amyotrophic lateral sclerosis. *Annals of neurology*, 76(5):643–57.

Smith, M. (1960). Nerve fibre degeneration in the brain in amyotrophic lateral sclerosis. *Journal of Neurology, Neurosurgery & Psychiatry*.

Smith, S. M., Jenkinson, M., Johansen-Berg, H., Rueckert, D., Nichols, T. E., Mackay, C. E., Watkins, K. E., Ciccarelli, O., Cader, M. Z., Matthews, P. M., and Behrens, T. E. J. (2006). Tract-based spatial statistics: voxelwise analysis of multi-subject diffusion data. *NeuroImage*, 31(4):1487–1505.

Smith, S. M., Jenkinson, M., Woolrich, M. W., Beckmann, C. F., Behrens, T. E., Johansen-Berg, H., Bannister, P. R., De Luca, M., Drobnjak, I., Flitney, D. E., Niazy, R. K., Saunders, J., Vickers, J., Zhang, Y., De Stefano, N., Brady, J. M., and Matthews, P. M. (2004). Advances in functional and structural MR image analysis and implementation as FSL. *NeuroImage*, 23:S208–S219.

Smith, S. M. and Nichols, T. E. (2009). Threshold-free cluster enhancement: Addressing problems of smoothing, threshold dependence and localisation in cluster inference. *NeuroImage*, 44(1):83–98.

Song, S.-K., Sun, S.-W., Ramsbottom, M. J., Chang, C., Russell, J., and Cross, A. H. (2002). Dysmyelination Revealed through MRI as Increased Radial (but Unchanged Axial) Diffusion of Water. *NeuroImage*, 17(3):1429–1436.

Song, S. S.-K., Yoshino, J., Le, T. T. Q., Lin, S.-J. S., Sun, S. S.-W., Cross, A. A. H., and Armstrong, R. C. (2005). Demyelination increases radial diffusivity in corpus callosum of mouse brain. *NeuroImage*, 26(1):132–40.

Stagg, C. J., Knight, S., Talbot, K., Jenkinson, M., Maudsley, A. A., and Turner, M. R. (2013). Whole-brain magnetic resonance spectroscopic imaging measures are related to disability in ALS. *Neurology*, 80(7):610–5.

Stonnington, C. M., Tan, G., Klöppel, S., Chu, C., Draganski, B., Jack, C. R., Chen, K., Ashburner, J., and Frackowiak, R. S. (2008). Interpreting scan data acquired from multiple scanners: A study with Alzheimer's disease.

Sun, S.-W., Liang, H.-F., Trinkaus, K., Cross, A. H., Armstrong, R. C., and Song, S.-K. (2006). Noninvasive detection of cuprizone induced axonal damage and demyelination in the mouse corpus callosum. *Magnetic resonance in medicine*, 55(2):302–8.

Sundgren, P. C., Dong, Q., Gómez-Hassan, D., Mukherji, S. K., Maly, P., and Welsh, R. (2004). Diffusion tensor imaging of the brain: review of clinical applications. *Neuroradiology*, 46(5):339–50.

Tabrizi, S. J., Langbehn, D. R., Leavitt, B. R., Roos, R. A., Durr, A., Craufurd, D., Kennard, C., Hicks, S. L., Fox, N. C., Scahill, R. I., Borowsky, B., Tobin, A. J., Rosas, H. D., Johnson, H., Reilmann, R., Landwehrmeyer, B., and Stout, J. C. (2009). Biological and clinical manifestations of Huntington's disease in the longitudinal TRACK-HD study: cross-sectional analysis of baseline data. *The Lancet Neurology*, 8(9):791–801.

Tabrizi, S. J., Reilmann, R., Roos, R. A., Durr, A., Leavitt, B., Owen, G., Jones, R., Johnson, H., Craufurd, D., Hicks, S. L., Kennard, C., Landwehrmeyer, B., Stout, J. C., Borowsky, B., Scahill, R. I., Frost, C.,

and Langbehn, D. R. (2012). Potential endpoints for clinical trials in premanifest and early Huntington's disease in the TRACK-HD study: analysis of 24 month observational data. *The Lancet Neurology*, 11(1):42–53.

Tabrizi, S. J., Scahill, R. I., Owen, G., Durr, A., Leavitt, B. R., Roos, R. A., Borowsky, B., Landwehrmeyer, B., Frost, C., Johnson, H., Craufurd, D., Reilmann, R., Stout, J. C., and Langbehn, D. R. (2013). Predictors of phenotypic progression and disease onset in premanifest and early-stage Huntington's disease in the TRACK-HD study: analysis of 36-month observational data. *Lancet Neurol*, 12(7):637–649.

Tang, C. C., Poston, K. L., Dhawan, V., and Eidelberg, D. (2010). Abnormalities in metabolic network activity precede the onset of motor symptoms in Parkinson's disease. *J Neurosci*, 30(3):1049–1056.

Teipel, S., Drzezga, A., Grothe, M. J., Barthel, H., Chételat, G., Schuff, N., Skudlarski, P., Cavedo, E., Frisoni, G. B., Hoffmann, W., Thyrian, J. R., Fox, C., Minoshima, S., Sabri, O., and Fellgiebel, A. (2015a). Multimodal imaging in Alzheimer's disease: validity and usefulness for early detection. *The Lancet Neurology*.

Teipel, S. J., Kurth, J., Krause, B., and Grothe, M. J. (2015b). The relative importance of imaging markers for the prediction of Alzheimer's disease dementia in mild cognitive impairment - Beyond classical regression. *NeuroImage. Clinical*, 8:583–93.

Teipel, S. J., Peters, O., Heuser, I., Jessen, F., Maier, W., Froelich, L., Arlt, S., Hüll, M., Gertz, H.-J., Kornhuber, J., Wiltfang, J., Thome, J., Rienhoff, O., Meindl, T., Hampel, H., and Grothe, M. (2011a). Atrophy outcomes in multicentre clinical trials on Alzheimer's disease: Effect of different processing and analysis approaches on sample sizes. *The World Journal of Biological Psychiatry*, 12(sup1):109–113.

Teipel, S. J., Reuter, S., Stieltjes, B., Acosta-Cabronero, J., Ernemann, U., Fellgiebel, A., Filippi, M., Frisoni, G., Hentschel, F., Jessen, F., Klöppel, S., Meindl, T., Pouwels, P. J., Hauenstein, K.-H., and Hampel, H. (2011b).

Multicenter stability of diffusion tensor imaging measures: A European clinical and physical phantom study. *Psychiatry Research: Neuroimaging*, 194(3):363–371.

The Lancet Neurology (2014). Bringing forward the diagnosis of Alzheimer's disease. *The Lancet. Neurology*, 13(10):961.

Toosy, A. T., Werring, D. J., Orrell, R. W., Howard, R. S., King, M. D., Barker, G. J., Miller, D. H., and Thompson, A. J. (2003). Diffusion tensor imaging detects corticospinal tract involvement at multiple levels in amyotrophic lateral sclerosis. *Journal of neurology, neurosurgery, and psychiatry*, 74(9):1250–7.

Trouillas, P., Takayanagi, T., Hallett, M., Currier, R., Subramony, S., Wessel, K., Bryer, A., Diener, H., Massaquoi, S., Gomez, C., Coutinho, P., Hamida, M., Campanella, G., Filla, A., Schut, L., Timann, D., Honnorat, J., Nighoghossian, N., and Manyam, B. (1997). International Cooperative Ataxia Rating Scale for pharmacological assessment of the cerebellar syndrome. *Journal of the Neurological Sciences*, 145(2):205–211.

Turner, M., Hammers, A., and Al-Chalabi, A. (2005). Distinct cerebral lesions in sporadic and 'D90A'SOD1 ALS: studies with flumazenil PET. *Brain*.

Turner, M. M. R., Grosskreutz, J., Kassubek, J., Abrahams, S., Agosta, F., Benatar, M., Filippi, M., Goldstein, L. H., van den Heuvel, M., Kalra, S., Lulé, D., and Mohammadi, B. (2011). Towards a neuroimaging biomarker for amyotrophic lateral sclerosis. *The Lancet. Neurology*, 10(5):400–403.

Turner, M. R., Agosta, F., Bede, P., Govind, V., Lulé, D., and Verstraete, E. (2012). Neuroimaging in amyotrophic lateral sclerosis. *Biomarkers in Medicine*, 6(3):319–337.

Turner, M. R., Kiernan, M. C., Leigh, P. N., and Talbot, K. (2009). Biomarkers in amyotrophic lateral sclerosis. *The Lancet. Neurology*, 8(1):94–109.

Van den Berg, J. P., Kalmijn, S., Lindeman, E., Veldink, J. H., de Visser, M., Van der Graaff, M. M., Wokke, J. H. J., and Van den Berg, L. H. (2005). Multidisciplinary ALS care improves quality of life in patients with ALS. *Neurology*, 65(8):1264–7.

van der Graaff, M. M., Sage, C. a., Caan, M. W. a., Akkerman, E. M., Lavini, C., Majoie, C. B., Nederveen, A. J., Zwinderman, A. H., Vos, F., Brugman, F., van den Berg, L. H., de Rijk, M. C., van Doorn, P. a., Van Hecke, W., Peeters, R. R., Robberecht, W., Sunaert, S., and de Visser, M. (2011). Upper and extra-motoneuron involvement in early motoneuron disease: a diffusion tensor imaging study. *Brain : a journal of neurology*, 134(Pt 4):1211–1228.

Van Laere, K., Vanhee, A., Verschueren, J., De Coster, L., Driesen, A., Dupont, P., Robberecht, W., and Van Damme, P. (2014). Value of 18fluorodeoxyglucose-positron-emission tomography in amyotrophic lateral sclerosis: a prospective study. *JAMA neurology*, 71(5):553–561.

Verstraete, E. and Heuvel, M. P. V. D. (2010). Motor network degeneration in amyotrophic lateral sclerosis: a structural and functional connectivity study. *PLoS One*.

Verstraete, E., Veldink, J. H., Hendrikse, J., Schelhaas, H. J., van den Heuvel, M. P., van den Berg, L. H., van den Heuvel, M. P., and van den Berg, L. H. (2012). Structural MRI reveals cortical thinning in amyotrophic lateral sclerosis. *Journal of Neurology, Neurosurgery & Psychiatry*, 83(4):383–388.

Verstraete, E., Veldink, J. J. H. J., van den Berg, L. H., and van den Heuvel, M. P. (2014). Structural brain network imaging shows expanding disconnection of the motor system in amyotrophic lateral sclerosis. *Human brain mapping*, 35(4):1351–1361.

Walhout, R., Schmidt, R., Westeneng, H.-J., Verstraete, E., Seelen, M., van Rheenen, W., de Reus, M. A., van Es, M. A., Hendrikse, J., Veldink, J. H., van den Heuvel, M. P., and van den Berg, L. H. (2015). Brain morphologic

changes in asymptomatic C9orf72 repeat expansion carriers. *Neurology*, 85(20):1780–8.

Wang, S. and Summers, R. M. (2012). Machine learning and radiology. *Medical image analysis*, 16(5):933–51.

Wang, Y., Wang, Q., Haldar, J. P., Yeh, F.-C., Xie, M., Sun, P., Tu, T.-W., Trinkaus, K., Klein, R. S., Cross, A. H., and Song, S.-K. (2011). Quantification of increased cellularity during inflammatory demyelination. *Brain : a journal of neurology*, 134(Pt 12):3590–601.

Welsh, R. C., Jelsone-Swain, L. M., and Foerster, B. R. (2013). The utility of independent component analysis and machine learning in the identification of the amyotrophic lateral sclerosis diseased brain. *Frontiers in human neuroscience*, 7(June):251.

Westin, C.-F., Maier, S., Mamata, H., Nabavi, A., Jolesz, F., and Kikinis, R. (2002). Processing and visualization for diffusion tensor MRI. *Medical Image Analysis*, 6(2):93–108.

Whitwell, J., Jack, C., Boeve, B., and Senjem, M. (2009). Voxel-based morphometry patterns of atrophy in FTLD with mutations in MAPT or PGRN. *Neurology*.

Winkler, A. M., Kochunov, P., Blangero, J., Almasy, L., Zilles, K., Fox, P. T., Duggirala, R., and Glahn, D. C. (2010). Cortical thickness or grey matter volume? The importance of selecting the phenotype for imaging genetics studies. *NeuroImage*, 53(3):1135–1146.

Winkler, A. M., Ridgway, G. R., Webster, M. A., Smith, S. M., and Nichols, T. E. (2014). Permutation inference for the general linear model. *NeuroImage*, 92:381–397.

Wokke, J. H. (2009). Confounding effects of mimicking disorders in the early diagnosis of amyotrophic lateral sclerosis. *Amyotrophic Lateral Sclerosis and Other Motor Neuron Disorders*.

Wolf, J., Safer, A., Wöhrle, J. C., Palm, F., Nix, W. A., Maschke, M., and Grau, A. J. (2014). Factors predicting one-year mortality in amyotrophic lateral sclerosis patients - data from a population-based registry. *BMC Neurology*, 14(1):197.

Wong, J. C. T., Concha, L., Beaulieu, C., Johnston, W., Allen, P. S., and Kalra, S. (2007). Spatial profiling of the corticospinal tract in amyotrophic lateral sclerosis using diffusion tensor imaging. *Journal of neuroimaging : official journal of the American Society of Neuroimaging*, 17(3):234–40.

Woolley, S. C., Zhang, Y., Schuff, N., Weiner, M. W., and Katz, J. S. (2011). Neuroanatomical correlates of apathy in ALS using 4 Tesla diffusion tensor MRI. *Amyotrophic lateral sclerosis : official publication of the World Federation of Neurology Research Group on Motor Neuron Diseases*, 12(1):52–58.

Zhang, J., Aggarwal, M., and Mori, S. (2012). Structural insights into the rodent CNS via diffusion tensor imaging. *Trends in neurosciences*, 35(7):412–21.

Zhang, Y., Schuff, N., Woolley, S. C., Chiang, G. C., Boreta, L., Laxamana, J., Katz, J. S., and Weiner, M. W. (2011). Progression of white matter degeneration in amyotrophic lateral sclerosis: A diffusion tensor imaging study. *Amyotrophic lateral sclerosis : official publication of the World Federation of Neurology Research Group on Motor Neuron Diseases*, 12(6):421–9.

Zoccolella, S., Beghi, E., Palagano, G., Fraddosio, A., Samarelli, V., Lamberti, P., Lepore, V., Serlenga, L., and Logroscino, G. (2006). Predictors of delay in the diagnosis and clinical trial entry of amyotrophic lateral sclerosis patients: A population-based study. *Journal of the Neurological Sciences*, 250(1-2):45–49.